Master's thesis

NTNU
Norwegian University of Science and Technology
Faculty of Information Technology and Electrical Engineering
Department of Electric Power Engineering

Fredrik Bjørken

Toward the New Grid Code: Implications of the Fault Ride-Through

Master's thesis in Energy and the Environment

Supervisor: Jonas Kristiansen Nøland

June 2020

NTNU
Norwegian University of Science and Technology

Fredrik Bjørken

Toward the New Grid Code: Implications of the Fault Ride-Through

Master's thesis in Energy and the Environment
Supervisor: Jonas Kristiansen Nøland
June 2020

Norwegian University of Science and Technology
Faculty of Information Technology and Electrical Engineering
Department of Electric Power Engineering

NTNU
Norwegian University of
Science and Technology

Abstract

Norway's history in hydropower goes as far back as the 1800s and since has hydro been the main source of electrical power production. In the past years, there has been an increased utilization of renewable energy sources. The fault ride-through requirement was first implemented to wind power generators and has later become a requirement for synchronous generators. In Norway, the utilization of wind power has grown the past years, but hydropower is still the largest in electrical power production.

The fault ride-through requirement has been implemented to many synchronous generators worldwide, where the requirement is described as a voltage profile the synchronous generator should stay within without losing synchronism. In Norway, the fault ride-through requirement was first described in FIKS 2012. Later in 2019, a draft was published by Statnett suggesting a new, improved voltage-time profile, with easier fault clearing time. Both FIKS 2012 and the draft NVF 2020 will be described in the thesis, NVF 2020 will be used in the simulations.

Usually a consultant is hired to test the generators fault ride-though capability by putting a voltage profile on the generator. This thesis will show how the actual voltage profile is during a three-phase fault, by changing its distance from the high voltage side of the transformer. The thesis is intended as a detailed support document to aid the fault ride-through analysis.

The model is created in MATLAB Simulink where the critical clearing time and the voltage profile at each distance is presented and describe. A total of six cases is chosen. A short-circuit power of 20 [p.u], 10 [p.u], and 6,67 [p.u] is used, where each of them is simulated with a reactive power at zero and maximum. The reactive power is measured on the HV-side of the step-up transformer connected to the synchronous generator.

What is observed in the result is that the synchronous machines pre-fault operation conditions have a significant effect on the fault ride-through capability. A change in reactive power from zero to maximum improved the critical fault clearing time of the synchronous generator, and the critical fault distance was closer to the terminals.

Sammendrag

Norge har en lang historie innen vannkraft og den går helt tilbake til 1800-tallet, og har vært den primære kilden for produksjon av elektrisk energi siden. I de siste årene har det vært en økt utnyttelse av fornybar energi. Fault ride-through-kravet ble først krevd til vindkraftgeneratorer, og ble senere krevd for synkrone generatorer. Utnyttelsen av vindkraft har økt de siste årene i Norge, men vannkraft er fortsatt den største kilden til elektrisk energi.

Fault ride-through-kravet har blitt implementert i mange synkrone generatorer over verden. Kravet blir beksrevet av en spenningsprofil som generatoren må holde seg innnenfor uten å miste synkronisme. I Norge ble kravet først beskrevet i FIKS 2012, og senere i 2019 ble det publisert et høringsutkast av Statnett med en forbedret spenningsprofil, og lettere feilklareringstid. Både FIKS 2012 og høringsutkastet NVF 2020 vil bli presentert i avhandlingen. NVF 2020 vil bli benyttet i simuleringene.

Det er vanlig å leie inn en konsulent som tester generatorens fault ride-through-egenskap ved å sette på en spenningsprofil på generatoren. Denne avhandlingen vill vise den faktiske spenningsprofilen under en tre-fase feil ved å endre dens avnstand til høyspent siden av transformatoren. Avhandligen er tenkt som et detaljert underliggende dokument for å analysere fault ride-through egenskapene.

Modellen av systemet med den synkrone generatoren er gjort i MATLAB Simulink. En symmetrisk tre-fasefeil er satt på en linje hvor feilens avstand er dynamisk endret. Den kritiske feilklareringstiden og spenningsprofilen er presentert og beskrevet. Det er utført totalt seks scenarioer. Det er brukt en kortslutningsytelse på 20 [p.u], 10 [p.u] og 6,67 [p.u], hvor hver av de er simulert med en reaktiv effekt på null og maks. Den reaktive effekten er målt på høyspenningssiden av transformatoren som er tilkoblet generatoren.

Det som ble observert i resultatene er at driftsforholdet til generatoren før feilen har stor innvirkning på fault ride-through-egenskapene. En endring i reaktiv effekt fra null til maks bedret den kritiske feilklareringstiden til generatorene, og det kritiske feilavstanden er nærmere terminalene.

Preface

What you are about to read is a thesis about a fault ride-through event on a synchronous generator used in hydro-plants. Statkraft has provided technical data to set up a simulation model in Matlab Simulink. The model simulates a three-phase fault on a parallel line at different distances and how the synchronous generator will handle the fault. The master thesis is written as a part of the master degree at Norwegian University of Science and Technology from January 2020 to june 2020.

The task was given by Jonas Kristian Nøland where we contacted Statkraft late 2019 about possibilities in synchronous machine parameters to use in a simulation. The task has been difficult in many areas, but creating a working model has been one of the most demanding. With steady reading, learning and help from my supervisor Jonas a possible model was created.

I would like to thank my supervisor Jonas Kristian Nøland for aiding me in the thesis, and Geir Aalvik from Statkraft on providing technical data to create a simulation model. It has been a tough period with a lot of ups and downs. With steady help from both, friends and family, progress has been made.

I hope you enjoy the thesis.

Fredrik Bjørken

June, 13, 2020

Table of Contents

List of Figures

List of Tables

Abbreviations

AVR	Automatic voltage regulator
ENTSO-E	European Network of Transmission System Operators for Electricity
FIKS 2012	Funksjonskrav i kraftsystemet 2012
FRT	Fault ride-through
HV	High Voltage
NVF 2020	Nasjonal Veileder for Funksjonskrav i kraftsystemet 2020
PCC	Point of Common Coupling
PI	Proportional and Integral
POC	Point of Connection
PSS	Power system stabiliser
tc	Critical clearing time

Chapter 1

Introduction

1.1 Background

As early as the 1800s, the pioneer Sam Eyde made sure to get the rights to establish an industry in Telemark to use the power from the water to produce electricity. This made the foundation of "Norsk Hydro" and "Elkem." Later on, the Norwegian prime minister Gunnar Knutsen wrote a letter about the potential of electrical power production from water to the Norwegian parliament. The goal was to cooperate with the parliament to make Norway a rich country were the water resources should benefit the population.

The first municipal hydropower was put into operation in 1891 in Hammerfest and was the first town to have electric lights in the streets in Norway. Oslo followed along later in the 1890s. Hammeren power in Maridalen in Oslo was built in the 1900 and is the oldest power station still in operation to this day in Norway. The power produced over a year from Hammeren power station can supply Oslo for half a day. This gives a good illustration of how much electrical power consumption has increased over the years.

Vemork powerplant was put into operation in 1911 and considered the largest hydropower in the world at that time. During the industrial revolution, other countries used oil and coal, while Norway used the benefit of water resources. Hydropower plants have since been the gateway into the modernization and industrialization in Norway [2].

Three percent of the total energy production in Norway in 2018 was produced by wind power[3], and in 2019 the number increased to four percent[4], while 93 percent of the power production was by hydro in 2019 [5]. The increase in renewable penetration is increasing each year. Renewable sources like solar and wind are more challenging to control since the power produced is determined by the weather conditions. The requirement for fault-ride through was first implemented to wind turbines generators [6] and has later become a topic for synchronous generators.

Fault ride-through requirement describes a voltage profile which the generator should be able to stay within, without losing synchronism with the grid. ENTSO-E published a report which gives the basis of the regulation each transmission system operator (TSO) has published. In Norway, that is Statnett. The first regulation published was called "Funksjonskrav i kraftsystemet 2012" (FIKS 2012) [7], but there is a new, improved regulation published as a draft called "Nasjonal veilder for funksjonskrav i kraftsystemet 2020" (NVF 2020)[1].

1.2 Problem description

A fault in the grid will cause the voltage to drop. This drop of voltage will cause the speed of the rotor in the synchronous machine to increase to produce the required active power to the grid. Should the fault stay connected too long, the rotor may lose synchronism.

The thesis will look at the draft published by Statnett, NVF 2020 [1], in the fault ride-through analysis. The draft describes a voltage profile which the generator should stay within. The voltage produced by the generator should be above the curve, and synchronism with the grid must be kept. One of the voltage profiles described in the draft can be observed in Figure 1.1.

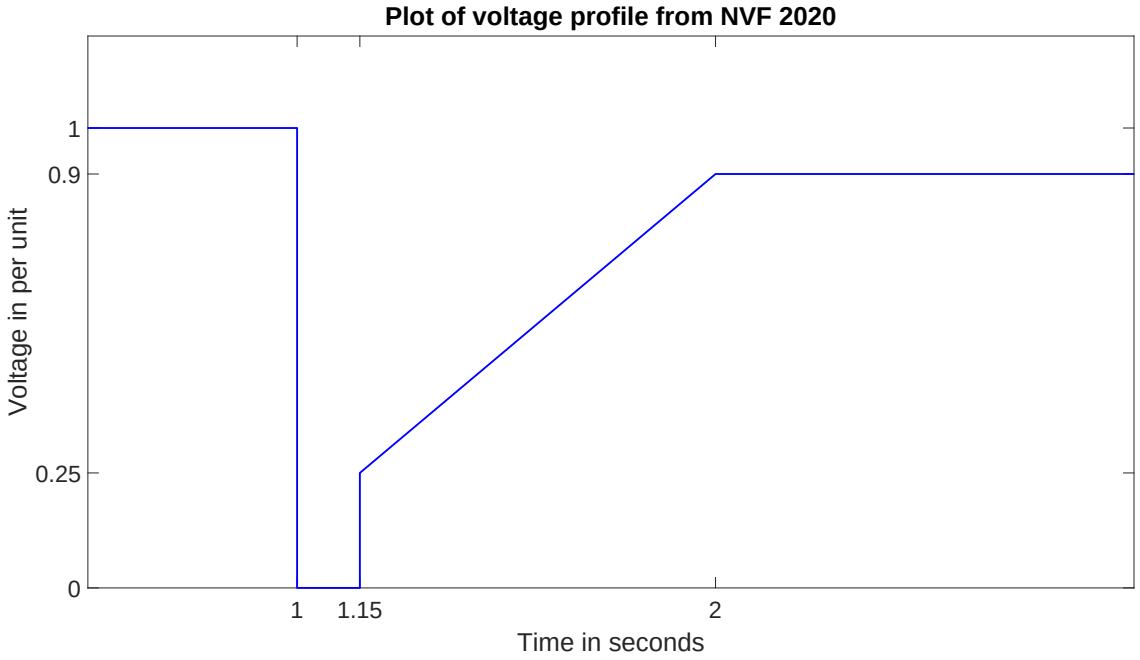

Figure 1.1: A figure of the voltage profile given in the NVF 2020 draft. The voltage profile is for a generator with P $\geq$ 30 MW and U $\geq$ 110 kV. Fault occurs at 1 second, and is cleared after 150 ms where the voltage steps up to 0.25 per unit, and then recovers to 0,9 per unit after another 850 ms.

This thesis investigates how the drop of voltage affects the synchronous generator. The generator is connected to a step-up transformer, which is connected to the grid with two parallel lines in between. The fault will be dynamically changed with a distance "a" from the high voltage (HV) side of the step-up transformer, and the critical clearing time will be found for each distance. A figure of the model can be seen in Figure 1.2. The magnetization system used in the model is a PI regulator without a power system stabilizer (PSS), and the mechanical torque is constant. Since the model does not have a PSS the focus will be on the generators survival capability during the fault period.

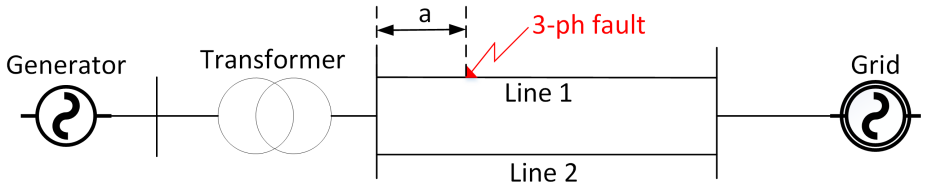

Figure 1.2: A figure of the case model used in the simulation in the thesis. A 3-phase fault occurs at a distance "a" from the HV side of the step-up transformer.

1.3 Objective

- The thesis will test the fault ride-through requirement described in NVF 2020 on a hydro power synchronous generator.
- How the pre-fault operation conditions of the synchronous generator will affect its fault ride-through capability.
- Does the NVF 2020 suggest a better voltage profile?
- Recommendations to NVF 2020.

1.4 Thesis structure

Chapter 2 describes the theory required to set up the simulation model in chapter 3. Chapter 2 also gives an explanation of how the reactive power flows, and how the load angle oscillates and recovers when the line is cleared after the fault. How the simulation is created in Simulink with the step-up transformer built into the generator model with the help of the d- and q-axis is explained in chapter 3. The excitation system setup and tuning is also explained. In the simulations, the requirement from NVF 2020 will be used. Chapter 4 describes the fault ride-through requirement from NVF 2020 and FIKS 2012. Before the results are presented in chapter 6, the six cases are described along with the generator parameters and how the model is tuned with for each case in chapter 5. After the results are presented in chapter 6, the model and the results are discussed in chapter 7 and then the conclusion is presented in chapter 8.

Chapter 2

The synchronous machine

The theory required is presented in this chapter, which is needed to build the simulation model in MATLAB Simulink. Some of the methods were described in the specialization project [8] and will be covered again. The theory presented in the chapter is from the book Power System Stability and Control by Kundur [9].

2.1 d- and q- axis equivalent circuits

The voltages in a synchronous machine are usually represented by the equivalent circuits in form the d- and q- axis. These equivalent circuits gives a visual representation of the machine. The d-axis can be observed in Figure 2.1 and the q-axis in Figure 2.2. The inductance $L_{f1d} - L_{ad}$ in Figure 2.1 is the flux circulates the field winding and the amortisseur [9]. The parameter p in Figure 2.1 and 2.2 represents the derivative term $\frac{d}{dt}$.

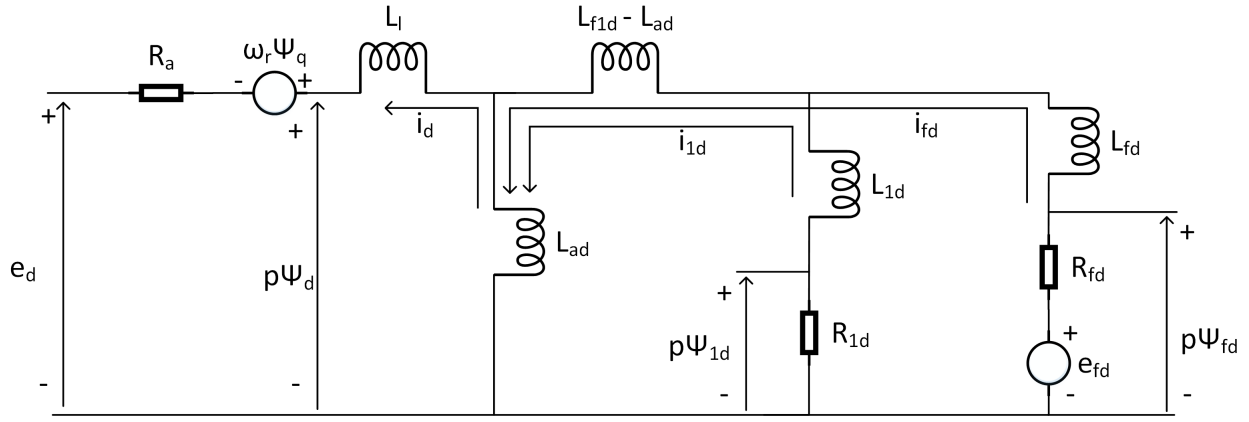

Figure 2.1: Figure of the d-axis equivalent circuit. The parameter p in the model represents the derivative term $\frac{d}{dt}$.

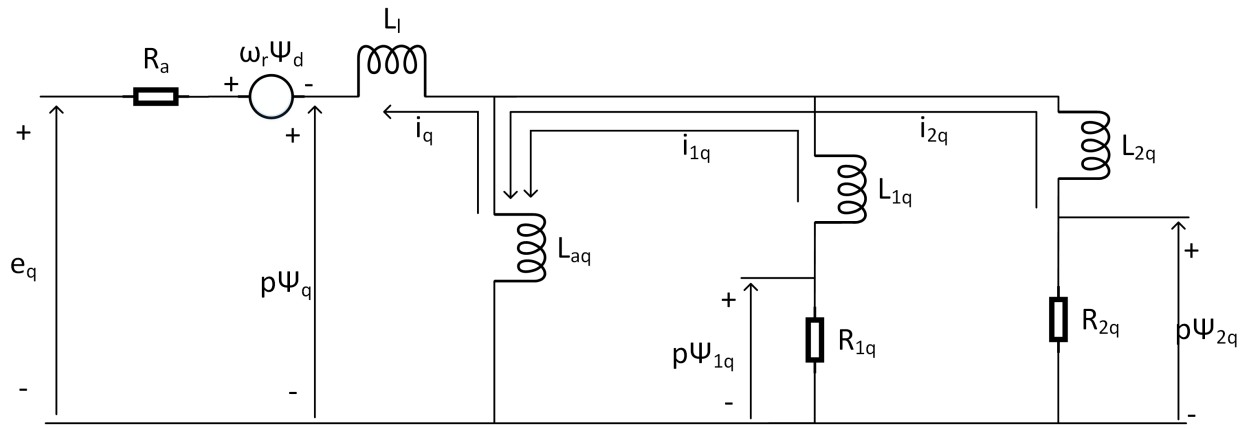

Figure 2.2: Figure of the q-axis equivalent circuit. The parameter p in the model represents the derivative term $\frac{d}{dt}$.

The d- and q- axis voltage and fluxes are represented by equation 2.1 to equation 2.6. Subscript *d* is the d-axis, *q* is the q-axis and *fd* is the field winding. Subscript *a* is the armature winding. L_l is the leakage inductance. L_{ad} and L_{aq} are the mutual inductance. Subscripts 1q and 2q denotes the amortisseur circuits [9].

$$e_d = \frac{d}{dt}\Psi_d - \Psi_q \omega_r - R_a i_d \tag{2.1}$$

$$e_q = \frac{d}{dt}\Psi_q + \Psi_d \omega_r - R_a i_q \tag{2.2}$$

$$e_{fd} = \frac{d}{dt}\Psi_{fd} + R_{fd} i_{fd} \tag{2.3}$$

$$\Psi_d = -(L_{ad} + L_l) i_d + L_{ad} i_{fd} + L_{ad} i_{1d} \tag{2.4}$$

$$\Psi_q = -(L_{aq} + L_l) i_q + L_{aq} i_{1q} + L_{aq} i_{2q} \tag{2.5}$$

$$\Psi_{fd} = L_{ffd} i_{fd} + L_{fld} i_{1d} - L_{ad} i_d \tag{2.6}$$

It can be observed from equations 2.1 and 2.2 that the d-axis voltage is dependent on the q-axis flux and the q-axis voltage on the d-axis flux. It is assumed the q-axis leads the d-axis, therefore the negative term $-\Psi_q \omega_r$, in equation 2.1, and the positive term $+\Psi_d \omega_r$ in equation 2.2.

The resistance R_a can be neglected from equations 2.1 and 2.2 since its usually of a small value. By neglecting the resistance R_a, equation 2.1 and equation 2.2 can be written as equation 2.7 and 2.8[9].

$$e_d = \frac{d}{dt}\Psi_d - \Psi_q \omega_r \tag{2.7}$$

$$e_q = \frac{d}{dt}\Psi_q + \Psi_d \omega_r \tag{2.8}$$

In per unit the reactance *X* equals the inductance *L*. But the reactance in the d-axis and q-axis during a sub-transient, transient and steady-state period has different values. The sub-transient $X_d^{''}$ and $X_q^{''}$, corresponds to the first oscillation of a fault period. The transient, $X_d^{'}$ and $X_q^{'}$, is the values until the fault dissipates and steady state, X_d and X_q, is reached [9].

2.2 Time constants

The time constants was explained in the project thesis [8]. When creating the Simulink model some of the equations is needed, and will therefore be mentioned in this chapter.

The fault period which happens is described by time constants. Those time constants are referred to the sub-transient, transient and the steady state period. The sub-transient is the first oscillation period, the transient is the period until steady state is reached. Each of these time constants describes one part on the fault oscillations, the corresponding equations for the d-axis time constants can be observed in equations 2.9 to 2.12. Equation 2.9 is the subtransient time constant and equation 2.10 is the transient time constant. The open circuit subtransient time constant is described by equation 2.11 and the open circuit transeient time constant is described by equation 2.12 [9].

$$T_d^{''} = \frac{1}{R_{1d}}\left(L_{1d} + \frac{L_{ad}L_{pl}L_{fd} + L_l L_{fd} L_{ad} + L_l L_{fd} L_{pl}}{L_{fd}L_{ad} + L_{fd}L_l + L_{pl}L_{ad} + L_{pl}L_l + L_{ad}L_l}\right) \tag{2.9}$$

$$T_d^{'} = \frac{1}{R_{fd}}\left(L_{fd} + L_{pl} + \frac{L_{ad}L_l}{L_{ad} + L_l}\right) \tag{2.10}$$

$$T_{d0}^{''} = \frac{1}{R_{1d}}\left(L_{1d} + \frac{L_{fd}(L_{ad} + L_{pl})}{L_{fd} + L_{ad} + L_{pl}}\right) \tag{2.11}$$

$$T_{d0}^{'} = \frac{L_{ad} + L_{fd} + L_{pl}}{R_{fd}} \tag{2.12}$$

However the open circuit time constants may also be expressed in terms of the d-axis transient and subtransient inductances. Rearranging equation 2.13 to be expressed by the steady state d-axis inductance, as in equation 2.14. The steady state d-axis inductance in equation 2.14 may now be inserted into equation 2.15 obtaining equation 2.16. The subtransient open circuit time constant can now be expressed by the d-axis transient time constants and inductances, observed in equation 2.17 [9].

$$L_d^{'} = L_d \frac{T_d^{'}}{T_{d0}^{'}} \tag{2.13}$$

$$L_d = L_d^{'} \frac{T_{d0}^{'}}{T_d^{'}} \tag{2.14}$$

$$L_d^{''} = L_d \frac{T_d^{'} T_d^{''}}{T_{d0}^{'} T_{d0}^{''}} \tag{2.15}$$

$$L_d^{''} = L_d^{'} \frac{T_d^{''}}{T_{d0}^{''}} \tag{2.16}$$

$$T_{d0}^{''} = T_d^{''} \frac{L_d^{'}}{L_d^{''}} \tag{2.17}$$

For the q-axis only the sub-transient and steady state time constants is present. This is due to the laminated core in a salient pole machine, consequently, there is only a damper circuit. The q-axis damper circuit is usually represented by the subscript $1q$. The subtransient open circuit time constant can be observed in equation 2.18 [9].

$$T_{q0}^{''} = \frac{L_{aq} + L_{1q}}{R_{1q}} \tag{2.18}$$

2.3 Excitation system

The excitation system regulates the field current to maintain the terminal voltage of the synchronous generator. During transient disturbance the excitation system must also be able to give field forcing to improve the synchronous generators stability [9].

The excitation system may consist of an exciter, regulator, voltage transducer and load compensator and a power system stabilizer (PSS). The exciter should give a dc power to the field winding in the synchronous generator. A load compensator is used to sense the desired voltage, and the voltage transducer rectifies the sensed voltage signal to DC quantity. The PSS task is to give additional damping to reduce the oscillations of the synchronous generator. Excitation systems can be put in three categories, DC excitation system, AC excitation system and Static excitation system [9]. The focus will be put on the Static excitation system.

Static excitation system get their power from the terminals where it is stepped down by a transformer, and then the power is fed to the synchronous generators field. There is thre different types of static excitation systems which is commonly used [9].

Compound-source rectifier system get its power from the current and the voltage at the generator terminals. A saturation limiter is used to control the output voltage. During a fault, with a larger voltage drop, the power is supplied from the terminal current [9].

Potential-source controlled-rectifier gets the power from the generator terminals. The power may also be supplied from an auxiliary bus. A rectifier then regulates and controls the power. Since the power is supplied from the terminals the ceiling voltage is reduced [9].

Compound controlled rectifier excitation system, the power is supplied from the generator stator. To provide the power from the stator is usually by current and voltage-derived sources which are compounded in the generator [9].

The ceiling voltage is the maximum voltage the excitation system can provide. Since static excitation system receives their power from the terminals of the transformer, the ceiling voltage is therefore defined by the terminal voltage and terminal current. The synchronous generators stability is usually improved with a higher ceiling voltage [9].

2.3.1 Excitation system per unit representation

During normal operation conditions the per unit values for the excitation system field voltage is very low, therefore it is usually referred to its own system. This system is referred to as the *"non-reciprocal per unit system"* in Power system

stability and control by Kundur [9].

To begin with, the machine is in open circuit condition, and therefore the currents I_d and I_q equals to zero. Equations 2.1 and 2.2 can therefore be written as in equations 2.19 and 2.20 [9].

$$e_d = -\Psi_q = -L_q i_q = 0 \tag{2.19}$$

$$e_q = \Psi_d = L_{ad} i_{fd} \tag{2.20}$$

The field current is determined by the mutual inductance L_{ad} and the terminal voltage, were the terminal voltage is 1.0 per unit. Substituting $E_t = e_q = 1.0$, allows equation 2.20 to be written as in equation 2.21 [9].

$$i_{fd} = \frac{1}{L_{ad}} \tag{2.21}$$

Equation 2.21 is expressed in per unit form. If the values were to be expressed in SI units, the denominator would be multiplied with ω_{base}. Expressed by per unit values, the field voltage can then be written as in equation 2.22 [9].

$$e_{fd} = R_{fd} i_{fd} = \frac{R_{fd}}{L_{ad}} \tag{2.22}$$

E_{fd} and I_{fd} in equations 2.23 and 2.24 is the *non-reciprocal per unit system*, and, e_{fd} and i_{fd} is the per unit system referred to the synchronous model [9].

$$I_{fd} = L_{ad} i_{fd} \tag{2.23}$$

$$E_{fd} = \frac{Lad}{R_{fd}} e_{fd} \tag{2.24}$$

When the synchronous generator is in steady state the field voltage and the field current has the same per unit value. However, as soon as a transient disturbance occurs the field voltage and field current per unit values differ [9].

2.4 Reactive power

With varying loads in the system will cause the reactive power to change. A synchronous generator will absorb reactive power when it is underexcited and produce reactive power when it is overexcited. The AVR providing the field current will control the field voltage depending on the reference voltage. Consequently, the armature voltage is also controlled [9].

Considering a simple system, with two sources, a receiving end and a sending end. Between the two sources there is a reactance X. A model of the figure can be observed in Figure 2.3. V_r is the voltage at the receiving end with the load angle equal to zero. V_s is the voltage at the sending end, with a load angle δ. The current flows from the sending end to the receiving end [9].

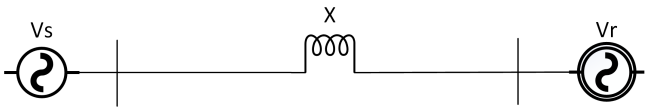

Figure 2.3: Figure of two sources, a sending end and a receiving end with a reactance in between.

The complex power, referred to the receiving can be observed in equation 2.25 [9].

$$S_r = P_r + jQ_r = V_r I^* V_r \left(\frac{V_s - V_r}{jX} \right) = V_r \left(\frac{V_s cos(\delta) + jV_s sin(\delta) - V_r}{jX} \right) \tag{2.25}$$

The active and the reactive power at the receiving end can be observed in equation 2.26 and 2.27 [9].

$$P_r = \frac{V_s V_r}{X} sin(\delta) \tag{2.26}$$

$$Q_r = \frac{V_s V_r cos(\delta) - V_r^2}{X} \tag{2.27}$$

While at the sending end the active and reactive power are as in equation 2.28 and 2.29 [9].

$$P_s = \frac{V_s V_r}{X} sin(\delta) \tag{2.28}$$

$$Q_s = \frac{V_s^2 - V_s V_r cos(\delta)}{X} \tag{2.29}$$

If the load angle δ is zero, the active power in both the sending and receiving end is zero. The reactive power in the sending end and the receiving end is then according to equation 2.31 and 2.30 [9].

$$Q_r = \frac{V_s V_r - V_r^2}{X} \tag{2.30}$$

$$Q_s = \frac{V_s^2 - V_s V_r}{X} \tag{2.31}$$

With a positive reactive power at the receiving end and the sending end, the voltage V_s larger then V_r, the reactive power flows from the sending end to the receiving end. The reactance X consumes a certain amount of reactive power determine by equation 2.32 [9].

$$Q_s - Q_r = \frac{(V_s - V_r)^2}{X} = XI^2 \tag{2.32}$$

If the voltages V_s and V_r are equal, and the load angle δ is different from zero. The active and reactive power can then be expressed as in equation 2.33 and 2.34 [9].

$$P_s = P_r = \frac{V^2}{X} sin(\delta) \tag{2.33}$$

$$Q_s = -Q_r = \frac{(V)^2}{X}(1 - cos(\delta)) = \frac{1}{2}XI^2 \tag{2.34}$$

The load angle δ determines the power flow in the model. When the load angle δ is greater then zero, the active power in both ends is positive. The active power flow, will then be from the sending end to the receiving end. If the load angle is negative, the active power flow will change to the opposite direction. The reactive power is produced by each end, were they each produce half of the reactive power consumed by X. The active power is determined by the voltage magnitude and the load angle δ. But since the voltage magnitude has to stay within a certain range, the load angle is used to control the active power [9].

Considering any value of voltage V_r, V_s and load angle δ. The current will then be as observed in equation 2.35 [9].

$$I = \frac{V_s cos(\delta) + jV_s sin(\delta) - V_r}{jX} \tag{2.35}$$

The reactance X consumes the reactive power determined by equation 2.36 [9].

$$Q_s - Q_r = \frac{V_s^2 + V_r^2 - 2V_s V_r cos(\delta)}{X} = \frac{XI^2}{X} = XI^2 \tag{2.36}$$

The reactive power consumed by the reactance X is XI^2, which is the loss of reactive power in the model. The reactive power is determined by the magnitude of the voltage and the end with the higher voltage magnitude produces the reactive power. Observing equation 2.37 and 2.38, an increase in the reactive power will cause an increase in the active power and the active and reactive power losses [9].

$$Q_{loss} = XI^2 = X\frac{P_r^2 + Q_r^2}{E_r^2} \tag{2.37}$$

$$P_{loss} = RI^2 = R\frac{P_r^2 + Q_r^2}{E_r^2} \tag{2.38}$$

2.5 Swing equation

The derivation of the swing equation was also covered in the project report [8], and will be repeated here.

The swing equation for the system is developed from the equation of motion. Were the difference in mechanical (T_m) and electrical torque (T_e), or acceleration (T_a) torque gives the inertia of the generator. The equation of motion can be observed in equation 2.39 [9].

$$J\frac{d\omega_m}{dt} = T_a = T_m - T_e \tag{2.39}$$

Equation 2.39 can be expressed in terms of per unit. It is common to use the constant H instead of J when per unit is used. The per unit inertia is expressed by equation 2.40 [9].

$$H = \frac{1J\omega_{base,m}^2}{2S_{base}} \tag{2.40}$$

Substituting the inertia constant J from equation 2.40 into equation 2.39 results in equation 2.41. The equation of motion which was introduced is now expressed in terms of per unit values [9].

$$2H\frac{d}{dt}\omega_{r,pu} = T_{m,pu} - T_{e,pu} \tag{2.41}$$

The rotor speed ω_r is the rotor velocity in electrical rad/s, and ω_0 is the rated value in electrical rad/s. The relation between the mechanical and electrical rad/s is shown in equation 2.42 [9].

$$\omega_{r,pu} = \frac{\omega_m}{\omega_{0,m}} = \frac{\frac{\omega_m}{p_f}}{\frac{\omega_0}{p_f}} = \frac{\omega_r}{\omega_0} \tag{2.42}$$

The position of the rotor with respect to the rotating field in the stator is given by the load angle δ. If the load angle has a reference point equal to δ_0 and the difference in rotating speed is given by $\omega_r - \omega_{base}$. The load angle can be expressed in terms of the rotating speed ω as observed in equation 2.43 [9].

$$\delta = \omega_r t - \omega_0 t + \delta_0 \tag{2.43}$$

The derivative of the equation 2.43 can be observed in equation 2.44 [9].

$$\frac{d\delta}{dt} = \omega_r - \omega_0 \tag{2.44}$$

Taking the double derivative of the load angle in equation 2.44 and substituting ω_r from equation 2.42 into equation 2.44 results in equation 2.45 [9].

$$\frac{d^2\delta}{dt^2} = \omega_0 \frac{d\omega_{r,pu}}{dt} \tag{2.45}$$

Inserting the rotor speed $\frac{d\omega_{r,pu}}{dt}$ from equation 2.45 into equation 2.41. The swing equation can now be expressed in terms of the load angle instead of the rotor speed as in equation 2.41. The swing equation in terms of load angle can be observed equation 2.46 [9].

$$\frac{2H}{\omega_0}\frac{d^2\delta}{dt^2} = T_{m,pu} - T_{e,pu} \tag{2.46}$$

2.6 Power Swings

This subsection will cover how the rotor swings is associated with the disconnection of one of the lines in case of a three-phase fault. Rotor swing was covered in the specialization project [8], without parallel connected lines. This section covers the rotor swing when a single line is discounted but power is still transferred through a second line.

In per unit the deviation of rotor speed is so small that the actual rotor speed may be assumed to be equal to ω_{base}. The per unit torque in the air gap may consequently be assumed to be equal to the power in the air gap. The swing equation 2.46 may then be expressed in terms of power as observed in equation 2.47 [9].

$$\frac{d^2\delta}{dt^2} = \frac{\omega_0}{2H}(P_{m,pu} - P_{e,pu}) \tag{2.47}$$

By multiplying equation 2.47 with $\frac{d\delta}{dt}$ on both, equation 2.48 is obtained [9].

$$\frac{d}{dt}(\frac{d\delta}{dt})^2 = \frac{\omega_0}{2H}(P_{m,pu} - P_{e,pu})\frac{d\delta}{dt} \tag{2.48}$$

and by integrating both sides of equation 2.48, equation 2.49 is obtained [9].

$$(\frac{d\delta}{dt})^2 = \int \frac{\omega_0}{2H}(P_{m,pu} - P_{e,pu})d\delta \tag{2.49}$$

For the system to be stable the deviation in rotor angle $\frac{d\delta}{dt}$ should be zero. Equation 2.50 will then describe the criterion for the system to be stable. δ_{max} is max load angle [9].

$$\int_{\delta}^{\delta_{max}} \frac{\omega_0}{2H}(P_{m,pu} - P_{e,pu})d\delta = 0 \tag{2.50}$$

The electrical power generated by the synchronous machine can be described by equation 2.51 [9].

$$P_e = \frac{E^{'}V_{grid}}{X_{tot}}sin(\delta) \tag{2.51}$$

$E^{'}$ is the internal transient voltage, V_{grid} is the voltage at the grid, X_{tot} is the total reactance in the model and δ is the load angle [9].

A representation of the model which is crated in Simulink can be observed in Figure 2.4. The reactance X_t is the step up transformer, $X_d^{'}$ is the transient reactance, line one is represented by $X_{line\,1}$ and line two is represented by $X_{line\,2}$.

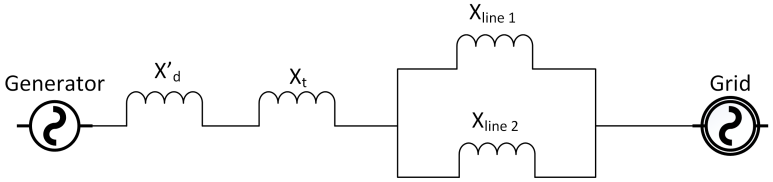

Figure 2.4: Figure of a generator connected to a step up transformer, through a parallel lines to a grid.

The total reactance in the model is expressed by equation 2.52. Line one and line two are assumed to have the same reactance, therefore the parallel connection can be represented as the half of one line reactance X_{line}.

$$X_{tot} = X_d^{'} + X_t + \frac{X_{line}}{2} \tag{2.52}$$

Figure 2.5 shows how Figure 2.4 can be represented, when a symmetrical three-phase fault occurs on line 1 with a distance "a" from the transformer terminals. The distance "a" is set in percentage. [10].

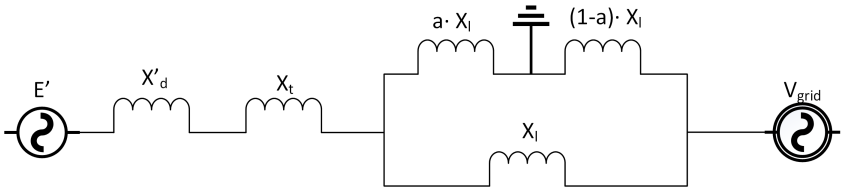

Figure 2.5: Figure of a generator connected to a step up transformer, through a parallel lines to a grid with a fault at a distance "a", in percentage, on line one.

The reactance on the parallel lines, and the grid voltage may be represented by a thevenin equivalent, pre fault, during the fault and post fault. The thevenin voltage and reactance during the fault can be observed in equation 2.53 and equation 2.54 [10].

$$X_{th} = \frac{aX_l \cdot X_l}{aX_l + X_l} = \frac{a}{1+a} X_l \tag{2.53}$$

$$V_{th} = \frac{aX_l}{aX_l + X_l} V = \frac{a}{1+a} V_{grid} \tag{2.54}$$

Pre fault and post fault the Thevenin voltage is equal to the voltage V_grid. While the thevenin reactance pre fault is $\frac{X_l X_l}{X_l + X_l}$. Post fault the thevenin reactance is X_l since line 1 is disconnected [10].

The electrical power from equation 2.51 can then be expressed as in equation 2.55.

$$P_e = \frac{E^{'} V_{th}}{X_d^{'} + X_t + X_{th}} sin(\delta) \tag{2.55}$$

When a three-phase fault occurs, there will be a decrease in the total reactance, however, the voltage V_{th} will decrease with a larger value, causing the peak value of the electrical power to decrease. The electrical power will then follow three curves, pre-fault by curve 1, during the fault by curve 3 and post fault by curve 2 in Figure 2.6. Pre fault, the load angle is set and stable at the operation point defined by $P_e = P_m$ at δ_1. As the fault occurs, the operation point drops to curve 3. The rotor will now accelerate since the electrical power is lower than mechanical power. Once the rotor has accelerated from the point defined by δ_1 to δ_2, were the fault is cleared and line 1 is isolated from the system, the operation point will now follow curve 2. The rotor will start to decelerate since the electrical power is larger than the mechanical power until it reaches δ_3, the blue shaded area absorbs the kinetic energy obtained from the red shaded area. Since the electrical power is greater than the mechanical power, the rotor will slowly decrease its speed to allow the load angle to settle at the operation condition satisfying $P_{e\,postfault} = Pm$. Without any damping in the system, the rotor will continue to oscillate with a constant amplitude around the operating point [9].

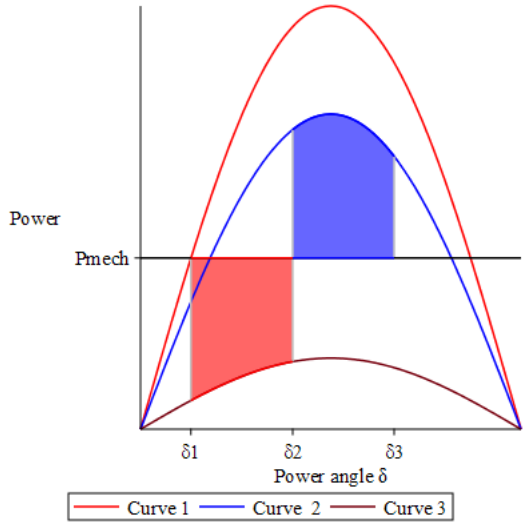

Figure 2.6: Figure of the power angle characteristics. Curve 1 is the electrical power pre fault, curve 2 is post fault, and curve 3 is during the fault.

The stability criteria is described by equation 2.50. Equation 2.56 describes the red area and 2.57 describes the blue area. For the system to be stable $A_{red} \leq A_{blue}$ [9].

$$\int_{\delta_1}^{\delta_2} \frac{\omega_{base}}{2H}(P_{m,pu} - P_{e,pu})d\delta = A_{red} \tag{2.56}$$

$$\int_{\delta_2}^{\delta_3} \frac{\omega_{base}}{2H}(P_{m,pu} - P_{e,pu})d\delta = A_{blue} \tag{2.57}$$

Chapter 3

The Simulink model

The fault ride-through is analysed using a model created in MATLAB Simulink. To simulate a fault ride-through the step up transformer is connected to parallel connected lines which again is connected to the grid. On one of these lines a three-phase fault will occur at a distance "a" from the step-up transformer. The voltage sensed by the AVR is 80% into the step up transformer. To save some simulation time the step-up transformer is added directly into the generator model. In the following section the simulation model will be explained. A figure of the model can be observed in Figure 3.1.

The simulation model will be similar to a Powerformer. Since the generator cannot supply the higher voltage required by the transmission lines a step-up transformer is connected to the generator to step the voltage up to the required voltage level of the transmission system. But in a Powerformer the step-up transformer is implemented into the generator [11].

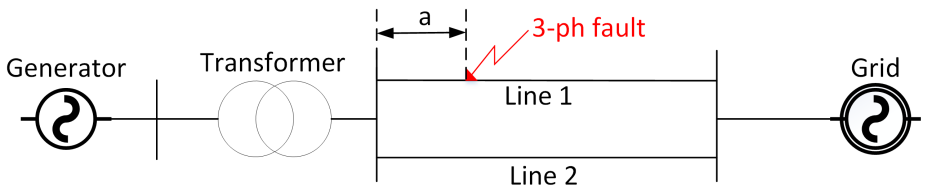

Figure 3.1: Illustration of the model which is created in MATLAB Simulink

3.1 The generator parameters

Before explaining how the model was created in Simulink the generator parameters will presented. The parameters used for the generator was can be observed in Table 3.1.

Apparent power	*S* [VA]	145
Active Power	*P* [W]	125
Reactive power	*Q* [VAr]	74
Voltage	*U* [kV]	15
Power factor	$cos\phi$	0.86
Frequency	*F* [Hz]	50
Inertia	*H* [s]	2.04
Rpm	*n* [rpm]	500
Pole pairs	*Pp*	12
Stator resistance	*R* [p.u]	0.0018
Leakage reactanc	X_l [p.u]	0.16
Synchronous direct reactance - unsaturated	X_d [p.u]	1.29
Transinet direct reactance - unsaturated	$X_d^{'}$ [p.u]	0.29
Subtransient direct reactance - unsaturated	$X_d^{''}$ [p.u]	0.21
Synchronous quadr. reactance - unsaturated	X_q [p.u]	0.83
Subtransient quadr. reactance - saturated	$X_q^{''}$ [p.u]	0.20
No load open circuit tdirect axis time constant	$T_{do}^{'}$ [s]	10.8
Transient direct axis time constant	$T_d^{'}$ [s]	2.15
Subtransient direct axis time constant	$T_d^{''}$ [s]	0.08
Subtransient quadr. axis time constant	$T_q^{''}$ [s]	0.09

Table 3.1: Table over the parameters used in the generator model in Simulink.

3.2 Adding the step-up transformer and calculating the generator terminal voltage

Because the step-up transformer is added into the generator model in Simulink. The measured voltage of the terminals will be at the high voltage (HV) side of the transformer. In order to measure the voltage 80% into the step up transformer the d- and q- axis equivalent circuits in Figure 2.1 and 2.2 was used to calculated the required voltage. The related equations to the d- and q-axis equivalent circuits in equation 2.1 and equation 2.2. [9].

Adding the step-up transformer into the model is done by adding it to the leakage inductance. This results in a new set of parameters, as observed in equation 3.3. All values used in the simulation model is in per unit.

$$L_{l\,new} = L_l + L_t \tag{3.1}$$

However since the d- and q- axis reactances is a part of the leakage inductance, as observed in equation 3.2, they will also have the step up transformer included in them. The new set of d- and q- axis reactances can be observed in equation 3.3.

$$L_d = L_{ad} + L_{l\,new} \tag{3.2}$$

$$
\begin{aligned}
L_{d\,new} &= L_d + L_t \\
L^{'}_{d\,new} &= L^{'}_d + L_t \\
L^{''}_{d\,new} &= L^{''}_d + L_t \\
L_{q\,new} &= L_q + L_t \\
L^{''}_{q\,new} &= L^{''}_q + L_t
\end{aligned}
\tag{3.3}
$$

The output voltage measured on the generator in the Simulink model is V_d and V_q observed in Figure 3.2 and 3.3. Since the step-up transformer is added in series with the generator parameters. The terminal voltage can be derived from the d- and q-axis voltage. Using equation 2.4 and 2.5 and substituting L_l for $L_{l\,new}$ from equation 3.3, the flux in the d- and q- axis can be represented by equation 3.4 and equation 3.5.

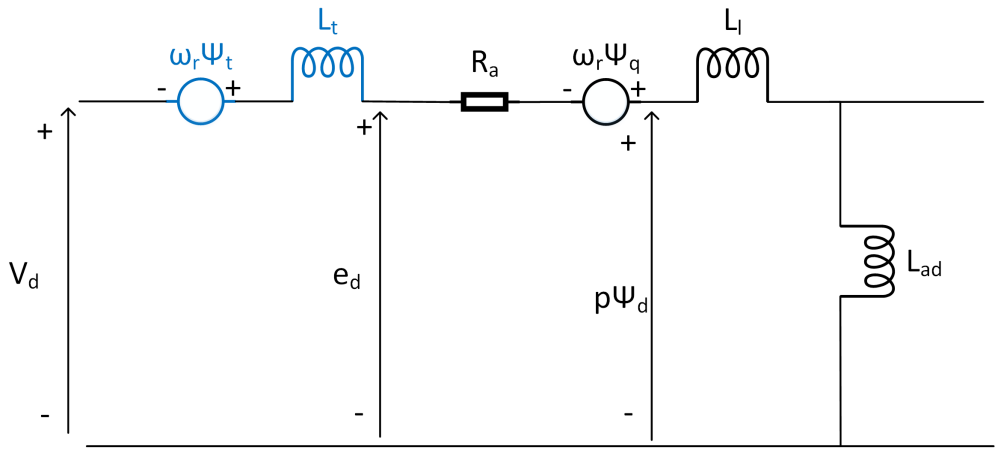

Figure 3.2: Figure of the d-axis equivalent circuit including the step-up transformer. The parameter p in the model represents the derivative term $\frac{d}{dt}$.

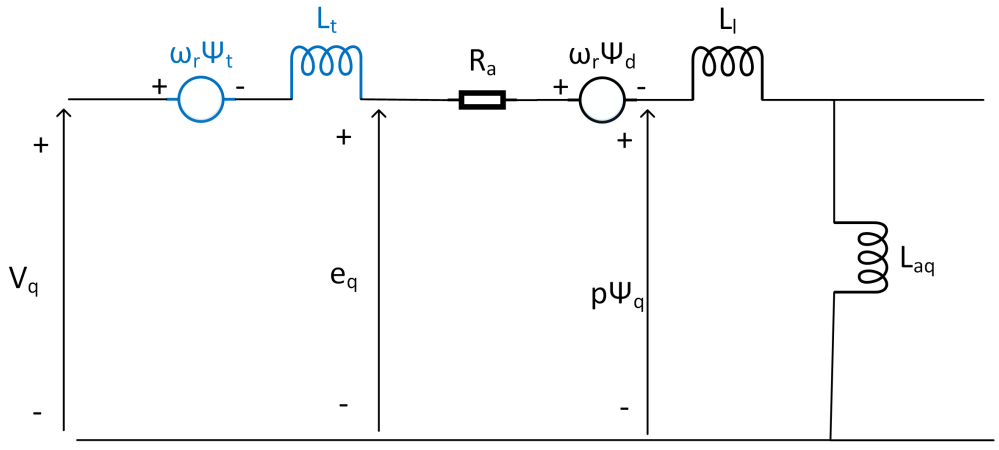

Figure 3.3: Figure of the q-axis equivalent circuit including the step-up transformer. The parameter p in the model represents the derivative term $\frac{d}{dt}$.

$$\Psi_d = -(L_{ad} + L_l + L_t)i_d + L_{ad}i_{fd} + L_{ad}i_{1d} \tag{3.4}$$

$$\Psi_q = -(L_{aq} + L_l + L_t)i_q + L_{aq}i_{1q} + L_{aq}i_{2q} \tag{3.5}$$

Inserting equation 3.4 and equation 3.5 into the d- and q- axis voltage equations 2.1 and 2.2 results in equations 3.6 and 3.7.

$$\begin{aligned} V_d = \frac{d}{dt}[-(L_{ad} + L_l + L_t)i_d + L_{ad}i_{fd} + L_{ad}i_{1d}] \\ -[-(L_{aq} + L_l + L_t)i_q + L_{aq}i_{1q} + L_{aq}i_{2q}]\omega_r - R_a i_d \end{aligned} \tag{3.6}$$

$$\begin{aligned} V_q = \frac{d}{dt}[-(L_{aq} + L_l + L_t)i_q + L_{aq}i_{1q} + L_{aq}i_{2q}] \\ +[-(L_{ad} + L_l + L_t)i_d + L_{ad}i_{fd} + L_{ad}i_{1d}]\omega_r - R_a i_q \end{aligned} \tag{3.7}$$

Equations 3.6 and 3.7 consist of the voltage drop across the step up transformer and the voltage at the terminals e_d and e_q from equations 2.1 and 2.2. Expanding equations 3.6 and 3.7 to isolate the terms related to the step up transformer results in equations 3.8 and 3.9.

$$\begin{aligned} V_d = -L_t\frac{d}{dt}i_d + i_q L_t\omega_r + \frac{d}{dt}[-(L_{ad} + L_l)i_d + L_{ad}i_{fd} + L_{ad}i_{1d}] \\ -[-(L_{aq} + L_l)i_q + L_{aq}i_{1q} + L_{aq}i_{2q}]\omega_r - R_a i_d \end{aligned} \tag{3.8}$$

$$\begin{aligned} V_q = -L_t\frac{d}{dt}i_d - i_q L_t\omega_r + \frac{d}{dt}[-(L_{aq} + L_l)i_q + L_{aq}i_{1q} + L_{aq}i_{2q}] \\ +[-(L_{ad} + L_l)i_d + L_{ad}i_{fd} + L_{ad}i_{1d}]\omega_r - R_a i_q \end{aligned} \tag{3.9}$$

Observing equations 3.8 and 3.9 the last terms is the voltage at the terminals, e_d and e_q from equations 2.1 and 2.2. Inserting the voltages e_d and e_q into equations 3.8 and 3.9, the d- and q- axis voltage at the terminals can be expressed as in equation 3.10 and equation 3.11.

$$e_d = V_d - \omega_r L_t i_q + L_t\frac{d}{dt}i_d \tag{3.10}$$

$$e_q = V_q + \omega_r L_t i_d + L_t\frac{d}{dt}i_q \tag{3.11}$$

Since the model chosen in Simulink works with per unit values the derivative terms in equations 3.10 and 3.11 has to be divided by $\omega_0 = 2\pi 50$. The values for $i_d,\ i_q,\ V_d,\ V_q$ and ω_r are all measured units.

To measure the correct voltage, 80% in on the step-up transformer, the parameter L_t is multiplied with 0,2. L_t is multiplied with 0,2 because the calculation is done in reverse, from the high-voltage side of the transformer towards the terminal voltage of the generator.

A figure of the complete calculation done in MATLAB Simulink can be observed in Figure 3.4.

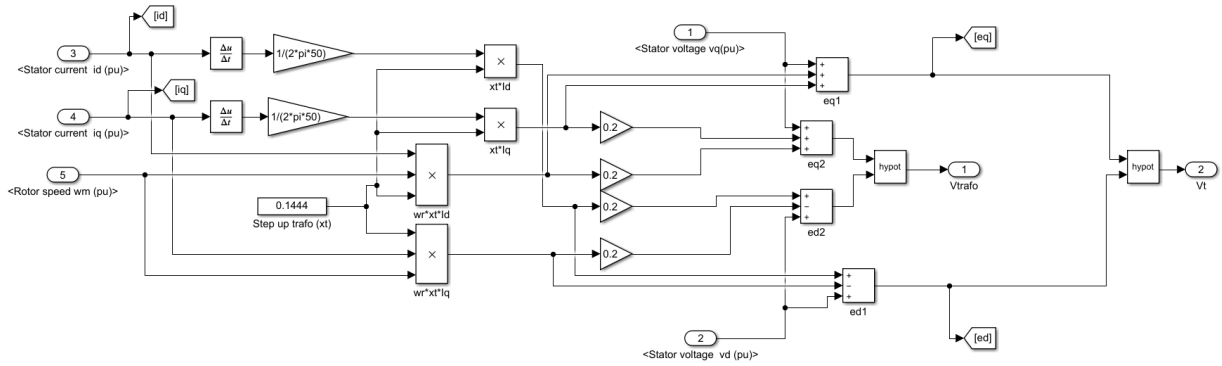

Figure 3.4: A figure of the calculated voltage in Simulink.

3.3 The new transient and subtransient d-axis time constants

As a consequence of adding the step-up transformer into the generator model, the sub-transient and transient time constants has to be recalculated. In the following chapter the time constants in chapter 2.2 will be used. Observing equation 3.12 and 3.13, the leakage inductance is a part of the time constants. Therefore the time constants $T_d^{'}$ and $T_d^{''}$ has to be recalculated introducing the inductance from the step-up transformer in the leakage inductance L_l. L_{pl} is usually a part of the equations, but is set to zero and therefore not present [9].

$$T_d^{'} = \frac{1}{R_{fd}}(L_{fd} + \frac{L_{ad}L_l}{L_{ad} + L_l}) \tag{3.12}$$

$$T_d^{''} = \frac{1}{R_{1d}}(L_{1d} + \frac{L_l L_{fd} L_{ad}}{L_{fd}L_{ad} + L_{fd}L_l + L_{ad}L_l}) \tag{3.13}$$

In order to calculate the new time constants, R_{fd}, L_{fd}, R_{1d} and L_{1d} is first required. To find these values, equations 3.14 to 3.17 is derived with respect to R_{fd}, L_{fd}, R_{1d} and L_{1d} [9].

$$L_d^{'} = L_l + \frac{L_{ad}L_{fd}}{L_{ad} + L_{fd}} \tag{3.14}$$

$$T_{d0}^{'} = \frac{L_{ad} + L_{fd}}{R_{fd}} \tag{3.15}$$

$$L_d^{''} = L_l + \frac{L_{ad}L_{fd}L_{1d}}{L_{ad}L_{fd} + L_{ad}L_{1d} + L_{fd}L_{1d}} \tag{3.16}$$

$$T_{d0}^{''} = \frac{1}{R_{1d}}(L_{1d} + \frac{L_{fd}(L_{ad})}{L_{fd} + L_{ad}}) \tag{3.17}$$

The resulting equations used to calculated R_{fd}, L_{fd}, R_{1d} and L_{1d} can be observed in equation 3.18 to equation 3.21.

$$L_{fd} = \frac{L_{ad}(L_d^{'} - L_l)}{L_{ad} - L_d^{'} + L_l)} \tag{3.18}$$

$$R_{fd} = \frac{L_{ad} + L_{fd}}{T_{d0}^{'}} \tag{3.19}$$

$$L_{1d} = \frac{-L_{ad}L_{fd}(L_d^{''} - L_l)}{L_{ad}L_d^{''} - L_{ad}L_{fd} - L_l L_{ad} + L_d^{''}L_{fd} - L_l L_{fd}} \tag{3.20}$$

$$R_{1d} = \frac{L_{ad}L_{1d} + L_{fd}L_{1d} + L_{ad}L_{fd}}{T_{d0}^{''}(L_{ad} - L_{fd})} \tag{3.21}$$

Substituting $L_{l\,new}$ from equation 3.3 for L_l in equation 3.12 and 3.13. The new time constants were the step-up transformer is included, is obtained from equation 3.22 and equation 3.23.

$$T_d^{'} = \frac{1}{R_{fd}}(L_{fd} + \frac{L_{ad}L_{l\,new}}{L_{ad} + L_{l\,new}}) \tag{3.22}$$

$$T_d^{''} = \frac{1}{R_{1d}}(L_{1d} + \frac{L_{l\,new}L_{fd}L_{ad}}{L_{fd}L_{ad} + L_{fd}L_{l\,new} + L_{ad}L_{l\,new}}) \tag{3.23}$$

3.3.1 Calculating the new d-axis time constants

In the following sub chapter the d-axis transient and subtransient time constants will be calculated with the equations derived in chapter 3.3. Table 3.1 contains the necessary parameters to do the calculations.

Since the calculations is done in per unit values, the time constants $T_{d0}^{'}$ and $T_{d0}^{''}$ has to be converted from seconds to per unit values. This is done by multiplying them with $2\pi 50$. The conversion of $T_{d0}^{'}$ to per unit can be observed in equation 3.24. Since $T_{d0}^{''}$ is not given, it is calculated, this is done by using equation 2.17. To obtain $T_{d0}^{''}$ in seconds the sub-transient time constant is first converted to per unit in equation 3.25, then $T_{d0}^{''}$ is calculated with equation 3.26.

$$T_{d0}^{'} = 10.8 \cdot 2\pi 50 = 3392.92 \tag{3.24}$$

$$T_d^{''} = 0.08 \cdot 2\pi 50 = 25.1327 \tag{3.25}$$

$$\frac{25.1327 \cdot 0.29}{0.21} = 34,7071 \tag{3.26}$$

First equations 3.18 to 3.21 is used to calculated L_{fd}, R_{fd}, L_{1d} and R_{1d}.

L_{fd} is calculated with equation 3.27

$$\frac{1.13(0.29 - 0.16)}{1.13 - 0.29 + 0.16)} = 0.1469 \tag{3.27}$$

R_{fd} is calculated with equation 3.28

$$\frac{1.13 + 0.1469}{3392.92} = 0.0003763 \tag{3.28}$$

L_{1d} is calculated with equation 3.29

$$\frac{-1.13 \cdot 0.1469 \cdot (0.21 - 0.16)}{1.13 \cdot 0.21 - 1.13 \cdot 0.1469 - 0.16 \cdot 1.13 + 0.21 \cdot 0.1469 - 0.16 \cdot 0.1469} = 0.08125 \tag{3.29}$$

R_{1d} is calculated with equation 3.30

$$\frac{1.13 \cdot 0.08125 + 0.1469 \cdot 0.08125 + 1.13 \cdot 0.1469}{11.0476 \cdot (1.13 - 0.1469)} = 0.006086 \tag{3.30}$$

Since L_{fd}, R_{fd}, L_{1d} and R_{1d} is now obtained, the new time constants can be calculated with equations 3.22 and equation 3.23.

$$T_d^{'} = \frac{1}{0.0003763}(0.1469 + \frac{1.13 \cdot 0.3044}{1.13 + 0.3044}) = 1027.5268[p.u] \tag{3.31}$$

Converting $T_d^{'}$ back to seconds by dividing by $2\pi 50$ gives 3,27 [s].

$$T_d^{''} = \frac{1}{0.006086}(0.08125 + \frac{0.3044 \cdot 0.1469 \cdot 1.13}{0.1469 \cdot 1.13 + 0.1469 \cdot 0.3044 + 1.13 \cdot 0.3044}) = 28.3153 \tag{3.32}$$

Converting $T_d^{''}$ back to seconds by dividing by $2\pi 50$ gives 0,0901 [s].

3.4 The excitation system

In the model a PI regulator is used as the regulator. For a PI regulator the steady state error is zero, and therefore the regulator is required to have a fast response and good damping. A good damping and fast response is achieved with a large phase-margin and open loop bandwidth. Tuning the PI regulator is done with the generator in no load. The correspodning transfer function for the synchronous machine is achieved from equation 3.33 [12].

$$\frac{d}{dt}E_q^{'} = \frac{1}{T_{d0}^{'}}(E_{fd} - E_q^{'} - (x_d - x_d^{'})I_d) \tag{3.33}$$

In no load $E_q^{'}$ equals to the terminal voltage and I_d is set equal to zero. By further deriving equation 3.33 with respect to the terminal voltage, V_t divided by the input voltage $E_f d$, equation 3.36 then is obtained [12].

$$\frac{d}{dt}V_t = \frac{1}{T_{d0}^{'}}(E_{fd} - Vt) \tag{3.34}$$

$$V_t(\frac{d}{dt}T_{d0}^{'} + 1) = E_{fd} \tag{3.35}$$

$$\frac{V_t}{E_{fd}} = \frac{1}{(\frac{d}{dt}T_{d0}^{'} + 1)} \tag{3.36}$$

Setting $\frac{d}{dt} = s$ and $\frac{Vt}{E_{fd}} = H_{gen}(s)$ equation 3.37 is obtained, which represents the transfer function for the synchronous generator in no load [12].

$$H_{gen}(s) = \frac{1}{(sT'_{d0} + 1)} \tag{3.37}$$

Equation 3.38 is the transfer function for the PI regulator for the excitation system [13].

$$H_{PI}(s) = K_{pr} + \frac{K_{ir}}{s} \tag{3.38}$$

The block diagram used to tune the system can be observed in Figure 3.5 [12].

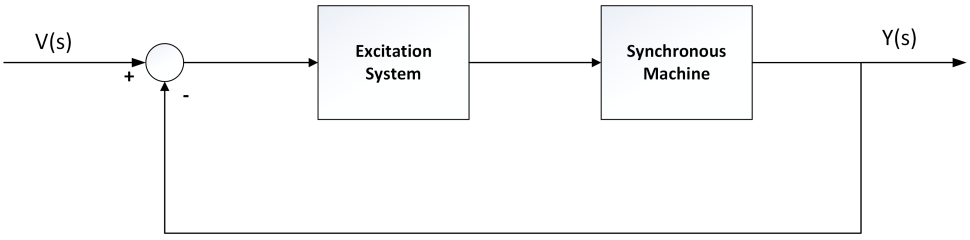

Figure 3.5: Block diagram of the excitation system and the synchronous machine

The open loop transfer function related to Figure 3.5 can be observed in equation 3.42. Equation 3.39 to 3.41 shows the derivation of the closed loop transfer function.

$$(V(s) - Y(s))H_{PI}(s)H_{gen}(s) = H_{PI}(s)H_{gen}(s)Y(s) \tag{3.39}$$

$$V(s)H_{PI}(s)H_{gen}(s) = Y(s)(1 + H_{PI}(s)H_{gen}(s)) \tag{3.40}$$

$$\frac{Y(s)}{V(s)} = \frac{H_{PI}(s)H_{gen}(s)}{1 + H_{PI}(s)H_{gen}(s)} \tag{3.41}$$

Were the open loop transfer function is given by the second term in the denominator $H_{PI}(s)H_{gen}(s)$. [13]

$$H_{CL}(s) = \frac{H_{PI}(s)H_{gen}(s)}{1 + H_{OL}(s)} \tag{3.42}$$

The PI regulator was tuned according to the recommendations given by Kundur [9] and [14]. The parameters the tuning was set according to can be observed Table 3.2.

Gain Margin	$\geq$	6 dB
Phase Marign	$\geq$	40°
Overshoot	=	(5 - 15)%

Table 3.2: Table of the parameters the tuning was done after.

Tuning the regulator the closed loop is used to plot the step response and the bode diagram, and the open loop is also used for the bode plot [14]. The tuning gave a proportional gain of 200 and the integral gain of 900. For the step response, in Figure 3.6, gave an overshoot of 12.91%. The closed loop response, observed in Figure 3.7, in the bode diagram gave an phase lag of -57 ° at -3 dB. For the open loop response in the bode diagram, observed in Figure 3.8, the phase lag was observed at $-103°$. The corresponding gain margin was "inf" and the phase margin was $77°$.

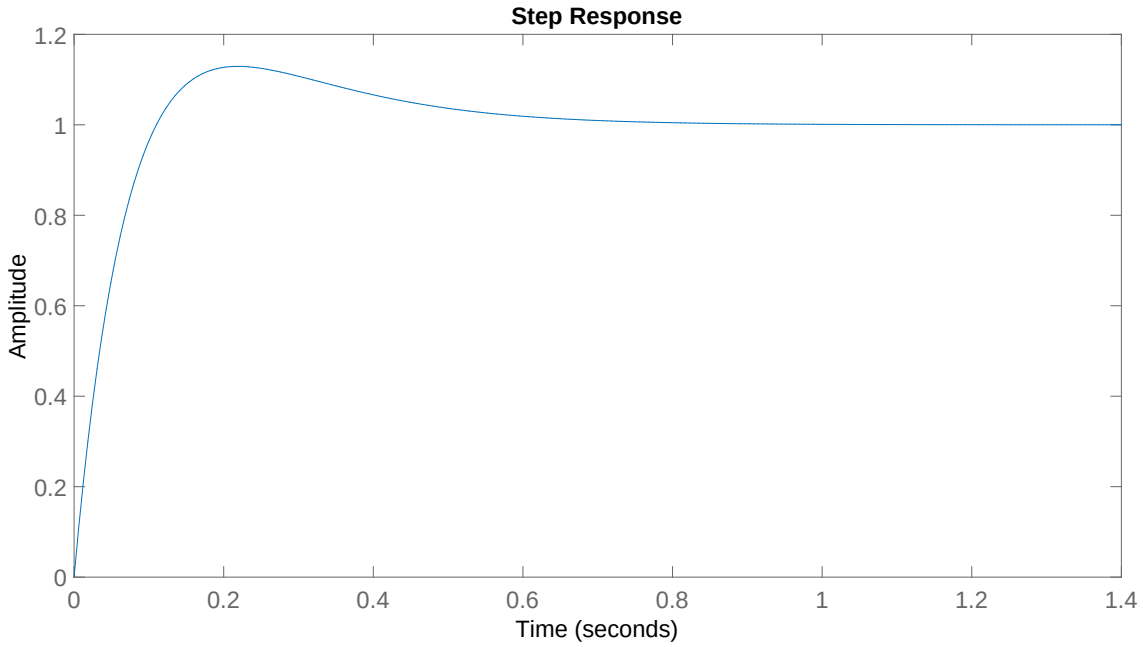

Figure 3.6: Figure of the step response with a proportional gain of 200 and integral gain of 900.

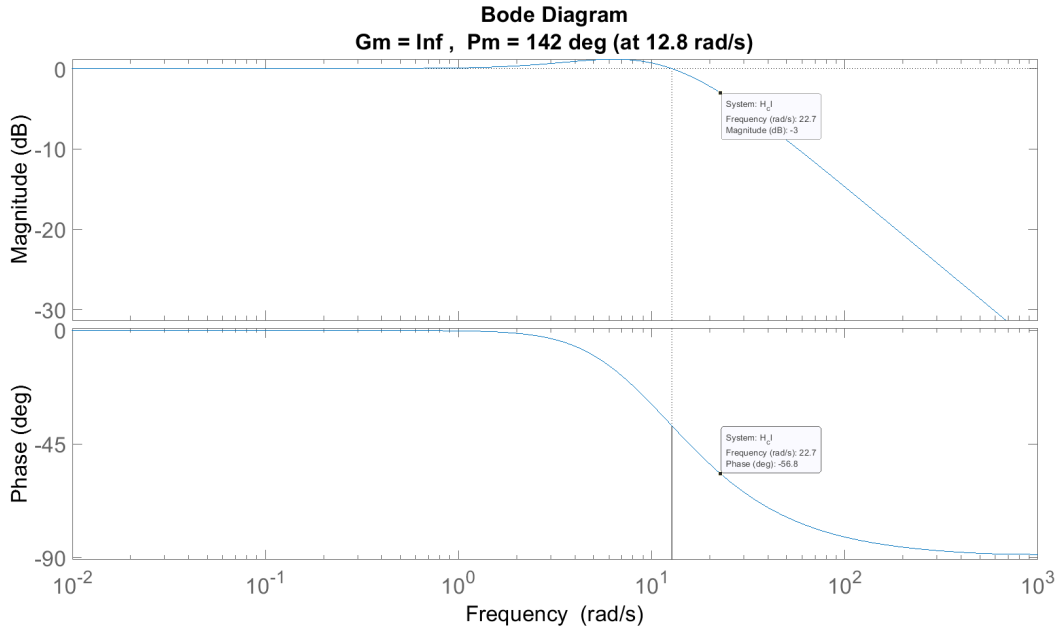

Figure 3.7: Figure of the closed loop bode plot with a proportional gain of 200 and integral gain of 900.

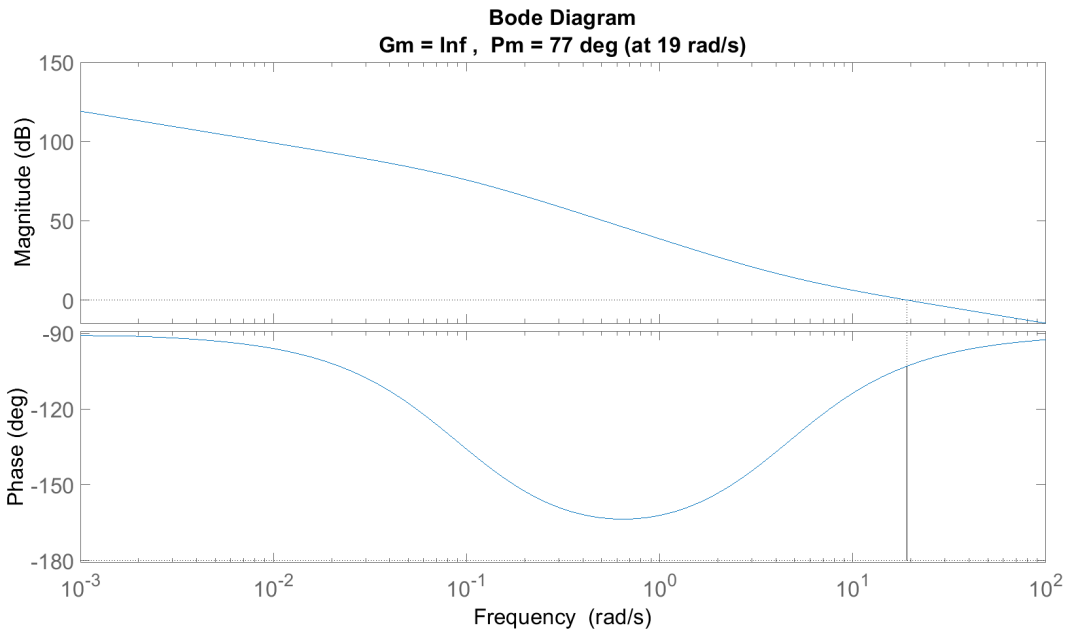

Figure 3.8: Figure of the open loop bode plot with a proportional gain of 200 and integral gain of 900.

3.5 Saturation, voltage transducer and wind up

The saturation is set to the ceiling voltage for the model. The terminal voltage depends on the field current, and the field current depends on the field voltage [15]. As mentioned in Chapter 2.3, a static excitation system receives its power from the terminals of the generator. Therefore during the fault, the field voltage will be restricted by the terminals voltage [9]. In the model the terminal voltage is multiplied with a ceiling factor of 2 for the upper and lower saturation [1].

The voltage entering the excitation system is usually rectified to DC voltage before entering the rotor. However when modelling a time constants is usually used to filter the signal. This time constant (T_r) is set according to the signal sensed [9]. In this case the signal is of 50 Hz, the time constant is therefore set to 0.02 seconds. The sensed voltage is multiplied with the transducer and the output is the measured voltage used for the PI regulator. The transfer function used can be observed in equation 3.43 [9].

$$H_{tr}(s) = \frac{1}{1 + T_r s} \tag{3.43}$$

A figure of the PI- regulator created in MATLAB Simulink can be observed in Figure 3.9. What can be observed is the voltage transducer connected in series with the voltage V_c which is the sensed voltage in the step-up transformer. V_t is the measured voltage on the terminals which is multiplied with a ceiling factor of 2. K_{pr} is the proportional gain and K_{ir} is the integral gain.

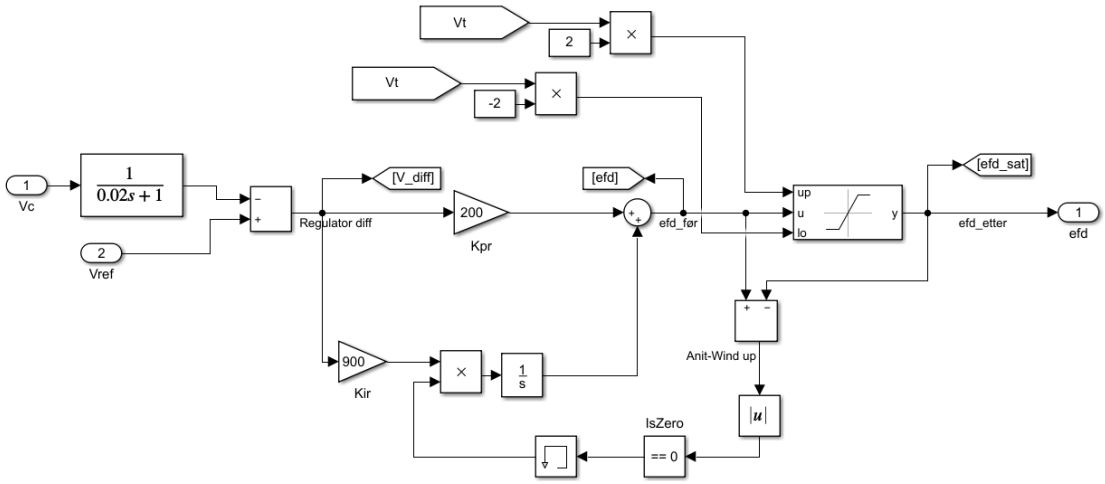

Figure 3.9: A figure of the PI regulator, with voltage transducer and saturation, created in MATLAB Simuink.

Anti- windup is used for integrals to prevent the integration after a certain limit is met [13]. In the model the limit used is the saturation limt. In Figure 3.9 the set-up for the anti-wind up is also shown. The anti-wind up measures the difference in the value before and after the saturation. If the value before the saturation should be higher then what is after the saturation the integral is multiplied with zero to turn it off.

3.6 Connecting to the grid

The model will be simulated with parallel connected lines between the step-up transformer and the grid. On one of those lines there will be a three-phase fault. The three phase fault will be adjusted with a parameter, "a", from the step up transformer, this parameter represents the distance in percentage of the line. The distance parameter "a" is illustrated in Figure 3.1.

The fault will be moved with the distance "a", but the lines will also be simulated with three different line inductances. In this case since there is two parallel lines, they can be represented by thevenin equivalent, explained in chapter 2.6, X_{th}. This Thevenin equivalent will be changed from a per unit value of 0.05, to 0.1 and 0.15. The inductance value in SI unites are given in Table 3.3.

$\mathbf{X_{th}}$ [p.u]	$\mathbf{X_L}$ [p.u]	L_{line} **[mH]**
0.05	0.1	0.24696
0.1	0.2	0.49393
0.15	0.3	1.5

Table 3.3: Table of the inductance values in SI and p.u values of the thevenin equivalent and the lines.

The thevenin equivalent X_{th} is the parallel connection of the lines between the step-up transformer and the grid. The actual value, per line, is therefore calculated from equation 3.44. Each line is assumed to have the same inductance, X_L.

$$X_{th} = \frac{X_L^2}{X_L + X_L} = \frac{X_L}{2} \tag{3.44}$$

To adjust the fault distance, two inductances is connected in series. The series inductance in the fault line is therefore simulated as in equation 3.45. The distance "a" will be adjusted in six steps from 0 to 100. The chosen distance of "a" is consequently, 0, 20, 40, 60, and 100. The faulty line can therefore divided into two reactances as described by equation 3.45. A figure of the model in Simulink can be observed in Figure 3.10.

$$X_{faulty\,line} = X_L a + X_L(1-a) \tag{3.45}$$

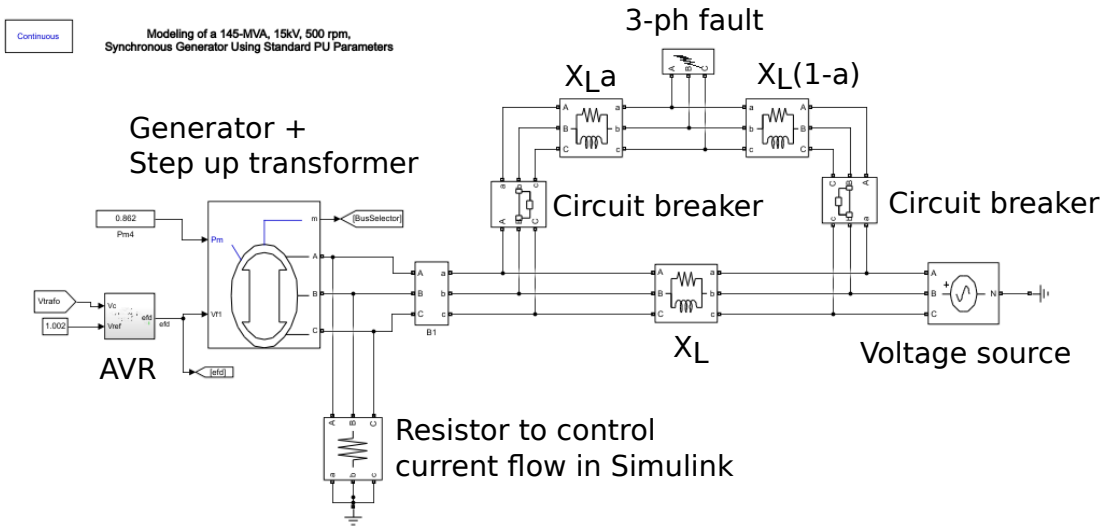

Figure 3.10: A figure of the model created in simulation in Simulink

Chapter 4

Fault Ride-Through Requirements

The master thesis will follow the fault ride-through requirements described by Statnett. The document is called *"Nasjonal Veileder for Funksjonskrav i kraftsystemet 2020"* (NVF 2020), which describes the voltage profile a synchronous generator should meet. However, in this chapter, the FRT requirement from both NVF 2020 [1] and FIKS 2012 [7] will be mentioned. The term fault ride-through is the capability of the synchronous machine to stay connected to the grid in case of a voltage drop. In NVF 2020, the FRT requirement given depends on the synchronous generator. The generators are divided into Type A, B, C, and type D generator. Where the type depends on the active power output. The four generator categories can be observed in Table 4.1 [1]. The FRT-requirement described in FIKS 2020 is dependent on the operation voltage, an operation voltage U < 220 [kV] or U $\geq$ 220 [kV].

Type	**Active power output**
A	0,8 [kW] $\leq P_{max}$ <1,5 [MW]
B	1,5 [MW] $\leq P_{max}$ <10 [MW]
C	10 [MW] $\leq P_{max}$ <30 [MW]
D	$P_{max} \geq$ 30 [MW] and $U_n \geq$ 110 [kV]

Table 4.1: Table of the 4 generator categories described in NVF 2020 [1]

The requirement given for FRT considers a symmetrical three-phase fault. Table 4.2 and Figure 4.1 describes the FRT requirement from NVF 2020 for type A, B, C and D generator connected to a voltage below 110 [kV] [1] and from FIKS for generators with an operation voltage below 220 [kV] [7]. In NVF the pre-fault voltage is at 1,0 [p.u], while at 1,0 [s] the fault occurs. The voltage then drops to 0,3 [p.u] for 150 [ms], where the fault is cleared and the voltage jump to 0,7 [p.u]. The voltage then recovers to 0,9 [p.u] after another 850 [ms][1]. In FIKS 2012 the pre-fault voltage is 1,0 [p.u], at 1 second the fault occurs and drops to 0,15 [p.u]. After 400 [ms] the fault is cleared and the voltage recovers to 0,85 [p.u] after another 600 [ms]. The voltage will then recover to 0,9 [p.u] 9 seconds after the fault [7].

NVF 2020		FIKS 2012	
Time in seconds	**Voltage in per unit**	**Time in seconds**	**Voltage in per unit**
1	1	1	1
1	0.3	1	0.15
1.150	0.3	1.4	0.15
1.150	0.7	2	0.85
2	0.9	10	0.9

Table 4.2: Table of the FRT requirement described in NVF 2020 and FIKS 2012. NVF 2020 is for type A, B, C, and D generators connected to a voltage below 110 [kV]. FIKS 2012 is for operation voltage below 220 [kV].

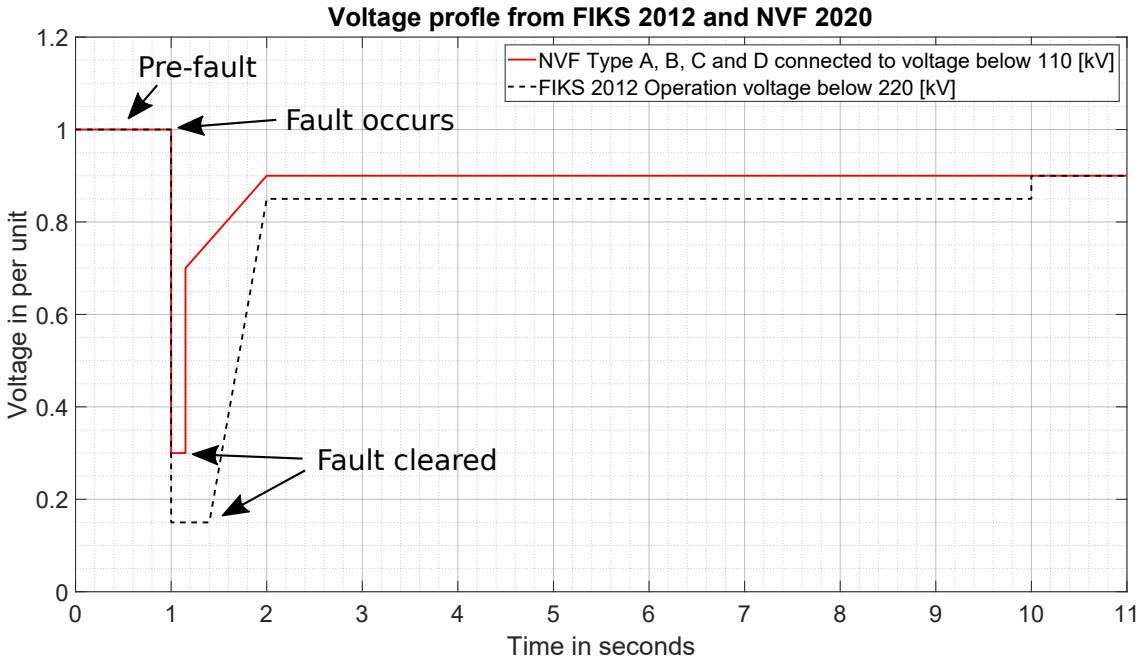

Figure 4.1: Figure of the voltage profile described in the document NVF 2020 and FIKS 2012. NVF 2020 is for type A, B, C, and D generators connected to a voltage below 110 [kV]. FIKS 2012 is for operation voltage below 220 [kV].

The FRT requirement from NVF 2020 for type D generators connected to a voltage at or above 110 [kV], and the FRT requirement from FIKS 2012 with an operation voltage at or above 220 [kV] is described in Table 4.3 and Figure 4.2. Pre-fault, the voltage is at 1,0 [p.u]. When the fault occurs at 1 [ms] the voltage drops to 0 [p.u]. The fault is then cleared at 1,150 [ms] were the voltage jumps to 0,25 [p.u]. After another 850 [ms] the voltage should recover to 0,9 [p.u] [1] [7].

NVF 2020		FIKS 2012	
Time in seconds	**Voltage in per unit**	**Time in seconds**	**Voltage in per unit**
1	1	1	1
1	0	1	0
1.150	0	1.150	0
1.150	0.25	1.150	0
2	0.9	2	0.9

Table 4.3: Table of the FRT requirement described in NVF 2020 and FIKS 2012. NVF 2020 is for type D generators connected to a voltage at 110 [kV] or above. FIKS 2012 is for operation voltage at 20 [kV] or above.

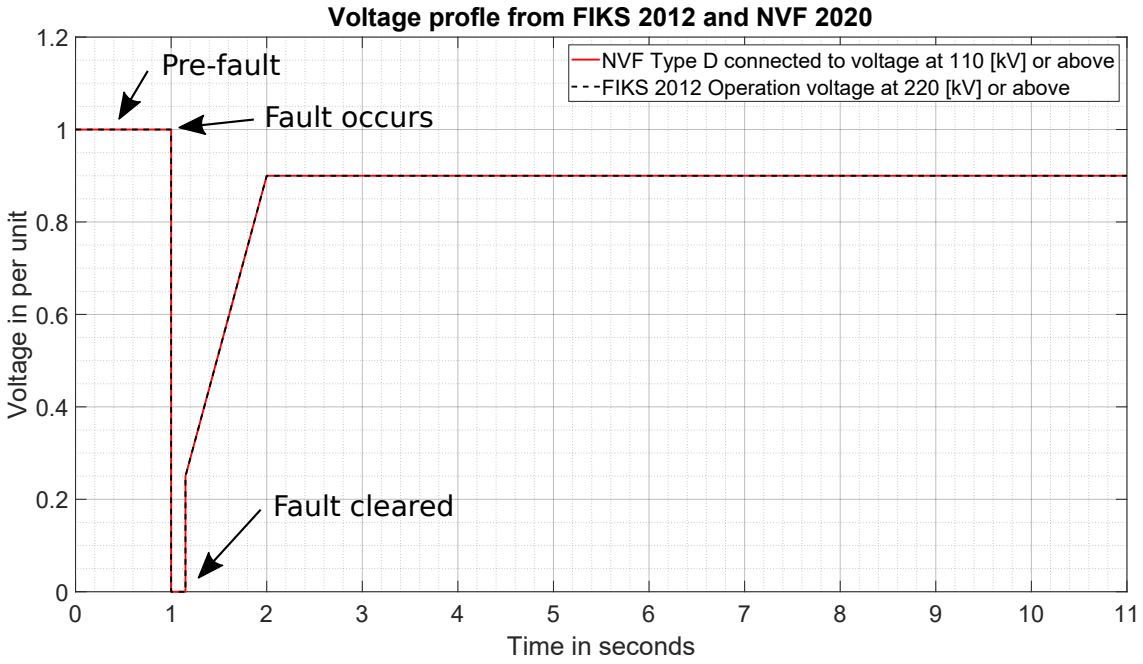

Figure 4.2: Figure of the voltage profile described in the document NVF 2020 and FIKS 2012. NVF 2020 is for type D generators connected to a voltage at 110 [kV] or above. FIKS 2012 is for operation voltage at 20 [kV] or above.

NVF 2020 also describes a set of pre-fault operation conditions for the synchronous generator before and after the fault. These conditions can be observed in Table 4.4[1]. For short-circuit power, the task will use a reference value, which is described in section 5.2.

Operation condition	**Prerequisite**
Active power before and after the fault	P = Pmax
Reactive power before the fault	Q = 0 (referred to POC)
Short circui-current and short circuit-power before and after the fault	$I_k = I_{k,min}$ and $S_{sc} = S_{sc,min}$

Table 4.4: Table of the pre-fault operation conditions for a synchronous generator [1].

NVF 2020 also mentions that if the generator is able to keep the voltage within the described voltage profile, but

synchronism is lost because of low short-circuit power, meaning the clearing time of the fault is larger then the critical clearing time. The short-circuit power can be increased until synchronism is kept [1].

Chapter 5

Case representation

The model used for the simulation was described in chapter 3. A total of six cases will be simulated, were each of them will have a distance parameter "a" with six values. The six cases consists of three different line inductances and each of them will be simulated with a reactive power of zero and maximum reactive power output. The automatic voltage regulator (AVR) used for the synchronous generator is a PI regulator as described in chapter 3.4, there is no power system stabilizer (PSS) used in the simulations. The genenrator parameters can be observed in Table 3.1 with the updated d-axis time constants in Table 5.1.

5.1 Model description

Instead of applying the fault at POC as mentioned in NVF 2020 [1], the model is extended with two parallel connected lines. The fault will then be applied on one of the lines with a fault distance given by the parameter "a". The model used for the simulation can be observed in Figure 5.1. The transformation ratio on the step-up transformer is $\frac{15[kV]}{70[kV]}$.

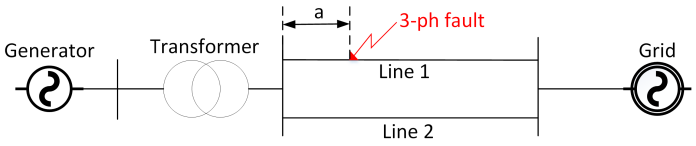

Figure 5.1: Figure shows the model used for the simulation. The original model given is extended with two parallel connected lines, and the fault is applied with a fault distance "a".

The parameters used for the generator can be observed in Table 3.1, the new d-axis time constants can be observed in Table 5.1. How the new d-axis time constants is calculated is mentioned in chapter 3.3.

Table 5.1: Table of the updated direct-axis time constants.

Transient direct axis time constant	$T_d^{'}$ [s]	3.27
Subtransient direct axis time constant	$T_d^{''}$ [s]	0.09

The base values used can be observed in Table 5.2 and 5.3.

Table 5.2: Table of base values.

Apparent power	S_b	145 [MW]
Voltage	U_b	15 [kV]
Electrical rad/s	ω_b	$2\pi 50$ [rad/s]

The base values for impedance Z_b and the inductance L_b and how they are calculated can be observed in Table 5.3 [9].

Table 5.3: Table of the impedance and the inductance base values, and how they are calculated.

Description	Parameter	Equation	Value
Impedance	Z_b	$\frac{U_b^2}{S_b}$	1.5517 [Ω]
Inductance	L_b	$\frac{Z_b}{\omega_b}$	0.0049 [H]

5.2 Case description

Defining the maximum reactive power output is done as described in NVF 2020. The reactive power output is defined by the active power output as observed in equation 5.1 [1].

$$Q_{max} = P \cdot 0.46 \tag{5.1}$$

Since the active power for the model is at 125 [MW] or $\frac{125[MW]}{145[MVA]} = 0.862\ [p.u]$, the maximum reactive power output at the HV side of the transformer is then 0.396 [p.u]. Adjusting and setting up the machine to generate 0 and 0.396 per unit reactive power at HV side of the transformer is done manually by adjusting the voltage reference input on the AVR.

A table of the cases can be observed in Table 5.4. The table sums up the six cases which is simulated, what line inductance, what reactive power at the HV side of the transformer and what distance parameter "a" on the faulty line is used.

Table 5.4: Table of the cases which will be simulated in Simulink

Case	L_{line} [mH]	Q[p.u]	a [%]
1A	0.49393	0	0, 20 ,30, 40, 60, 80 ,100
1B	0.49393	0.396	0, 20 ,30, 40, 60, 80 ,100
2A	0.98786	0	0, 20 ,30, 40, 60, 80 ,100
2B	0.98786	0.396	0, 20 ,30, 40, 60, 80 ,100
3A	1.5	0	0, 20 ,30, 40, 60, 80 ,100
3B	1.5	0.396	0, 20 ,30, 40, 60, 80 ,100

Table 5.5 shows the relationship between the short-circuit power (S_{sc}) and the line inductance chosen for each line. The short circuit power is calculated with equation 5.2 [1]. The voltage U_{th} in equation 5.2 is set to 1,0 [p.u] as a reference value in every case.

$$S_{sc} = \frac{U_t h^2}{Xth} \tag{5.2}$$

The line inductance used for each case is based on the thevenin reactance. They are chosen to be 0.05, 0.1 and 0.15. The line impedance will then be the double, 0.1, 0.2 and 0.3. Based on these values the line inductance is then calculated with equation 5.3 to 0.49393 [mH], 0.98786 [mH] and 1.5 [mH] with a L_b of 0.0049 [mH] as observed in Table 5.3.

$$L_{line} = X_{line,p.u} \cdot L_b \tag{5.3}$$

A full overview of the thevenin impedance in per unit, the line inductance and the corresponding short circuit power can be observed in Table 5.5.

Table 5.5: Table over the line inductance and their related short circuit powers

X_{th} **[p.u]**	X_{line} **[p.u]**	L_{line} **[mH]**	S_{sc} **[p.u]**
0,05	0,1	0,49393	20
0,1	0,2	0,98786	10
0,15	0,3	1,5	6,67

5.3 Tuning the model

Tuning the model for the required reactive power outputs will be done by adjusting the reference voltage on the AVR manually, since three different line parameters is chosen, three different reference voltages is also required.

In case 1 the Thevenin reactance was set to 0,05 [p.u], which corresponds to a line inductance of 0,49393 [mH] for each line. The short-circuit power is 20 [p.u] with U_{th} = 1,0 [p.u]. The voltage reference to the AVR is adjusted manually to achieve a reactive power as close as possible to zero on the HV side of the transformer. The resulting voltage reference was set to 1,002 per unit, with a measured reactive power of -0,001 per unit. To achieve a reactive power of 0,396 [p.u] on the HV side of the transformer, the approach was similar with a voltage reference of 1,033 [p.u] and a measured reactive power of 0,398 per unit. The measured reactive power after it was tuned to Q = 0 can be observed in Figure 5.2, and for Q = Qmax in Figure 5.3.

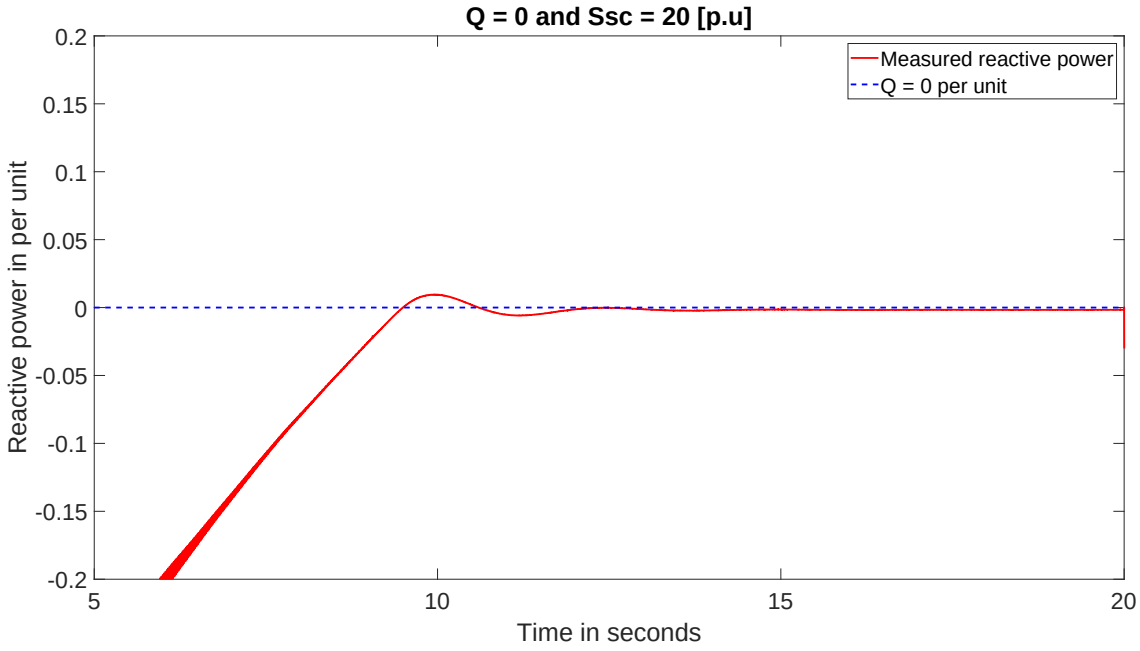

Figure 5.2: Figure of the measured reactive power with Q = 0 and S_{sc} = 20 [p.u].

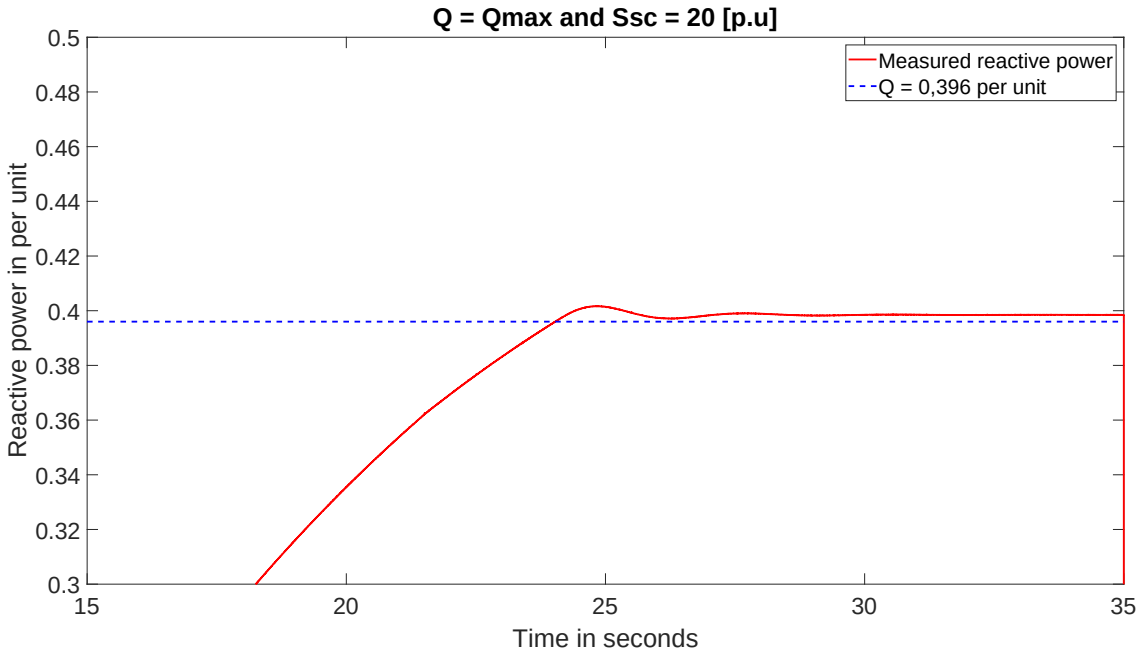

Figure 5.3: Figure of the measured reactive power with Q = Qmax and S_{sc} = 20 [p.u].

For case 2, the thevenin reactance was set to 0,1 [p.u], which gives a line inductance at 0,98786 [mH] for each line. The short-circuit power is 10 [p.u] with U_{th} = 1,0 [p.u]. Adjusting the voltage reference on the AVR manually to achieve a value of zero reactive power on the HV side of the transformer gave V_{ref} = 1,0 [p.u]. When the voltage reference was set to 1,0 [p.u] the measured reactive power on the HV side of the transformer was 0,005 [p.u]. Following the same procedure to achieve maximum reactive power of 0,396 [p.u] on the HV side of the transformer resulted in a reference

voltage at 1,049 per unit. The measured reactive power was then 0,397 [p.u]. The measured reactive power when it was tuned to Q = 0 can be observed in Figure 5.4, and for Q = Qmax in Figure 5.5.

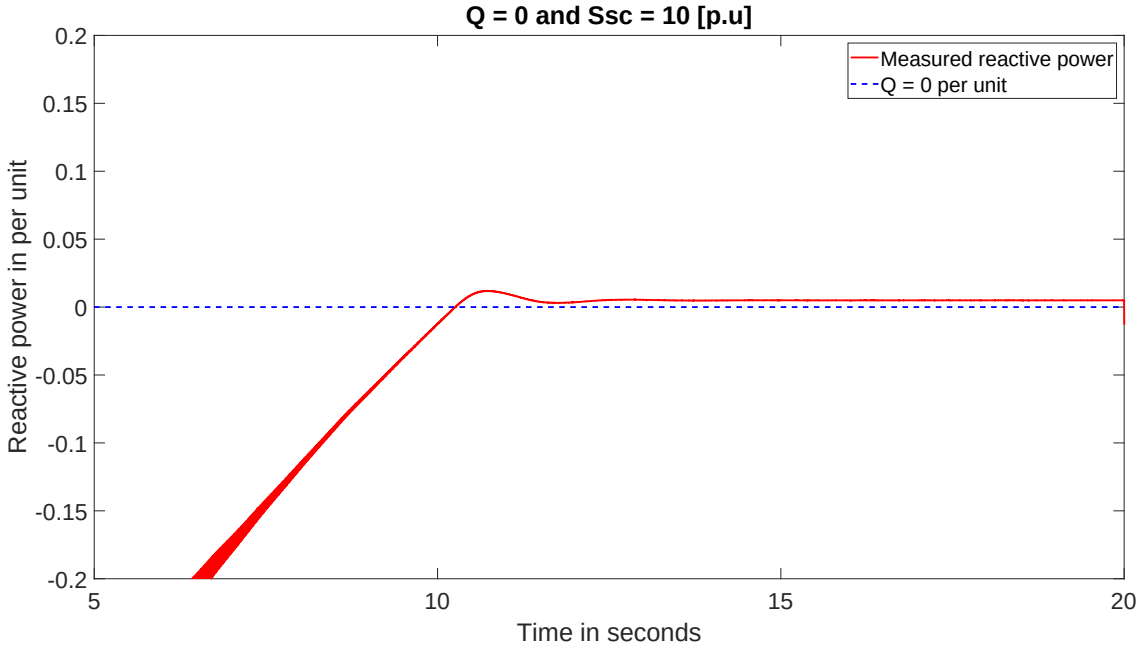

Figure 5.4: Figure of the measured reactive power with Q = 0 and S_{sc} = 10 [p.u].

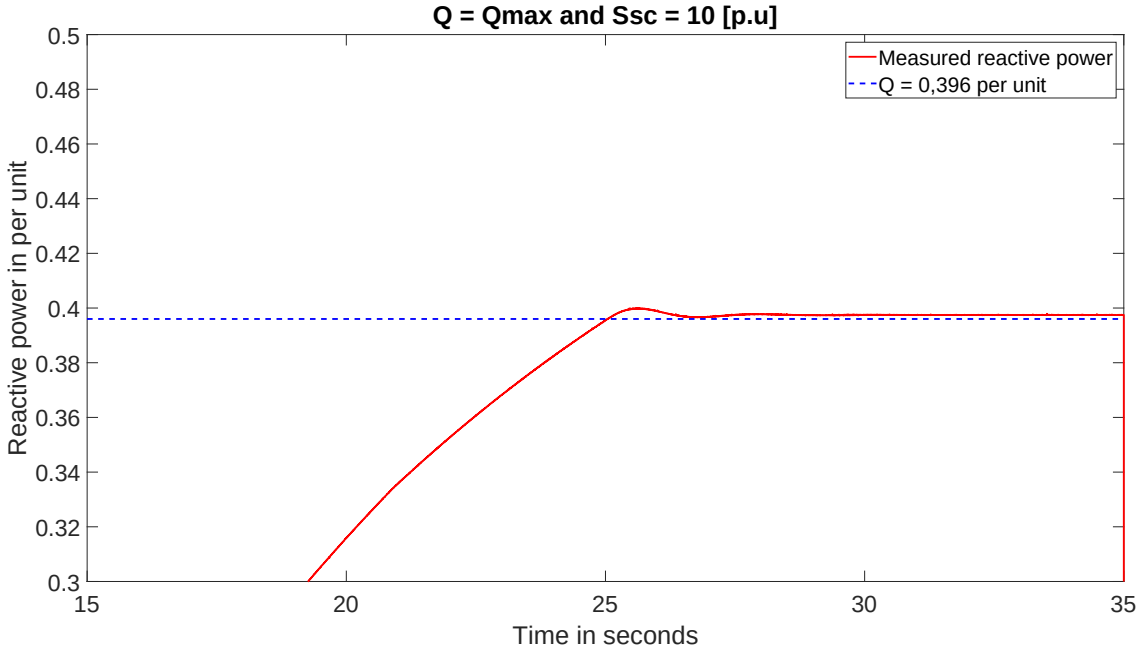

Figure 5.5: Figure of the measured reactive power with Q = Qmax and S_{sc} = 10 [p.u].

In case 3 the thevenin reactance was set to 0,15 [p.u], which corresponds to a line inductance of 1,5 [mH] for each line, and a short-circuit power of 6,67 [p.u] with U_{th} = 1 [p.u]. The reference voltage on the AVR was adjusted manually

to get a reactive power as close as possible to zero on the HV side of the transformer. The voltage reference was set to 0,995 per unit, and the measured reactive power at the HV side of the transformer was at 0,003 per unit. To get a reactive power of 0,396 [p.u] on the HV side of the transformer the same process was used. The voltage reference was set to 1,063 [p.u], and the reactive power was measured to 0,394 [p.u]. The measured reactive power when it was tuned to Q = 0 can be observed in Figure 5.6, and for Q = Qmax in Figure 5.7.

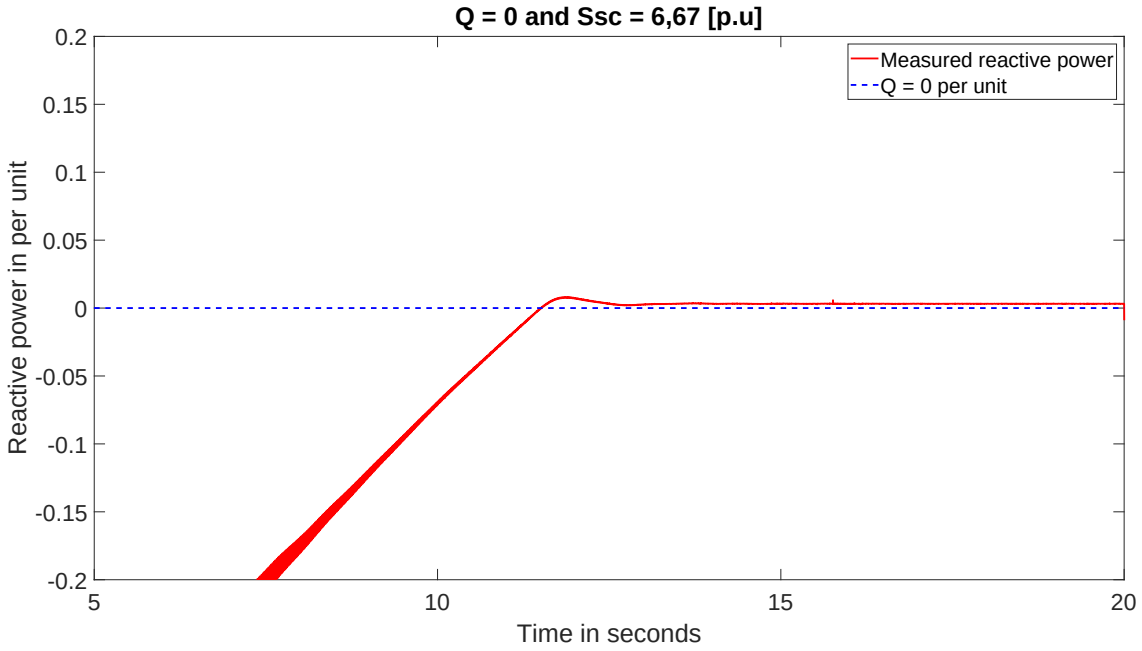

Figure 5.6: Figure of the measured reactive power with Q = 0 and S_{sc} = 6,67 [p.u].

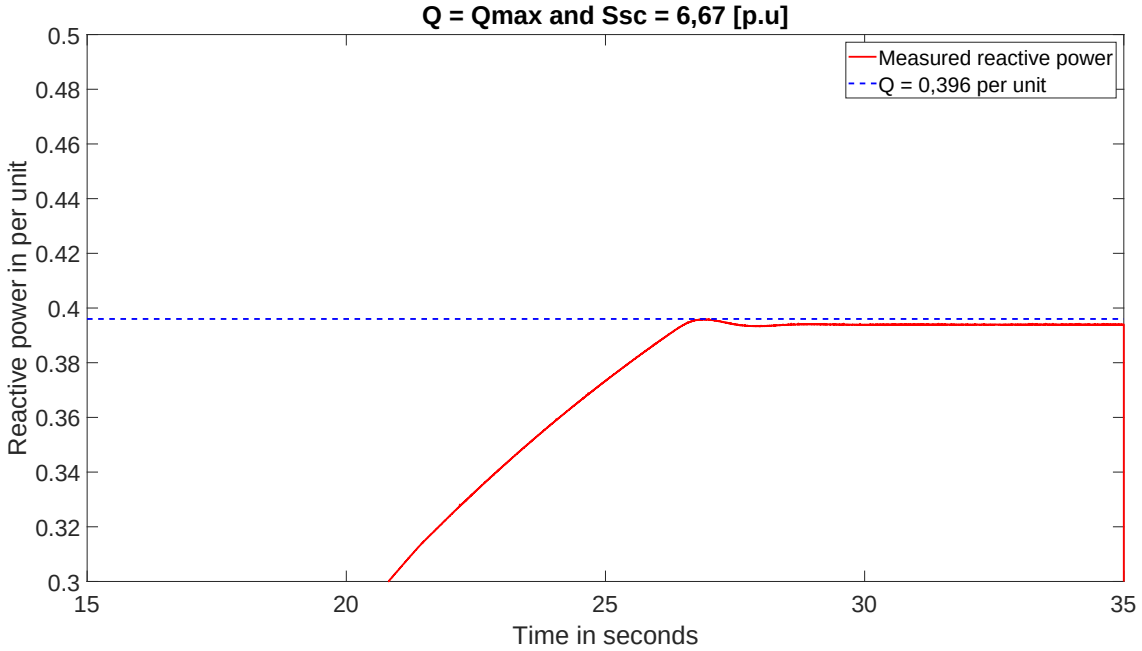

Figure 5.7: Figure of the measured reactive power with Q = Qmax and S_{sc} = 6,67 [p.u].

An overview of the tuning can be observed in Table 5.6.

Table 5.6: Table of the adjusted voltage references and the corresponding measured reactive powers for Q = 0 and Q = Qmax.

Line inductance [mH]	Q_{ref} **[p.u]**	V_{ref}	**Measured Q [p.u]**
0,49393	0	1,002	-0,001
	0,396	1,033	0,398
0,98786	0	1	0,005
	0,396	1,049	0,397
1,5	0	0,995	0,003
	0,396	1,063	0,394

Chapter 6

The simulation results

In this chapter a few results to confirm model will be presented as well as the results from the explained case in chapter 5 will be presented here. The active power measured for each case can be observed in appendix A.2.

6.1 Model outline

The following simulation results describes the behaviour of the machine before and under the applied three-phase fault. Case 1A will be used to assess the model. The Figures relevant for case 1B to 3B can be observed in appendix A.1 in Figure A.3 to A.14.

The field current and the field voltage can be observed in Figure 6.1. The blue curve is the field current and the red curve is the field voltage. As observed in Figure 6.1 the field current and the field voltage has the same per unit value pre-fault. When the fault occurs the field current increases and field voltage drops. The fault is then cleared and the field current and field voltage starts to oscillated, and they eventually stabilize at the same per unit value towards the end.

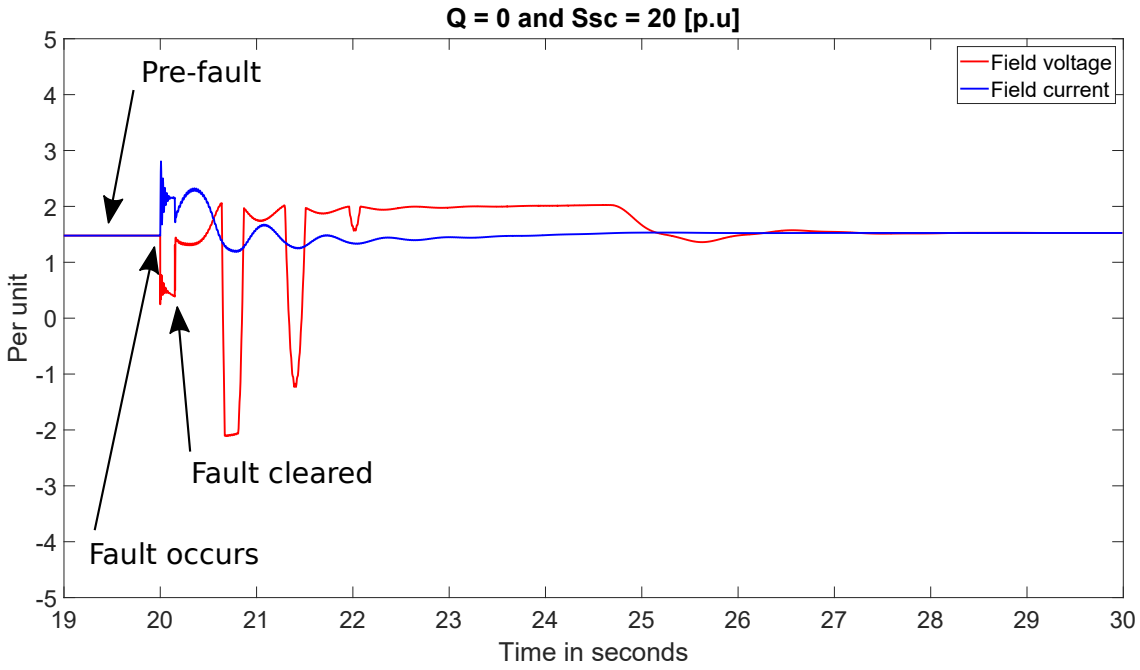

Figure 6.1: Plot of the field current and the field voltage with Q = 0 and X_{th} = 0,05 per unit.

Figure 6.2 shows the terminal voltage as the blue curve, and the field voltage as the red curve. Pre-fault, the terminal voltage is at 1,47 [p.u] and the field voltage is at 1,0 [p.u]. When the fault occurs both, the terminal voltage and field voltage drops. In the fault period, before the fault is cleared, the terminal voltage is at 0,42 [p.u] and the field voltage is at 0,21 [p.u].

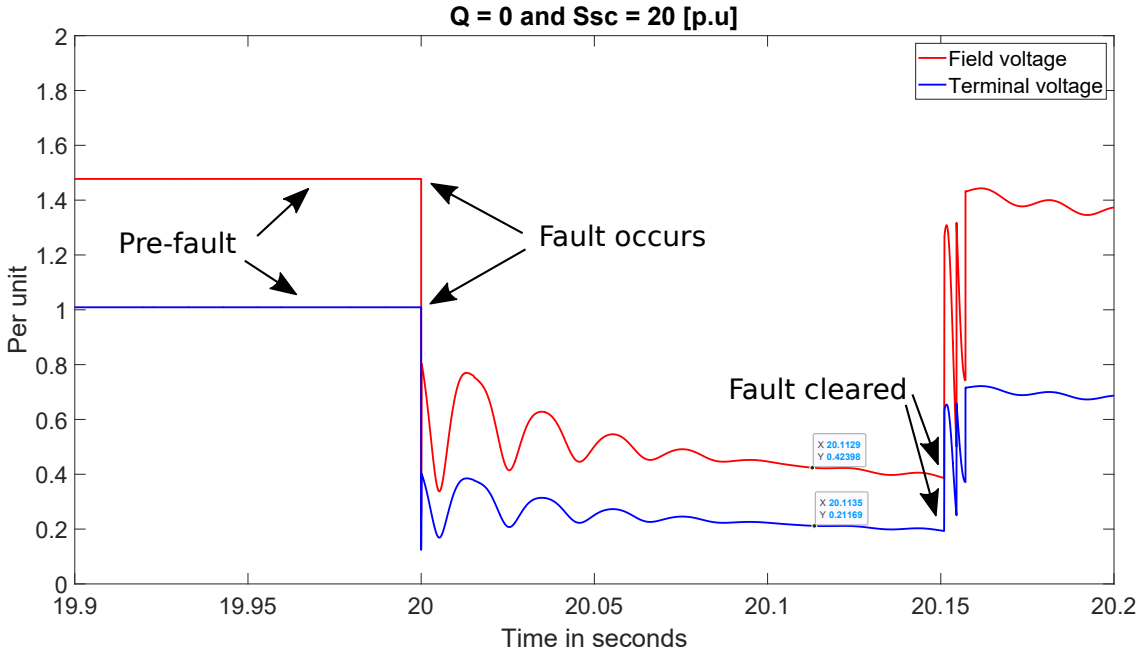

Figure 6.2: Plot of the terminal voltage and field voltage with Q = 0 and X_{th} = 0,05 per unit.

The reactive power measured, Q = 0 and Q = Qmax, is measured at the HV side of the transformer. The voltage drop between the terminals on the generator and the HV side of the transformer can be observed in Figure 6.3. The terminal voltage has a value of 1,0091 [p.u], the sensed voltage 1,002 [p.u] and the HV voltage 1,0017 [p.u]. The sensed voltage is the voltage measured 80 [%] into on the transformer.

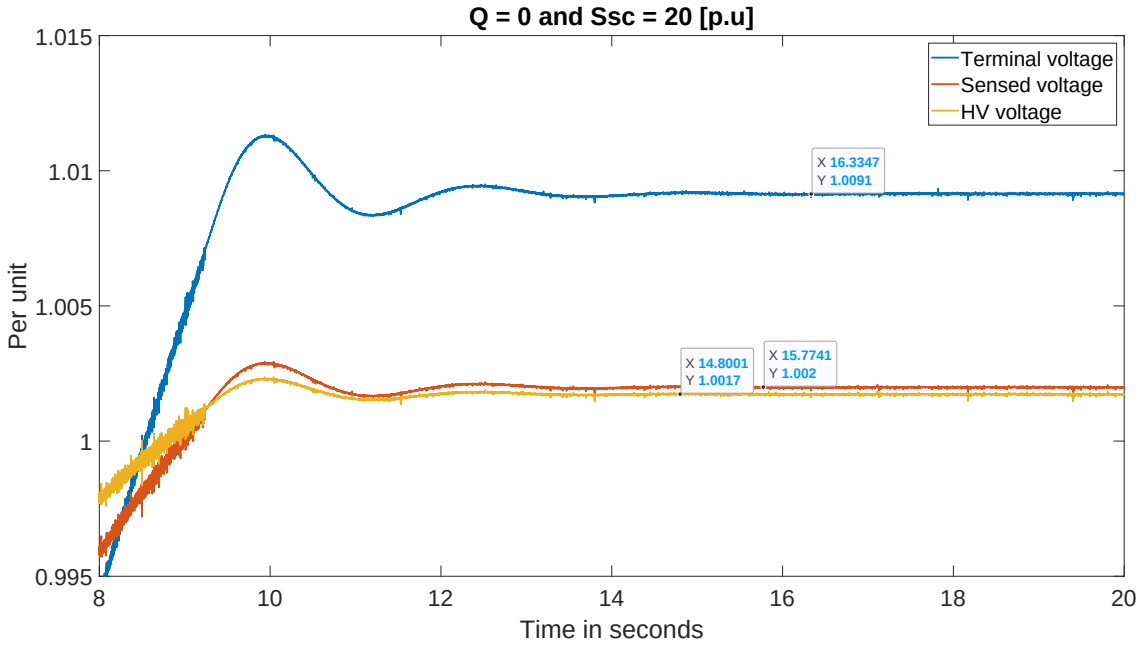

Figure 6.3: Figure of the voltage drop between the terminals and the HV side of the transformer, with Q = 0 and X_{th} = 0,05 [p.u].

Setting the reactive power to Q = Qmax was done by increasing the reference voltage. The voltage drop between the terminals of the generator and the HV side of the transformer can be observed in Figure 6.4. The terminal voltage is measured at 1,0846 [p.u], the sensed voltage at 1,033 [p.u] and the HV voltage at 1,0214 [p.u].

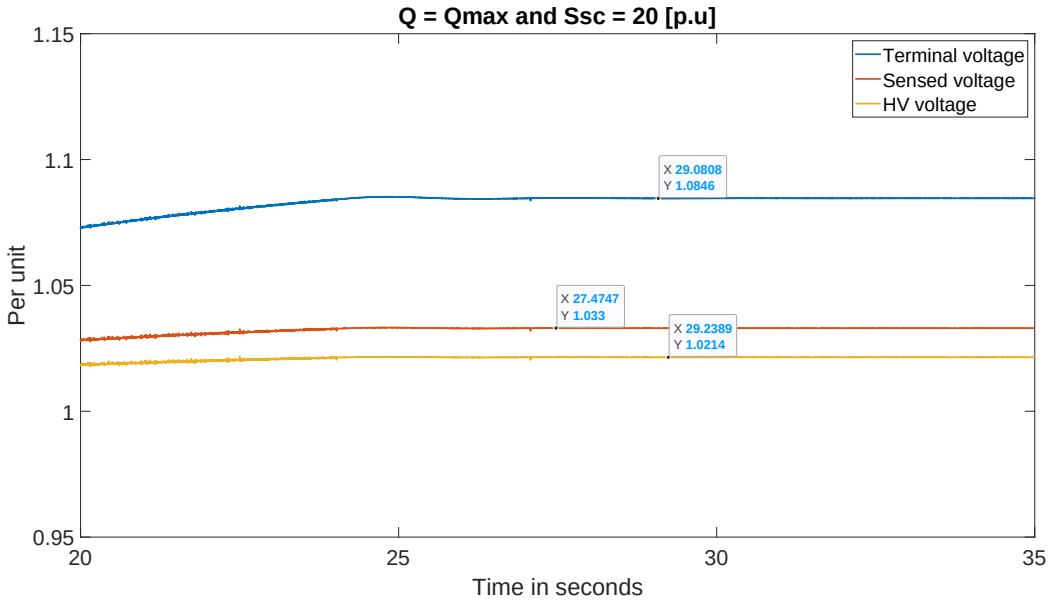

Figure 6.4: Figure of the voltage drop between the terminals and the HV side of the transformer, with Q = Qmax and X_{th} = 0,05 [p.u].

6.2 Case 1

Case 1 has a Thevenin reactance of 0,05 [p.u], which corresponds to a line inductance of 0,49393 [mH], and a short-circuit power of 20 [p.u].

6.2.1 Case 1A

Figure 6.5 and 6.6 shows the voltage profile when the AVR is tuned for a reactive power of Q = 0 in the HV side of the transformer. In Figure 6.5 the short circuit time is set to 150 [ms] and the distance parameter "a" is adjusted from 0 to 100 in steps of 20. What can be observed in Figure 6.5 is that the requirement for a type D generator connected to a voltage below 110 [kV] is not met for a distance below a = 40 [%]. The generator stays above the curve for type D generators connected to a voltage above 110 [kV] when the distance parameter "a" is at 0 [%].

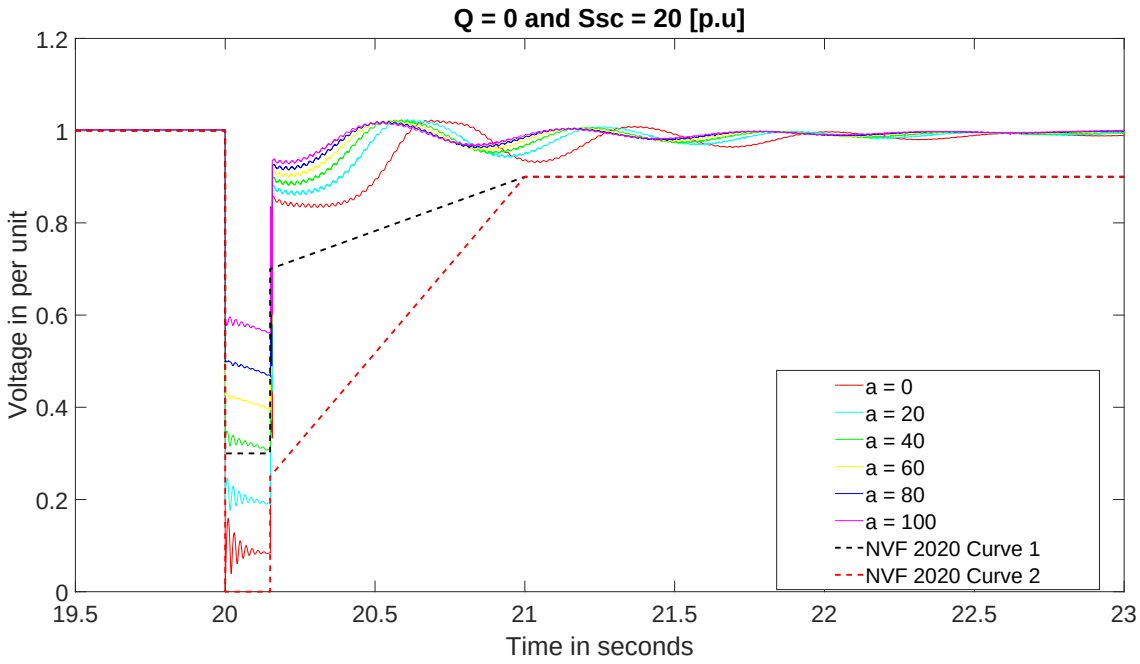

Figure 6.5: Plot of the voltage profiles on the HV side of the transformer with reactive power at Q = 0, and X_{th} = 0.05 [p.u]. The plot shows the voltage drop with a changed from 0 to 100 with a fault clearing time of 150 ms.

Figure 6.6 shows how the voltage profiles for the critical clearing time as the distance parameter is changed from 0 to 100, in steps of 20. When the distance parameter is set at 0 the critical clearing time is 160 [ms], increasing the distance parameter a to 100 gives a critical clearing time of 388. Figure 6.9 describes how the critical clearing time increases once the distance parameter "a" is increased from 0 to 100 with a reactive power of Q = 0 and Q = Qmax.

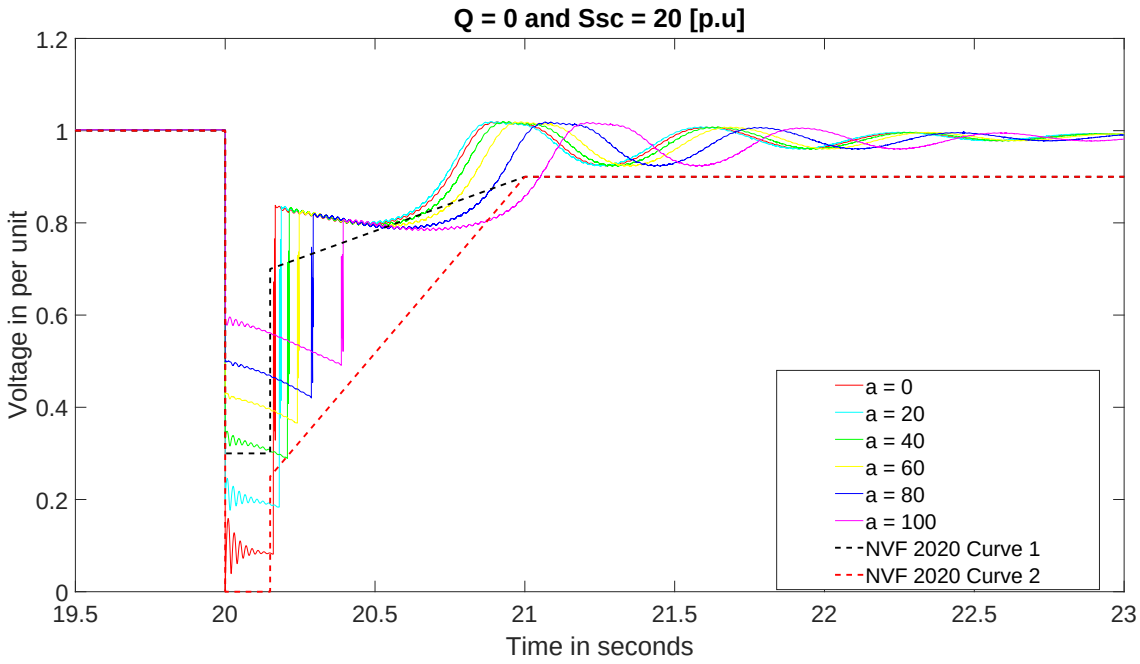

Figure 6.6: Plot of the voltage profiles on the HV side of the transformer with reactive power at Q = 0, and X_{th} = 0.05 [p.u]. The plot shows the voltage drop with a changed from 0 to 100 with the critical clearing time.

6.2.2 Case 1B

In Figure 6.7 and 6.8 the reactive power i set to Q = Qmax at the HV side of the transformer. The fault is cleared after 150 [ms] in Figure 6.7, and in Figure 6.8 the fault is cleared at the critical clearing time. In both Figure 6.7 and 6.8 the distance parameter "a" is adjusted from 0 to 100 in steps of 20.

Looking at Figure 6.7 and 6.8 the requirements for type D generators connected to a voltage above 110 [kV] is met once the distance parameter "a" is above 40 [%]. While for type D generators connected to a voltage above 110 [kV] the requirement is met for a = 0 [%].

Observing Figure 6.8. When the distance parameter "a" is set to 0 the critical clearing time is 204 [ms], once the distance parameter "a" is increased to 100 the critical clearing time is 5337 [ms]. Figure 6.9 shows how the critical clearing time increases when the distance parameter "a" is increased from 0 to 100 in steps of 20.

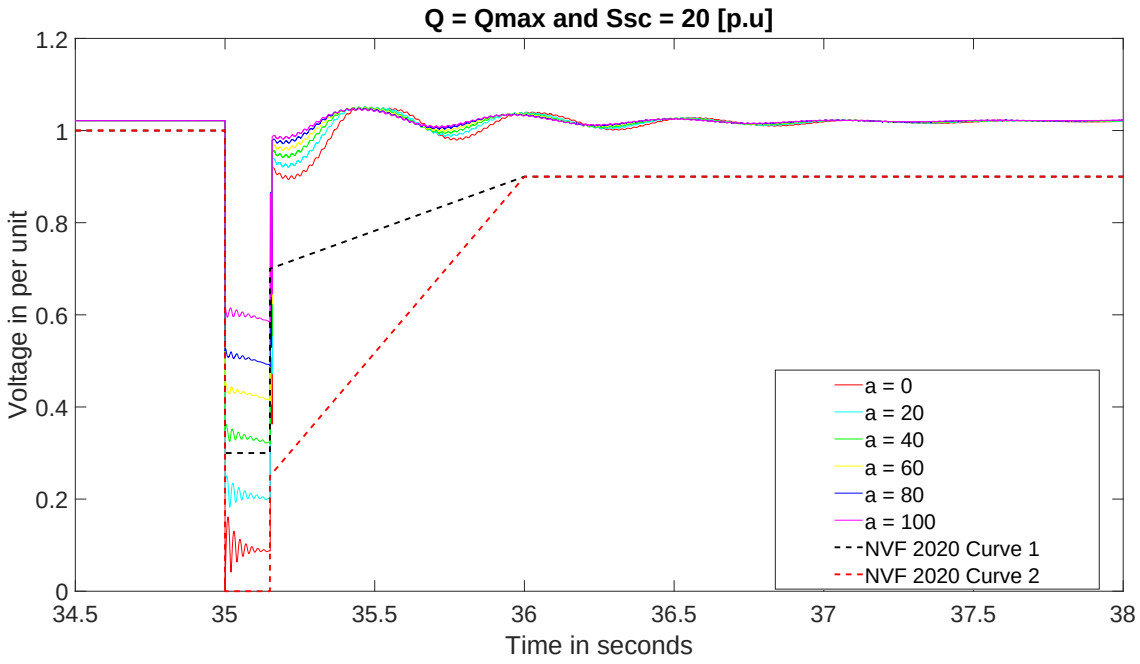

Figure 6.7: Plot of the voltage profiles on the HV side of the transformer with reactive power at Q = Qmax, and X_{th} = 0.05 [p.u]. The plot shows the voltage drop with a changed from 0 to 100 with a fault clearing time of 150 ms.

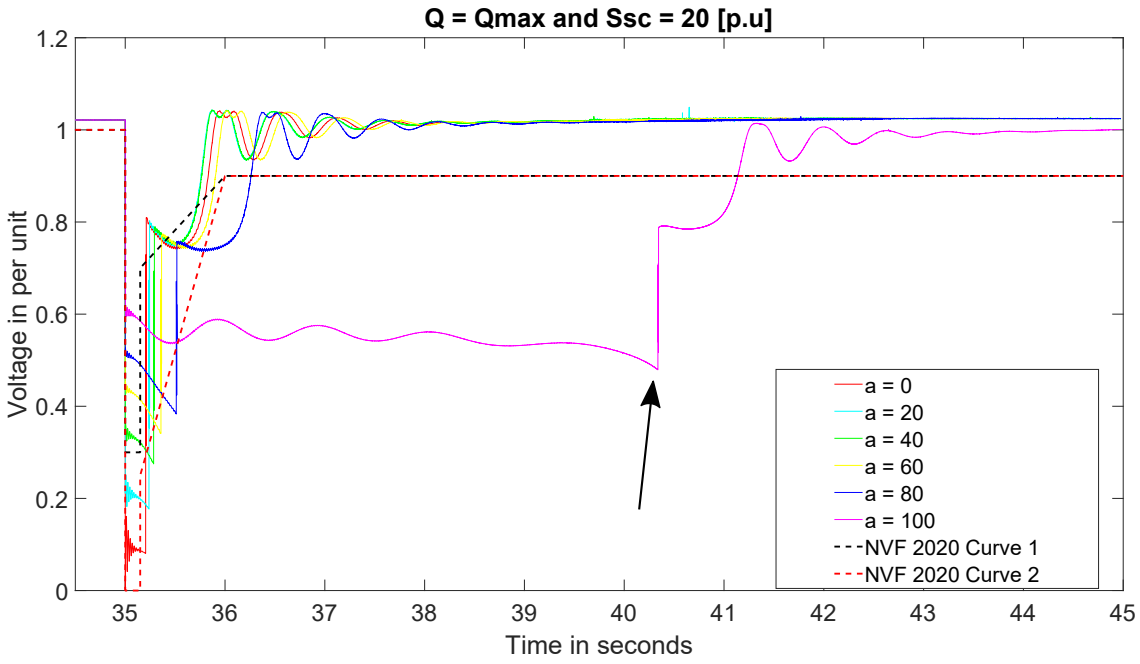

Figure 6.8: Plot of the voltage profiles on the HV side of the transformer with reactive power at Q = 0, and X_{th} = 0.05 [p.u]. The plot shows the voltage drop with a changed from 0 to 100 with the critical clearing time.

6.2.3 Case 1 - Critical clearing time

Figure 6.9 compares the critical clearing time (tc) in milliseconds for reactive power Q = 0 and Q = Qmax, were Qmax is 0,396 per unit at the HV side of the transformer. The critical clearing time is higher for an increased reactive power output. With a reactive power of Q = 0 the critical clearing time has a steady increase. While with a reactive power of Q = Qmax, the critical clearing time increases from a = 80 to a = 100 with 4827 [ms].

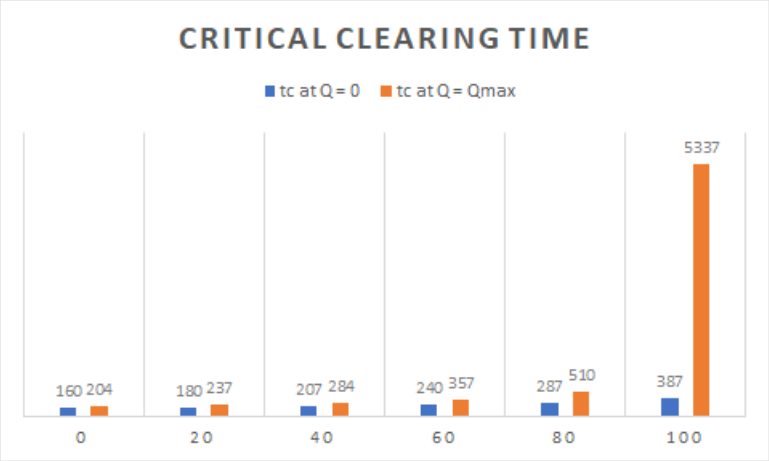

Figure 6.9: The figure compares the critical claering time (in milliseconds) for a reactive power at the HV side on the transformer of Q = 0 and Q = Qmax. The distance is parameter is changed from 0 to 100, in steps of 20.

6.3 Case 2

In case 2 the Thevenin reactance was set to 0,1 [p.u] which gives a line inductance at 0,98786 [mH]. The corresponding short-circuit power is 10 [p.u].

6.3.1 Case 2A

Figure 6.10 and 6.11 shows the voltage profile on the HV side of the transformer when the reactive power was tuned to be zero. In Figure 6.10 and 6.11 the distance parameter is adjusted from 0 to 100 in steps of 20. The clearing time for the fault in Figure 6.10 when a = 0 [%] is 125 [ms], while for a = 20 [%] then clearing time is 150 [ms]. Figure 6.11 shows the voltage profiles as the fault is cleared at the critical clearing time.

Looking at the voltage drop in Figure 6.10 and 6.11 it can be observed that the requirements for type D generators connected to below 110 [kV] is fulfilled when the distance parameters a is set to 40 [%] or above. For type D generators connected to 110 [kV] and above the requirement is met.

In Figure 6.11 the fault is cleared at the critical clearing time. The critical clearing time when the distance parameter "a" is set to zero is 134 [ms] while at a = 100 the critical clearing time is 310 [ms]. Figure 6.14 shows the critical clearing time for Q = 0 and Q = Qmax when the distance parameter is changed from 0 to 100 in steps of 20.

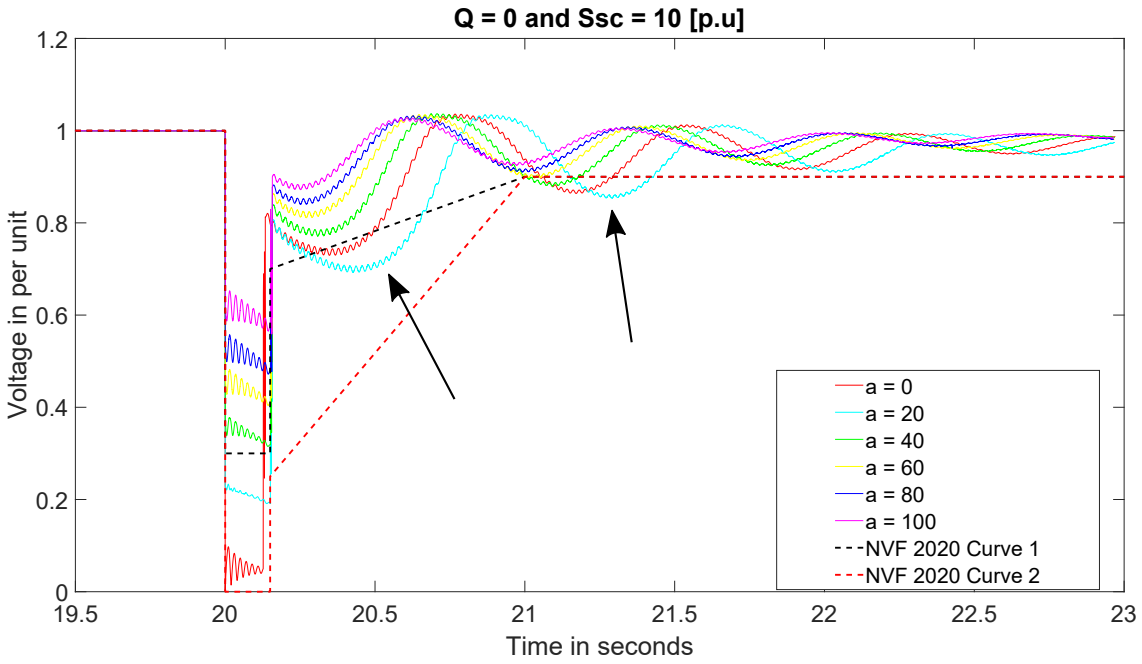

Figure 6.10: Plot of the voltage profiles on the HV side of the transformer with reactive power at Q = 0, and X_{th} = 0.1 [p.u]. The plot shows the voltage drop with a changed from 0 to 100 with a fault clearing time of 150 ms.

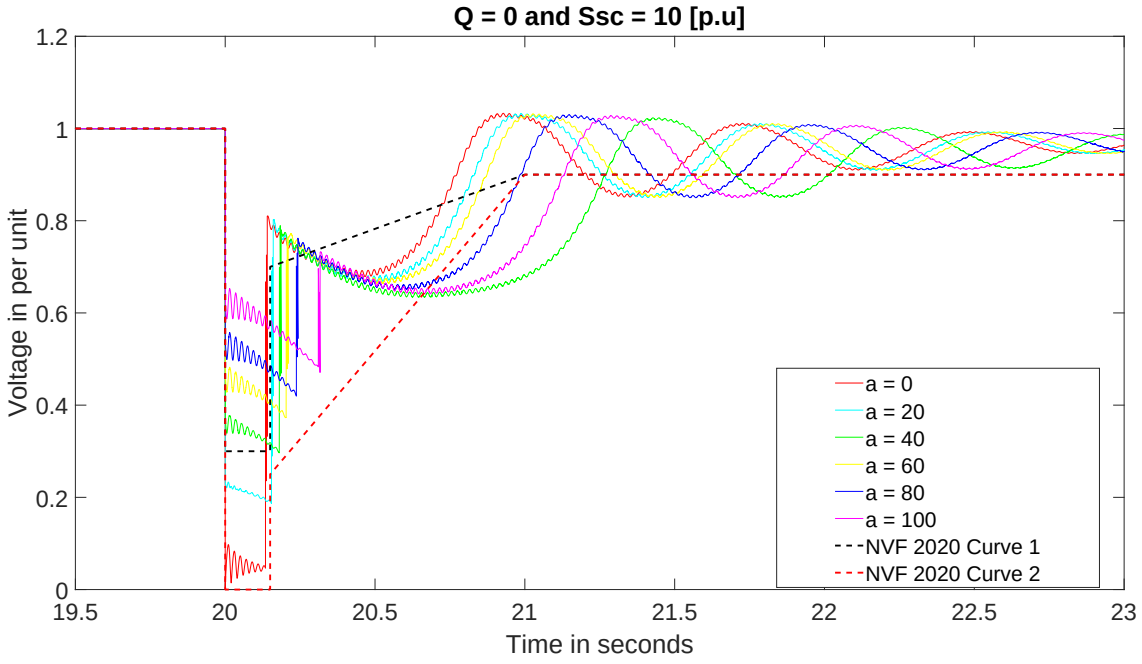

Figure 6.11: Plot of the voltage profiles on the HV side of the transformer with reactive power at Q = 0, and X_{th} = 0.1 [p.u]. The plot shows the voltage drop with a changed from 0 to 100 with the critical clearing time.

6.3.2 Case 2B

Figure 6.12 and 6.13 shows the voltage profile when the reactive power on the HV side of the transformer i set to Q = Qmax. In Figure 6.12 the fault is cleared after 150 [ms] while in Figure 6.13 the fault is cleared at the critical clearing time. The distance parameter "a" is changed from 0 to 100 in steps of 20.

The voltage drop in Figure 6.12 and 6.13 when the distance parameter "a" is below 40 [%] does not meet the requirements for type D generators connected to below 110 [kV]. While for type D generators connected to 110 [kV] and above the requirement is met.

In Figure 6.13 when the distance parameter "a" is set to 0 the critical clearing time is 180 [ms], while setting the distance parameter "a" to 100 gives a critical clearing time of 3530 [ms]. The critical clearing time for Q = 0 and Q = Qmax when the distance parameter is changed from 0 to 100 in steps of 20, can be observed ib Figure 6.14.

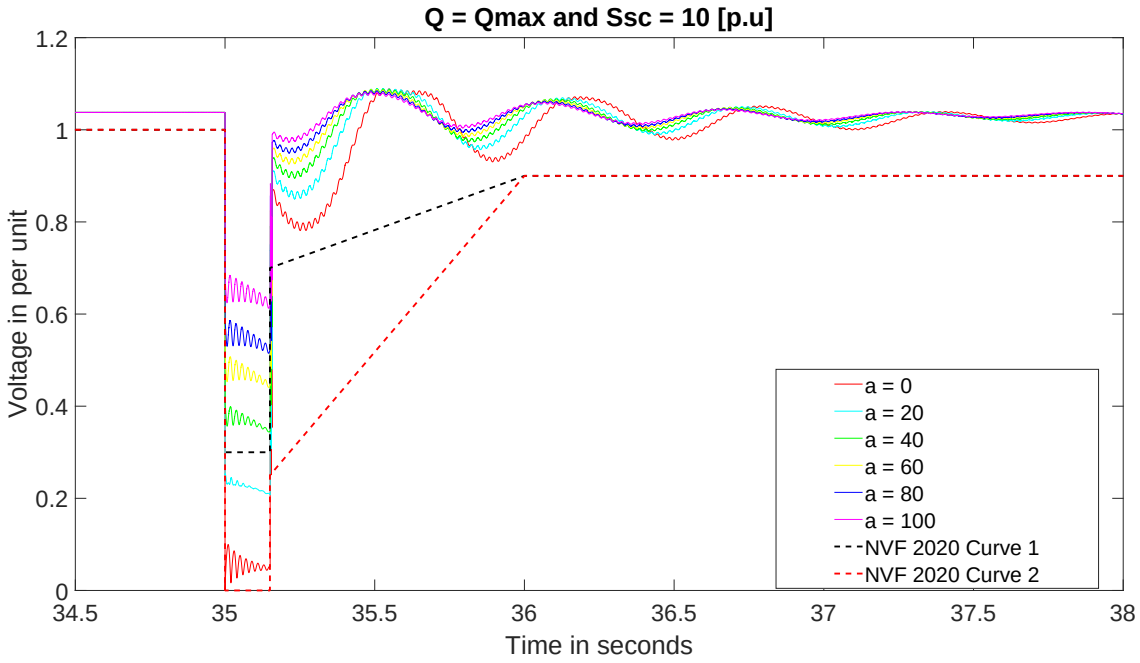

Figure 6.12: Plot of the voltage profiles on the HV side of the transformer with reactive power at Q = Qmax, and X_{th} = 0.1 [p.u]. The plot shows the voltage drop with a changed from 0 to 100 with a fault clearing time of 125 ms at a = 0 and 150 ms for a = 20 and above.

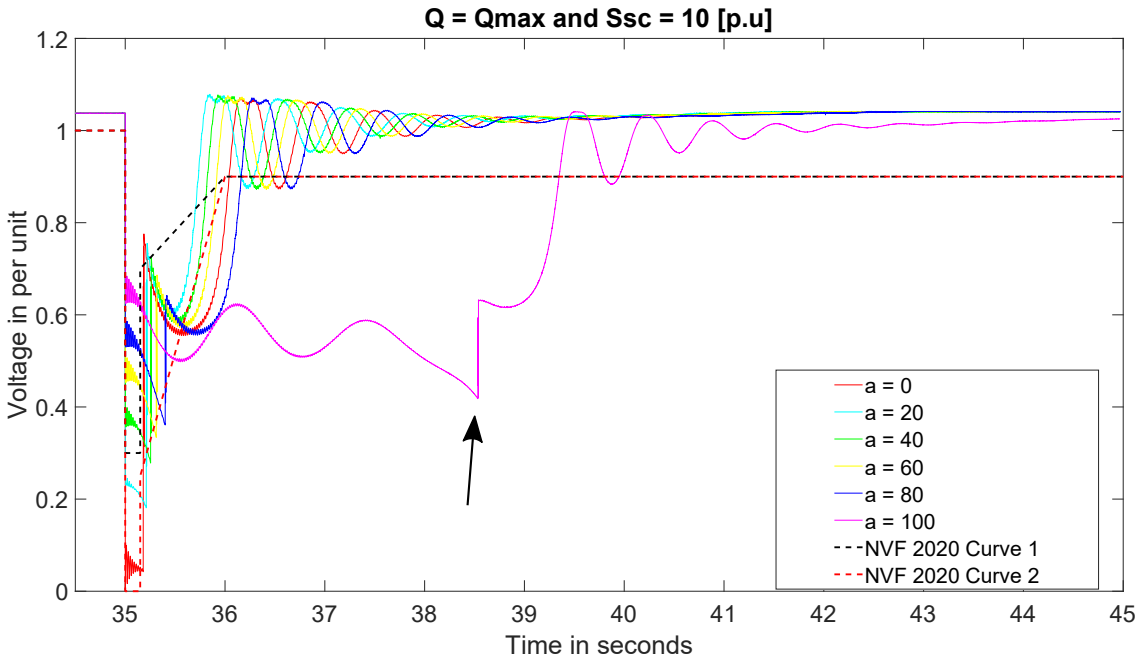

Figure 6.13: Plot of the voltage profiles on the HV side of the transformer with reactive power at Q = 0, and X_{th} = 0.1 [p.u]. The plot shows the voltage drop with a changed from 0 to 100 with the critical clearing time.

6.3.3 Case 2 - Critical clearing time

Figure 6.14 compares the critical clearing time (tc) when the reactive power at the HV side of the transformer is set to Q = 0 and Q = Qmax. The critical clearing time is in milliseconds when the distance parameter is changed from 0 to 100 in steps of 20. The critical clearing time for Q = Qmax is higher then Q = 0, and when Q = Qmax the critical clearing time increases by 3130 [ms] from a = 80 to a = 100.

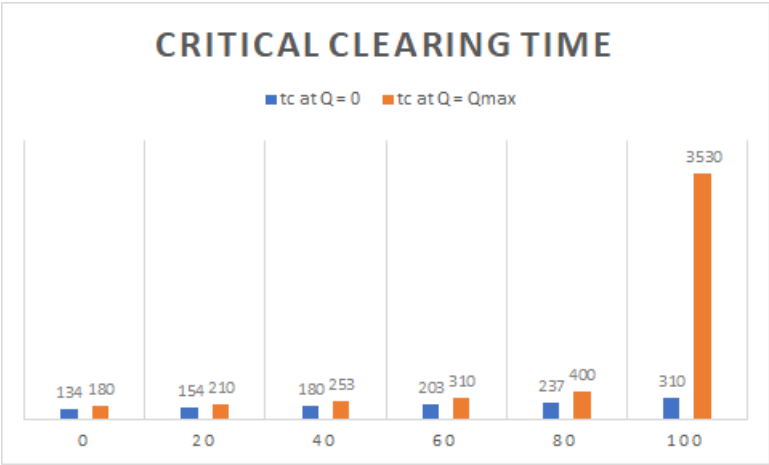

Figure 6.14: The figure compares the critical clearing time (in milliseconds) for a reactive power at the HV side on the transformer of Q = 0 and Q = Qmax. The distance is parameter is changed from 0 to 100, in steps of 20.

6.4 Case 3

In case 3 the Thevenin reactance was set to 0,15 [p.u] which gives a line inductance at 1,5 m[mH] each. The corresponding short-circuit power is 6,67 [p.u].

6.4.1 Case 3A

In case 3A the reactive power on the HV side of the transformer was adjusted to be zero. This case is represented by Figure 6.15 and 6.16. In Figure 6.15 and 6.16 the voltage profiles is shown with a distance parameter "a" from 0 to 100 in steps of 20.

In Figure 6.15 the fault is cleared after 100 [ms] when the distance parameter "a" is set to 0, for a = 20 and a = 40, the fault is cleared after 125 [ms] and for a = 60 and above the fault is cleared after 150 [ms]. It can be observed that with a distance parameter "a" below 40 [%] the requirements is not met for type D generators connected to below 110 [kV]. While for type D generators connected to 110 [kV] and above the requirement is met.

The critical clearing time in Figure 6.16 with a distance parameter "a" at 0 [%] is 110 [ms], while increasing a to 100 [%] gives a critical clearing time of 243 [ms]. The critical clearing time for each step change in "a" can be observed in Figure 6.19.

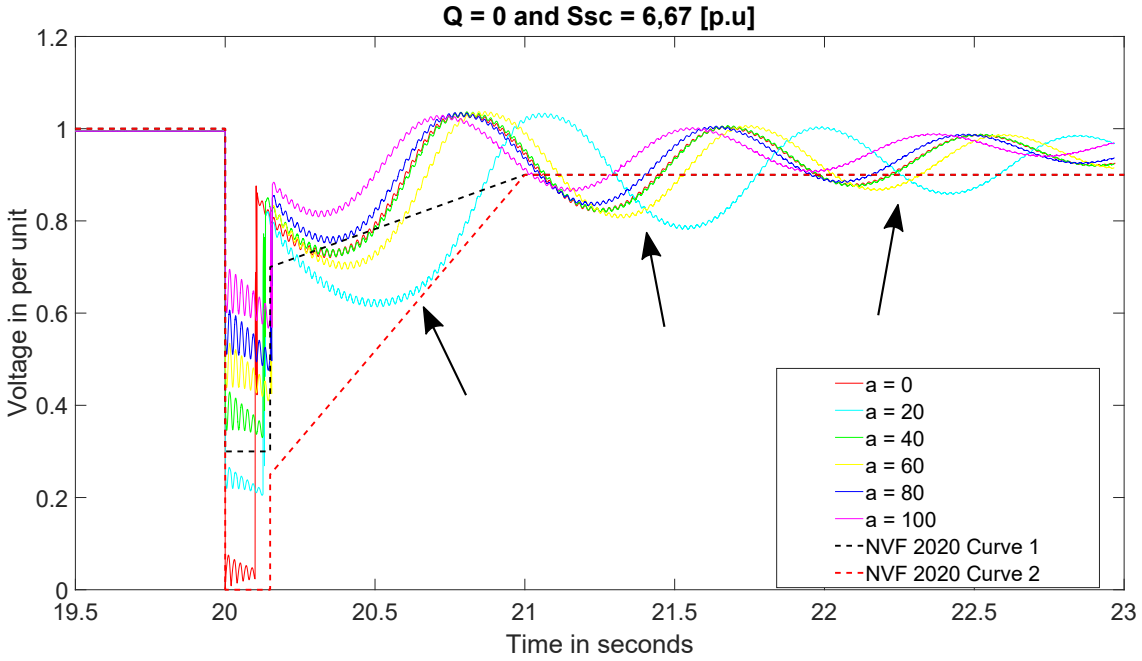

Figure 6.15: Plot of the voltage profiles on the HV side of the transformer with reactive power at Q = 0, and X_{th} = 0.15 [p.u]. The plot shows the voltage drop with a changed from 0 to 100 with a fault clearing time of 100 ms at a = 0, 125 ms at a= 20 and 40, and 150 ms for a = 60 and above.

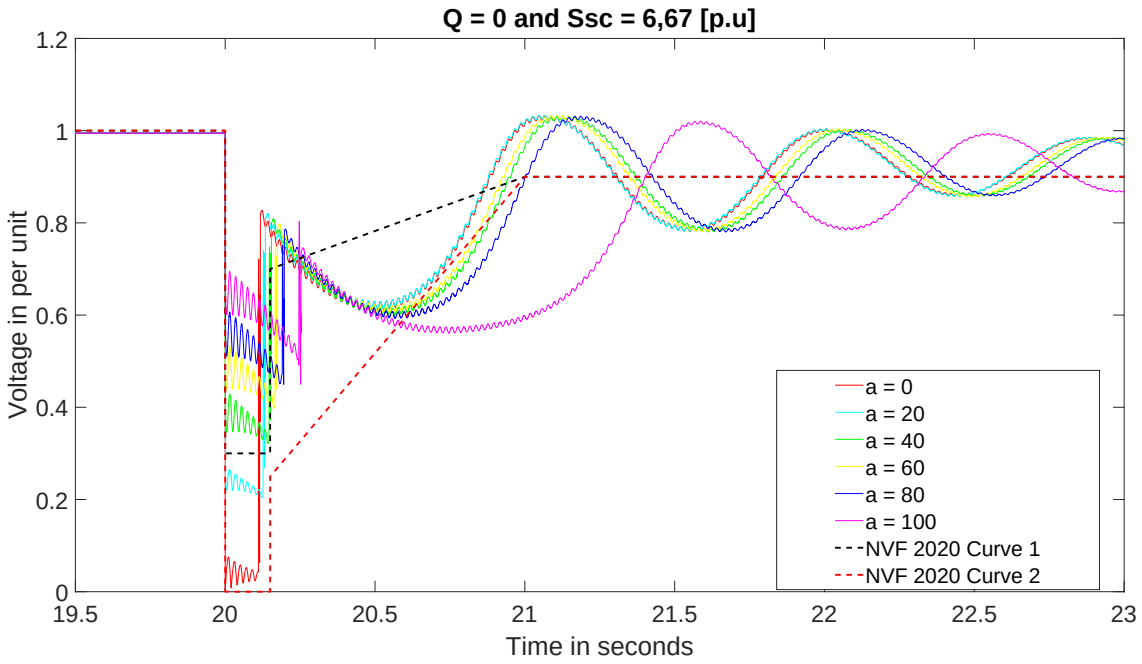

Figure 6.16: Plot of the voltage profiles on the HV side of the transformer with reactive power at Q = 0, and X_{th} = 0.15 [p.u]. The plot shows the voltage drop with a changed from 0 to 100 with the critical clearing time.

6.4.2 Case 3B

Figure 6.17 and 6.18 shows the voltage profile when the reactive power on the HV side of the transformer is at Q = Qmax. In Figure 6.17 the fault is cleared after 150 [ms], the distance parameter "a" is changed from 0 to 100 in steps of 20. The fault is cleared at the critical clearing time in Figure 6.18 and the distance parameter "a" is changed from 0 to 100 in steps of 20.

Observing Figure 6.15 and 6.16, when the distance parameter "a" is set to to 0 or 20[%], the requiremnt for type D generators connected to below 110 [kV] is not met. For type D generators connected to 110 [kV] and above the requirement is met.

The critical clearing time in Figure 6.16 when the distance parameter "a" is at 0 [%] is 163 [ms], while increasing a to 100 [%] the critical clearing time is 689 [ms]. In Figure 6.19 the critical clearing for each step change in "a" can be observed.

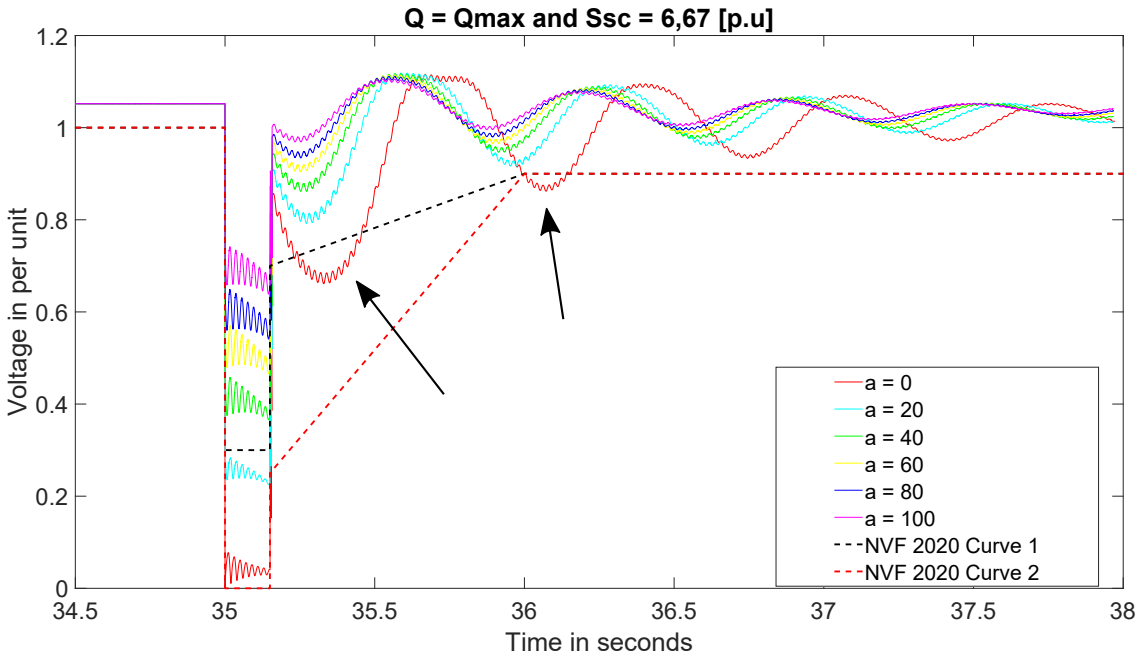

Figure 6.17: Plot of the voltage profiles on the HV side of the transformer with reactive power at Q = Qmax, and X_{th} = 0.15 [p.u]. The plot shows the voltage drop with a changed from 0 to 100 with a fault clearing time of 150 ms.

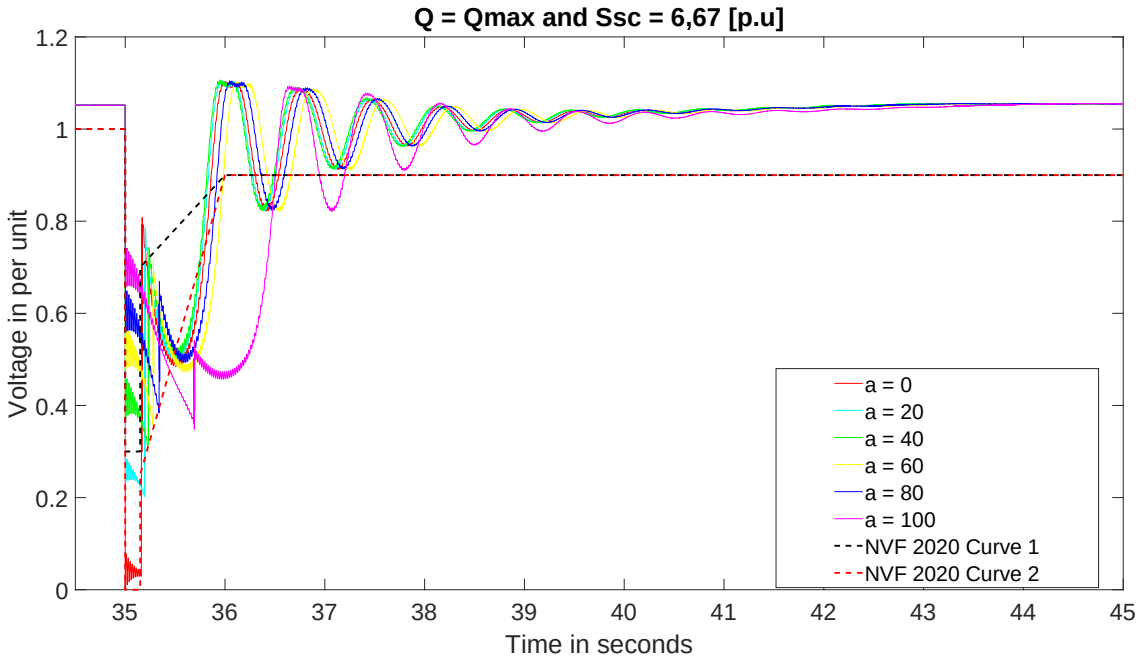

Figure 6.18: Plot of the voltage profiles on the HV side of the transformer with reactive power at Q = Qmax, and X_{th} = 0.15 [p.u]. The plot shows the voltage drop with a changed from 0 to 100 with the critical clearing time.

6.4.3 Case 3 - Critical clearing time

Figure 6.19 compares the critical clearing time when the reactive power on the HV side of the transformer is set to Q = 0 and Q = Qmax. The critical clearing time is in milliseconds, the distance parameter "a" is from 0 to 100 in steps of 20. When the distance parameter "a" is set to 100, the critical clearing time between Q = 0 and Q = Q max is 455 [ms].

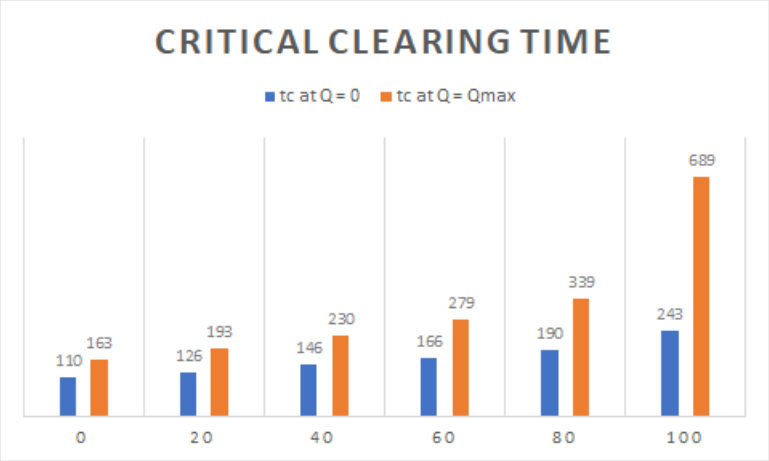

Figure 6.19: The figure compares the critical claering time (in milliseconds) for a reactive power at the HV side on the transformer of Q = 0 and Q = Qmax. The distance is parameter is changed from 0 to 100, in steps of 20.

Chapter 7

Discussion

In this chapter, the results presented in chapter 6 will be discussed, starting with the model used in the simulations and then fault ride-through capability of the synchronous machine.

7.1 Model assessment

The model created in MATLAB Simulink has the step-up transformer put inside the synchronous machine instead of adding it outside. The step-up transformer is implemented in the generator model to save some computation time in MATLAB Simulink. However, the model utilizes a PI regulator as an AVR, and there is no PSS added to the model. Therefore, the model lacks some damping, and the figure's oscillations are larger than what they would have been with a PSS. An example of this is the oscillations after the fault in Figure 6.10, 6.15. In appendix A.1, in Figure A.3, A.9 and A.12, it can also be observed that the generator does not reach steady-state since the field voltage and the field current has different per-unit values after the fault. Appendix A.2 shows the active power before and after the fault, but in Figure A.17, A.19 and A.20 the active power keeps oscillating after the fault. These oscillations could have been reduced by implementing a PSS to the Simulink model.

In chapter 6.1, a few simulation results were presented, showing how the field current and the field voltage is equal in the pre-fault state. As mentioned in 2.3, the field current and the field voltage have the same value per unit in steady-state, however as the fault occurs, the field current and the field voltage differ in per-unit values. Figure 6.1 confirms this theory.

In Figure 6.2, the terminal voltage is plotted with the field voltage. What can be observed from Figure 6.2 is during the fault period, after the fault occurs. The field voltage has a value of 0,42 [p.u] while the terminal voltage has a value of 0,21 [p.u]. In the pre-fault state, the AVR regulates the voltage according to the voltage reference set. When the fault occurs, the AVR uses the generated voltage error to supply power to the generator to maintain stability. During the fault, the field voltage is limited by the terminal voltage, as mentioned in chapter 2.3, and the recommended ceiling factor of 2 by NVF 2020 [1]. Therefore the field voltage has the same voltage profile as the terminal voltage during the fault and is twice as high because of the ceiling factor. A higher value would have been obtained if the field voltage had not been limited by the ceiling factor or the voltage obtained from the terminals. A higher field voltage during the fault would have increased the synchronous generator's FRT capability.

The synchronous generator is set to produce a reactive power of zero or 0,396 per unit at the HV side of the transformer.

The synchronous generator is therefore set to produce reactive power at its terminals. As mentioned in chapter 2.4, when the reactive power flows from the sending end to the receiving end, the voltage V_s is greater than V_r. This is confirmed by observing Figure 6.3 and 6.4, as there is a voltage drop from the terminals to the step-up transformer.

7.2 Reactive power set to Q = 0

The thesis presents six cases in total; three are simulated with a reactive power tuned to zero by manually adjusting the voltage reference to the AVR. The cases relevant for the reactive power set to Q = 0 are 1A, 2A, and 3A. These cases results are presented in chapter 6.2.1, 6.3.1 and 6.4.1 respectively.

Each of the three cases 1A, 2A, and 3A has their own short-circuit power. Case 1A has a S_{sc} = 20 [p.u], 2A has a S_{sc} = 10 [p.u] and 3A has a S_{sc} = 6,67 [p.u]. What is common in all these three cases is that none of them meets the requirement for a Type D generator connected to a voltage below 110 [kV]. For a type D generator connected to a voltage at 110 [kV] or above, the synchronous generator can stay above the described voltage profile even at "a" = 0 [%]. A distance parameter "a" = 0 [%] implies the fault occurs on the terminals of the step-up transformer.

In Table 7.1, the critical clearing time can be observed for case 1A, 2A, and 3A when the reactive power at the HV side of the transformer is set to Q = 0. An observed increase in the Thevenin reactance or a reduction in the short-circuit power causes the critical clearing time to decrease. The critical clearing time when S_{sc} = 10 [p.u] and "a" equals 0 [%] is 134 [ms] and "a" equals 20 [%] is 154 [ms]. Assumed the fault is detected and cleared within this time, the generator will maintain stability. If not, stability is lost. Decreasing the S_{sc} to 6,67 [p.u] causes a further drop in critical clearing time. When the fault is set to "a" = 0 [%] the critical clearing time is at 110 [ms] and at "a" = 20 [%] the critical clearing time is at 126 [ms]. This could be to low for the fault to be detected and cleared in time.

a [%]	0	20	40	60	80	100
Critical clearing time [ms] Case 1A	160	180	207	240	287	387
Critical clearing time [ms] Case 2A	134	154	180	203	237	310
Critical clearing time [ms] Case 3A	110	126	146	166	190	243

Table 7.1: Table of the critical clearing time when Q = 0 for Case 1A, 2A and 3A.

In Case 3A, when the reference voltage is set to give Q = 0 on the HV side of the step-up transformer, the voltage is measured at 0,994 [p.u]. This is not according to the requirement given in NVF 2020, where it should be above 1 [p.u] pre-fault. The measured voltage for case 3A can be observed in appendix A.1 in Figure A.11.

7.3 Reactive power set to Q = Qmax

In the remaining three cases the reactive power is tuned to be at Q = Qmax which is 0,396 [p.u] according to equation 5.1 when the active power, P_{max} = 0,862 [p.u]. The short circuit power is 20 [p.u], 10 [p.u] and 6,67 [p.u] for case 1B, 2B and 3B respectively. The results from the three cases are presented in chapter 6.2.2, 6.3.2 and 6.4.2.

Increasing the reactive power to Q = Qmax does not change the voltage drop significantly enough for the generator to meet the requirement for a type D generator connected to below 110 [kV]. The fault still has to be at "a" = 40 [%] or

above. Should the generator be connected to 110 [kV] or above the requirement is met, even at "a" = 0 [%]. Which means the fault occurs on the terminals of the step-up transformer.

The criticl clearing time when the reactive power is set to Q = Qmax can be observed in Table 7.2. With a short-circuit power at 10 [p.u] "a" = 0 [%] the critical clearing time is at 180 [ms]. Decreasing the short-circuit power to 6,67 [p.u] gives a critical clearing time of 163 [ms]. However, between "a" = 80 [%] and "a" = 100 [%] there is a large increase in critical clearing time. With a short-circuit power at 20 [p.u], the critical clearing time increases with 4828 [ms]. Setting the short-circuit power to 10 [p.u], the critical clearing time increases with 3130 [ms].

a [%]	0	20	40	60	80	100
Critical clearing time [ms] Case 1B	204	237	284	357	510	5337
Critical clearing time [ms] Case 2B	180	210	253	310	400	3530
Critical clearing time [ms] Case 3B	163	193	230	279	339	689

Table 7.2: Table of the critical clearing time when Q = Qmax for case 1B, 2B and 3B.

Figure 7.1 shows the critical clearing time with S_{sc} = 20 [p.u], when the distance parameter is increased from a = 80 [%] to a = 100 [%] in steps of 20. Observing the figure it is a clear exponential increase in critical clearing time between a = 80 [%] to a = 100 [%].

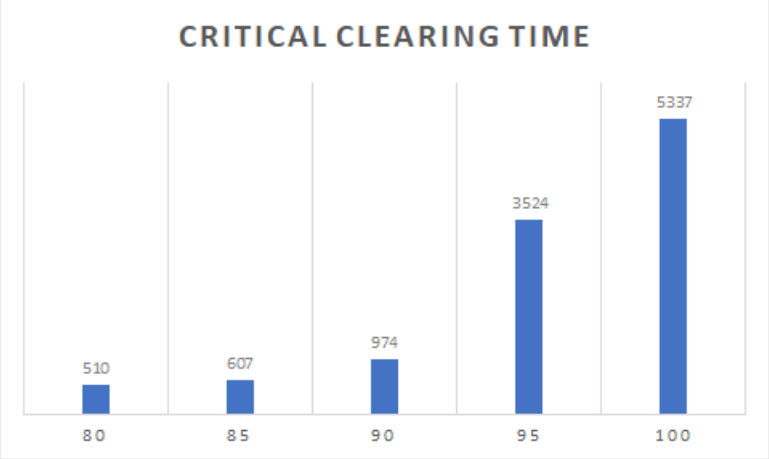

Figure 7.1: Figure of the exponential increase in critical clearing time between a = 80 [%] to a = 100 [%]. The short-circuit power is 20 [p.u] and Q = Qmax.

When the short-circuit power is set at 10 [p.u] the exponential increase in critical clearing time starts at "a" = 95 [%]. Figure 7.2 shows the increase in critical clearing time between a = 95 [%] to a = 100 [%].

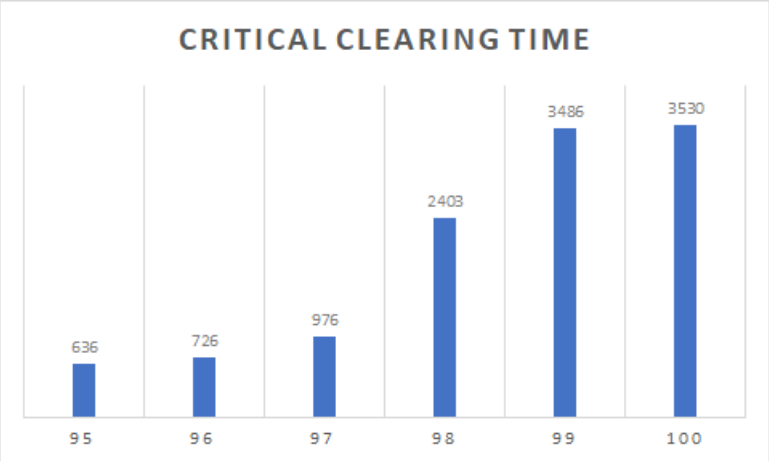

Figure 7.2: Figure of the exponential increase in critical clearing time between a = 95 [%] to a = 100 [%]. The short-circuit power is 10 [p.u] and Q = Qmax.

7.4 Critical clearing time comparison

Comparing the critical clearing time for each case shows that there are some linearities. However, when the fault is further out on the line, those linearities are lost. Table 7.3 show how the critical clearing time increases between each step change in "a". In the table, the critical clearing time of the next step is divided by the clearing time for the current step. For example, the number 1,125 in case 1A is achieved by dividing 180 [ms] when "a" = 20 [%] by 160 [ms] when "a" = 0 [%].

What can be observed in Table 7.3 is when the reactive power is set to Q = 0, that is case 1A, 2A and 3A shows that there are some linearities in each step change in "a." However, when the reactive power is increased, these linearities are lost when "a" is larger than 80 [%].

$\frac{tc\ at\ a_2=a_1+20}{tc\ at\ a_1=a_1}$	$\frac{tc\ at\ a=20}{tc\ at\ a=0}$	$\frac{tc\ at\ a=40}{tc\ at\ a=20}$	$\frac{tc\ at\ a=60}{tc\ at\ a=40}$	$\frac{tc\ at\ a=80}{tc\ at\ a=60}$	$\frac{tc\ at\ a=100}{tc\ at\ a=80}$
Case 1A	1,125	1,15	1,159	1,195	1,134
Case 2A	1,149	1,168	1,127	1,167	1,308
Case 3A	1,145	1,158	1,136	1,144	1,278
Case 1B	1,161	1,198	1,257	1,428	10,464
Case 2B	1,166	1,204	1,225	1,290	8,825
Case 3B	1,184	1,191	1,213	1,215	2,032

Table 7.3: The table shows how the critical clearing time increases between each step in "a" for each case.

7.5 Recommendations addressing NVF 2020 and proposed revisions of the guide lines

The pre-fault operation conditions is listed in Table 4.4. The active power should be at P = P_{max} before and after the fault and the reactive power should be Q = 0 referred to POC. In the three cases presented in the thesis, the active power does stabilise to the same degree after the fault, except for case 3A in Figure A.19. Another issue regarding the

FRT-requirement is the pre-fault voltage in case 2A and 3A. In Figure A.5 and A.11, the HV voltage is observed to be below 1,0 [p.u].

NVF 2020 set the fault at POC, which is on the terminals on the HV-side of the step-up transformer, in this thesis. This may not be fully realistic, since a fault occurs on the line. The critical clearing time, observed in Table 7.1, in case 2A and 3A is lower then the suggested clearing at 150 [ms]. [1]. To satisfy the clearing time, the fault has to be further out than "a" = 20 [%] for case 2A and "a" > 40 [%] for case 3A. An even larger distance may be suggested since 154 [ms] and 166 [ms] might be to close to the recommended 150 [ms] in NVF 2020. The clearing time also depends on the actual clearing time set for the system, since the critical clearing time is lower then 150 [ms] the generator may struggle to keep synchronism if the load should vary.

With the given cases in this thesis the clearing time at 150 [ms] still has some improvements, and can be reduced. However, if the reactive power in the pre-fault operation condition is increased, the generators FRT-capability increases and consequently the critical clearing time also increases. An increasing reactive power in the pre-fault conditions will allow case 2A and 3A to stay above the recommended 1,0 [p.u] voltage in NVF 2020. Considering Case 1A were the pre-fault voltage is measured above 1,0 [p.u]. As observed in Figure 6.5 the generator is able to keep to voltage profile above the recommended curve, NVF 2020 curve 2. For case 2A and 3A, after the fault the voltage oscillates out of the recommended profile by NVF 2020. The oscillations would have been reduced with a PSS. Based on the assumption that a PSS reduces the oscillations enough for the generator's voltage profile to stay within the recommended voltage profile by NVF 2020, and that the generator does not loose synchronism. NVF 2020 recommends a good profile for the synchronous generator.

Chapter 8

Conclusion

The model used in the simulation is based on a synchronous generator for hydro. In the simulations, a symmetrical three-phase fault is implemented to test the synchronous generator's survival capability in what is called a fault-ride through. The AVR in the model is a PI regulator, and there is no PSS added. As such, the oscillations after the fault could have been reduced further than what is presented in the simulations.

A total of six cases are presented in the thesis. Three of them are tuned to a measured reactive power of zero on the HV side of the step-up transformer, and with a short-circuit power of 20 [p.u], 10 [p.u] and 6,67 [p.u]. The remaining three are tuned to reactive power of 0,396 [p.u] (Q = Qmax) on the HV side of the step-up transformer, and with a similar short-circuit power of 20 [p.u], 10 [p.u] and 6,67 [p.u]. When the reactive power is increased from Q = 0 to Q = Qmax, the voltage drop is not changed much, considering the requirement for a type D generator connected to a voltage below 110 [kV]. Increasing the reactive power does, however, reduce the oscillations and improves the critical fault clearing time. Observing Table 7.1 the fault clearing time for "a" = 0 [%] and 20 [%] is close to or below 150 [ms]. With a short-circuit power of 10 [p.u] where the critical clearing time at a = 0 [%] is 134 [ms] and 154 [ms]. While for a short-circuit power at 6.67 [p.u] the fault clearing time is 110 [ms] for a = 0[%] and 126 [ms] for a = 20 [%]. It is, therefore, evident that the pre-fault conditions affect the synchronous machine fault-ride-through capability.

As mentioned in the discussion chapter 7.4 there are some linearities in how the critical clearing time increases in each step change of "a". However, they are lost when the distance parameter "a" is increased from 80 [%] to 100 [%], and especially for case 1B and 2B. For case 1B, the critical clearing was 5337 [ms] when the distance parameter "a" wast set to 100 [%]. In case 2B, the critical clearing time was 3530 [ms] when the distance parameter "a" was set to 100 [%].

What can be concluded from the thesis is that the critical spot for a short-circuit is closer to the terminals of the step-up transformer and for a fault distance below "a" = 40 [%]. The synchronous machine's pre-fault conditions also have an effect on the machines' stability capability. There is mentioned some recommendations for NVF 2020 in section 7.5. It is recommended to get a better understanding of the FRT-requirement from a practical view to under how realistic they are. A better practical understanding of the FRT-requirement will also allow for better and probably more realistic improvements.

8.1 Further work

- Improve the static excitation system used. Change the PI- regulator to a more commonly used excitation system.
- Add a PSS to the AVR to improve the damping of the system.
- Preform a similar simulation with a more extended system. A larger system with more generates, to see how one fault may effect the other generators.
- Use statical data from real short-circuit events to better asses recommendations for the FRT-requirements.

References

[1] Statnett, *Nasjonal Veilder for funksjonskrav i kraftsystemet 2020*. NVF 2020, 19-01229-12, 2020.

[2] Regjeringen. Norsk vannkrafthistorei på 5 minutter. [Online]. Available: https://www.regjeringen.no/no/tema/energi/fornybar-energi/norsk-vannkrafthistorie-pa-fem-minutter/id2346106/

[3] NVE. Vindkraft. [Online]. Available: https://www.nve.no/energiforsyning/vindkraft/

[4] ——. Vindkraft. [Online]. Available: https://www.nve.no/energiforsyning/kraftproduksjon/vindkraft/?ref=mainmenu

[5] ——. Kraftproduksjon. [Online]. Available: https://www.nve.no/energiforsyning/kraftproduksjon/?ref=mainmenu

[6] P. B. Eriksen, T. Ackermann, H. Abildgaard, P. Smith, W. Winter, and J. M. Rodriguez Garcia, *IEEE Power and Energy Magazine*, vol. 3, no. 6, pp. 65–74, 2005.

[7] Statnett. Funksjonskrav i kraftsystemet (fiks 2012) publisert. [Online]. Available: https://www.statnett.no/om-statnett/nyheter-og-pressemeldinger/Nyhetsarkiv-2012/funksjonskrav-i-kraftsystemet-fiks-2012-publisert-/

[8] F. Bjørken, "Parameter sensitivity in a synchronous generator during a fault-ride-through event," Department of Information Security and Communication Technology, NTNU – Norwegian University of Science and Technology, Project report in TET4510, Dec. 2019.

[9] P. Kundur, "Power system stability and control," New York, 1994.

[10] J. K. Nøland, *Unpublished note*, 2020.

[11] I. A. Metwally, R. M. Radwan, and A. m. ABOU-ELYAZIED, "Powerformers: A breakthrough of high-voltage power generators," *IEEE Potentials*, vol. 27, no. 3, pp. 37–44, May 2008.

[12] H. R. Pota, *The Essentials of Power System Dynamics and Control*. Springe Nature Singapore Pte. Ltd 2018, 2018.

[13] T. H. Karl J. Åström, *PID Controllers: Theory, Design, and Tuning, Second Edition*. ISA - The Instrumentation, Systems and Automation Society, 1995.

[14] Kiyong Kim and R. C. Schaefer, "Tuning a pid controller for a digital excitation control system," in *Conference Record of 2004 Annual Pulp and Paper Industry Technical Conference (IEEE Cat. No.04CH37523)*, 2004, pp. 94–101.

[15] "Ieee recommended practice for excitation system models for power system stability studies," *IEEE Std 421.5-2016 (Revision of IEEE Std 421.5-2005)*, pp. 1–207, 2016.

Appendix A

Appendices

The thesis contains three appendices:

Appendix A.1: Simulation results of the pre-fault conditions described in chapter 6.1 for case 1B to 3B.

Appendix A.2: Figures of the active power for each case.

Appendix A.3: Simulations results of voltage profile for case 1B and 2B. The voltage profile is for the critical clearing time proving the exponetial increase from "a" = 80 [%] to "a" = 100 [%].

A.1 Appendix 1: Model outline results

A.1.1 Case 1B

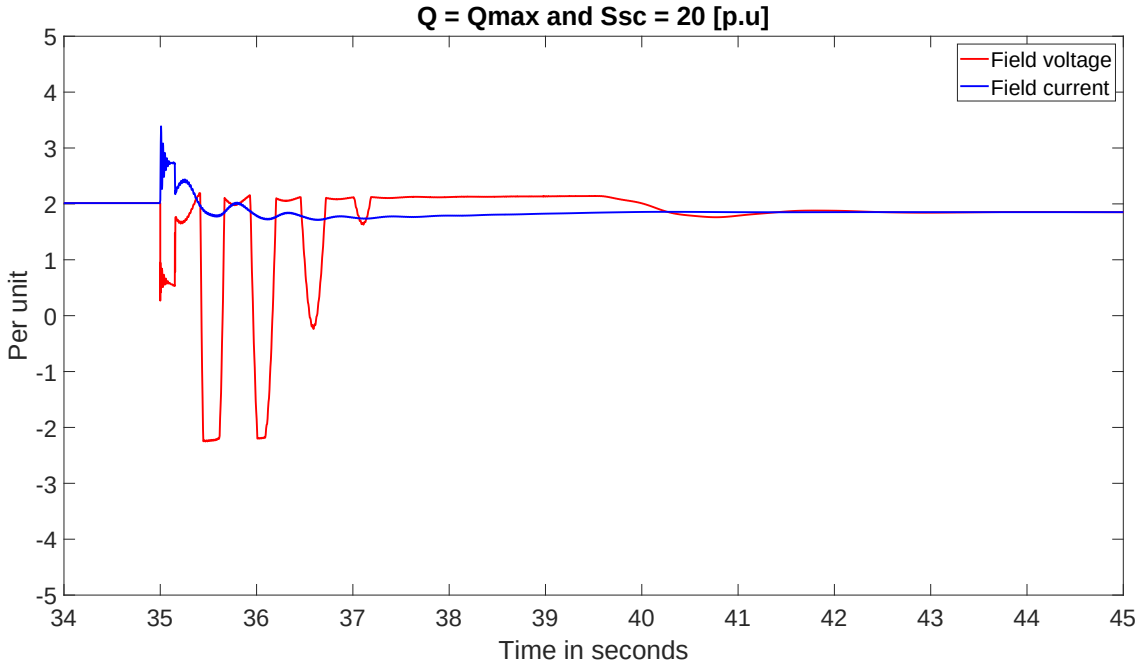

Figure A.1: Plot of the field current and the field voltage with Q = Qmax and X_{th} = 0,05 [p.u].

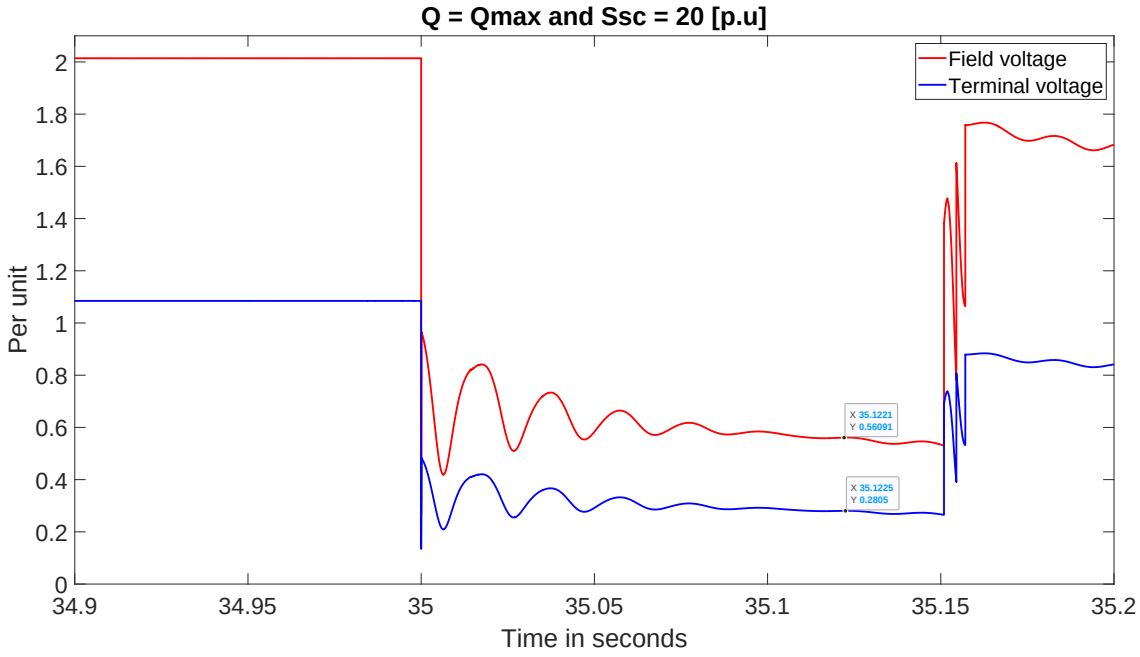

Figure A.2: Plot of the terminal voltage and field voltage with Q = Qmax and X_{th} = 0,05 [p.u].

A.1.2 Case 2A

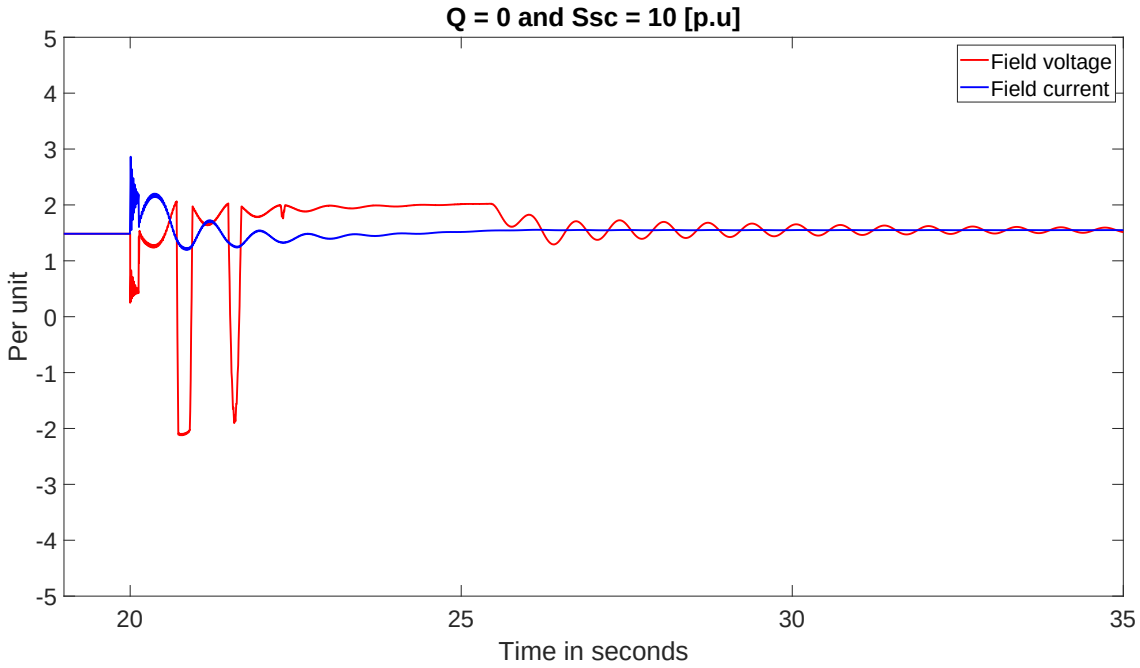

Figure A.3: Plot of the field current and the field voltage with Q = 0 and X_{th} = 0,1 [p.u].

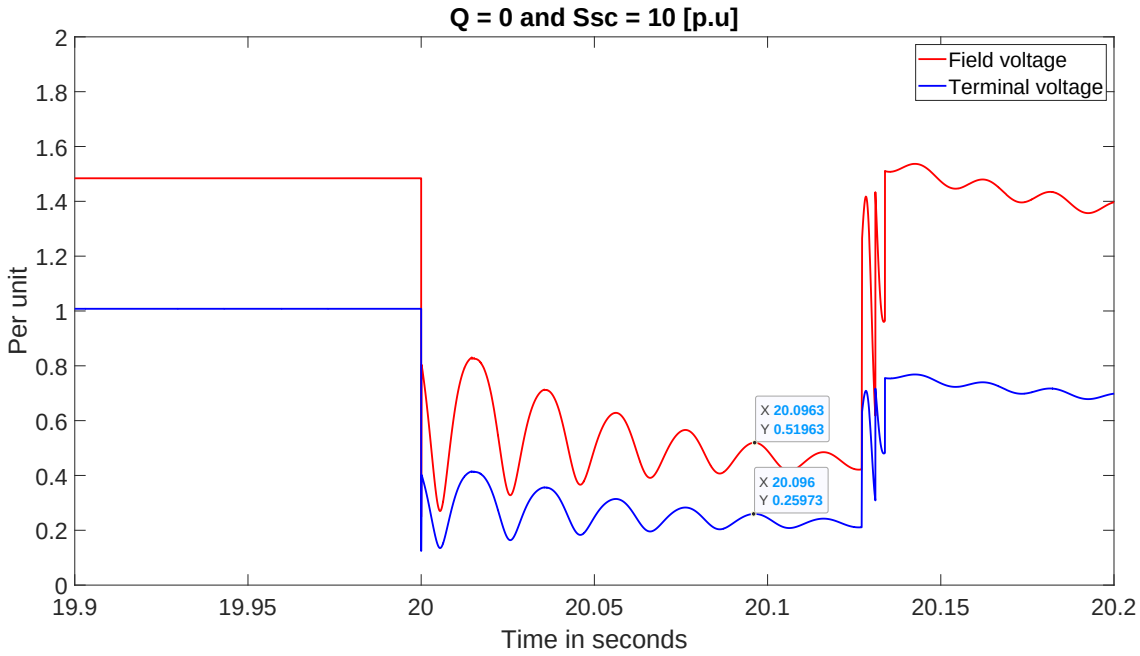

Figure A.4: Plot of the terminal voltage and field voltage with Q = 0 and X_{th} = 0,1 [p.u].

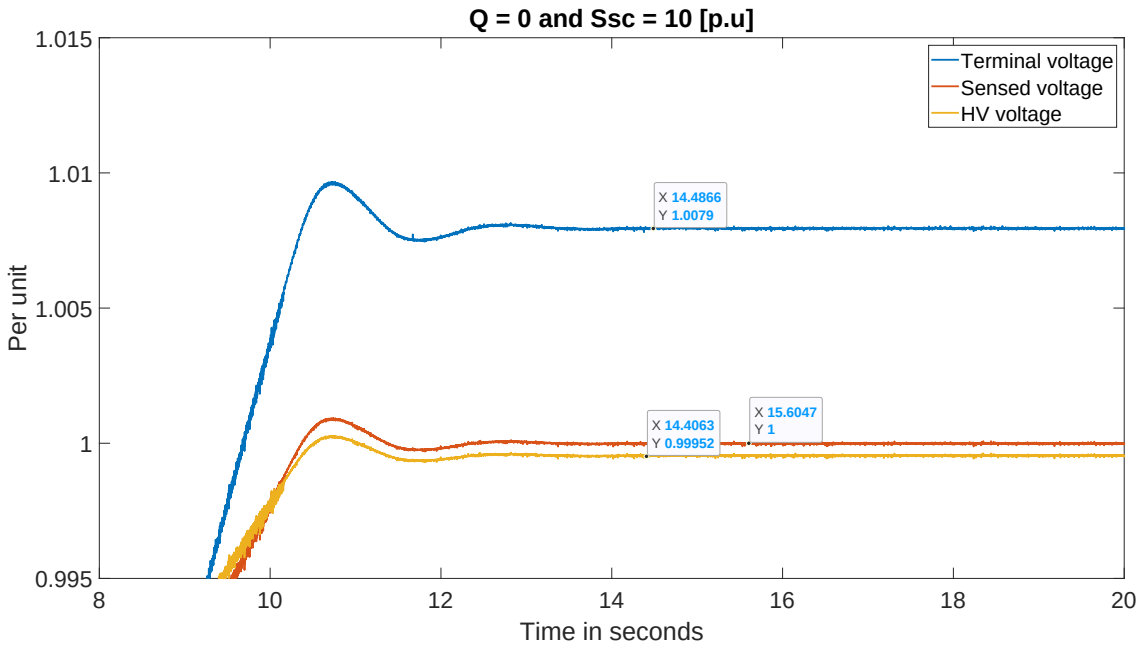

Figure A.5: Figure of the voltage drop between the terminals and the HV side of the transformer, with Q = 0 and X_{th} = 0,1 [p.u].

A.1.3 Case 2B

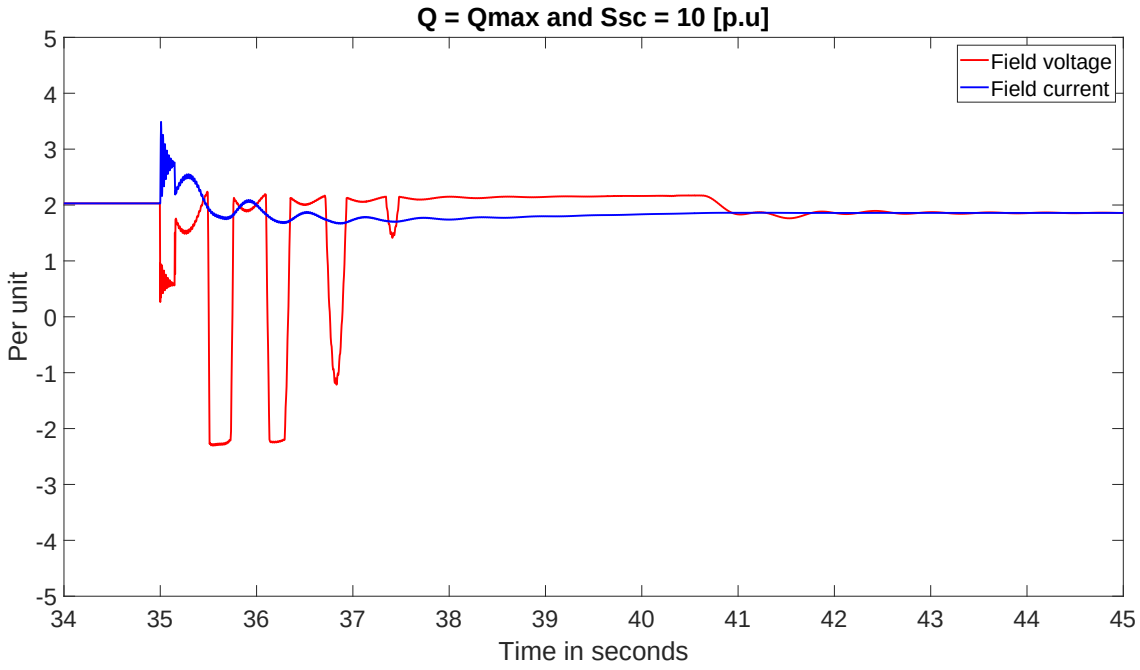

Figure A.6: Plot of the field current and the field voltage with Q = Qmax and X_{th} = 0,1 [p.u].

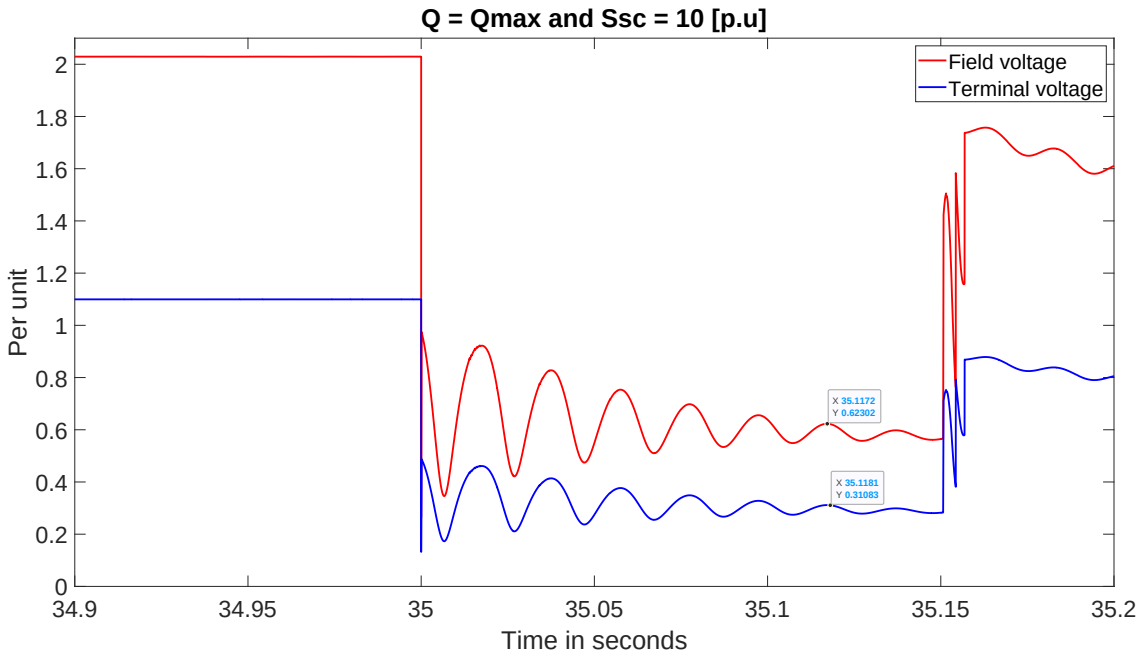

Figure A.7: Plot of the terminal voltage and field voltage with Q = Qmax and X_{th} = 0,1 [p.u].

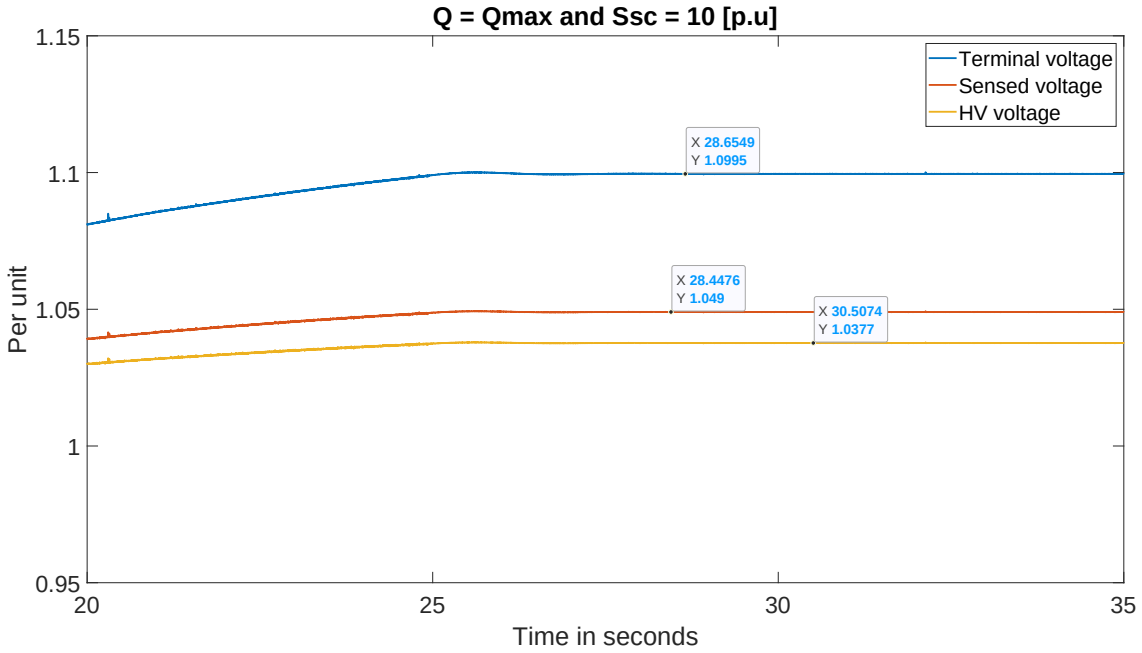

Figure A.8: Figure of the voltage drop between the terminals and the HV side of the transformer, with Q = Qmax and X_{th} = 0,1 [p.u].

A.1.4 Case 3A

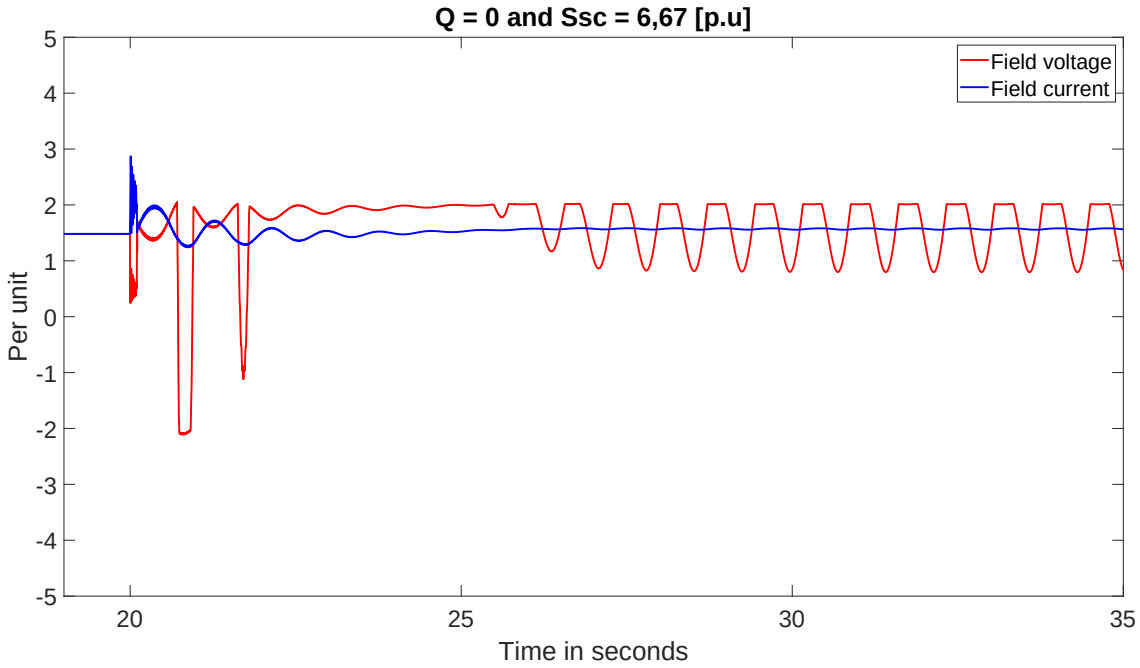

Figure A.9: Plot of the field current and the field voltage with Q = 0 and X_{th} = 0,15 [p.u].

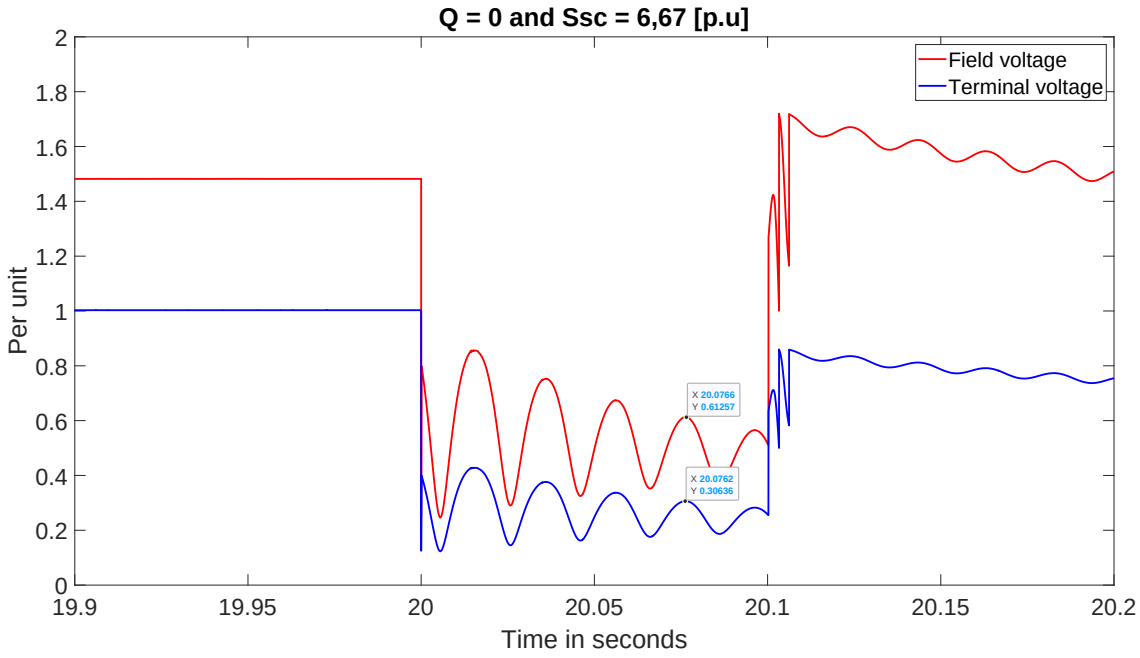

Figure A.10: Plot of the terminal voltage and field voltage with Q = 0 and X_{th} = 0,15 [p.u].

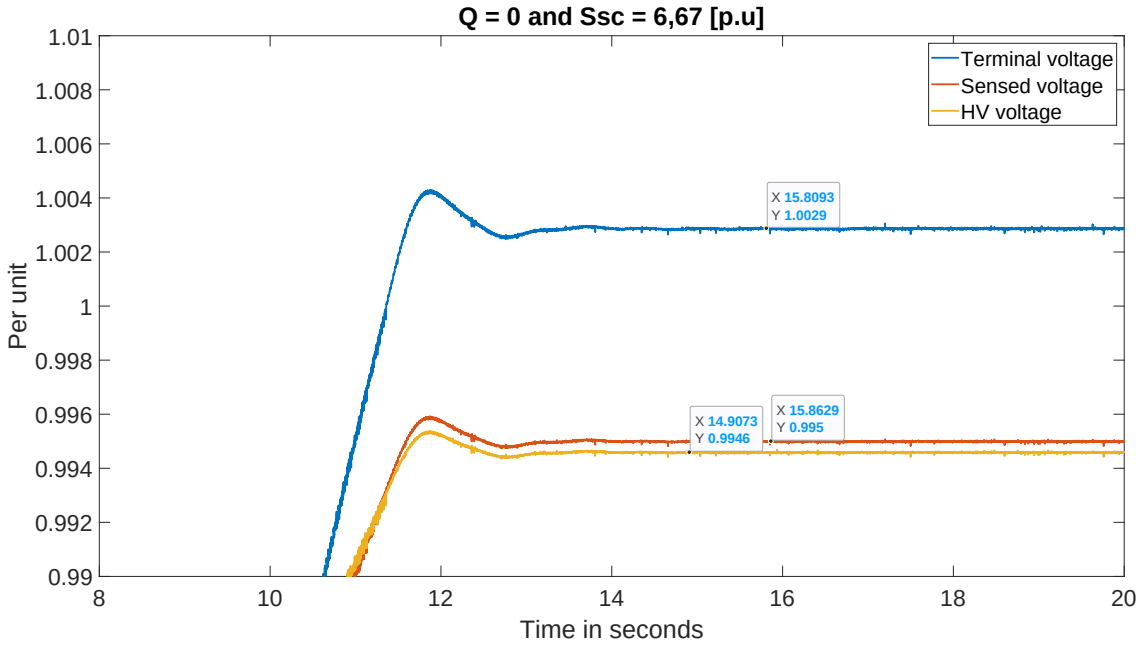

Figure A.11: Figure of the voltage drop between the terminals and the HV side of the transformer, with Q = 0 and X_{th} = 0,15 [p.u].

A.1.5 Case 3B

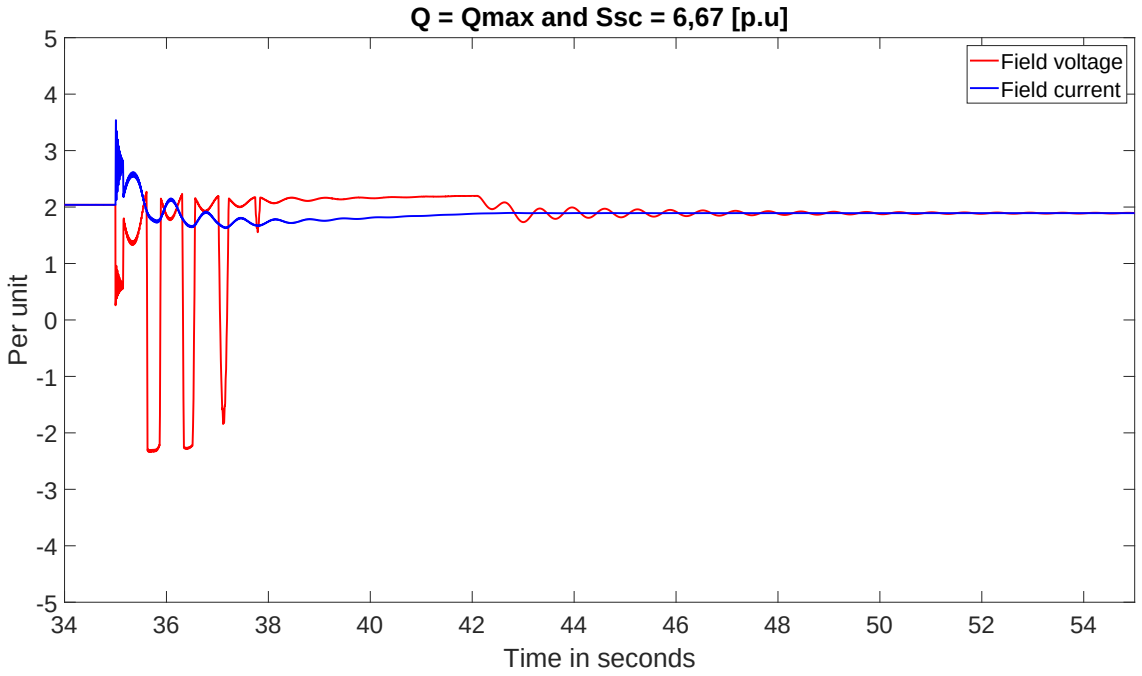

Figure A.12: Plot of the field current and the field voltage with Q = Qmax and X_{th} = 0,15 [p.u].

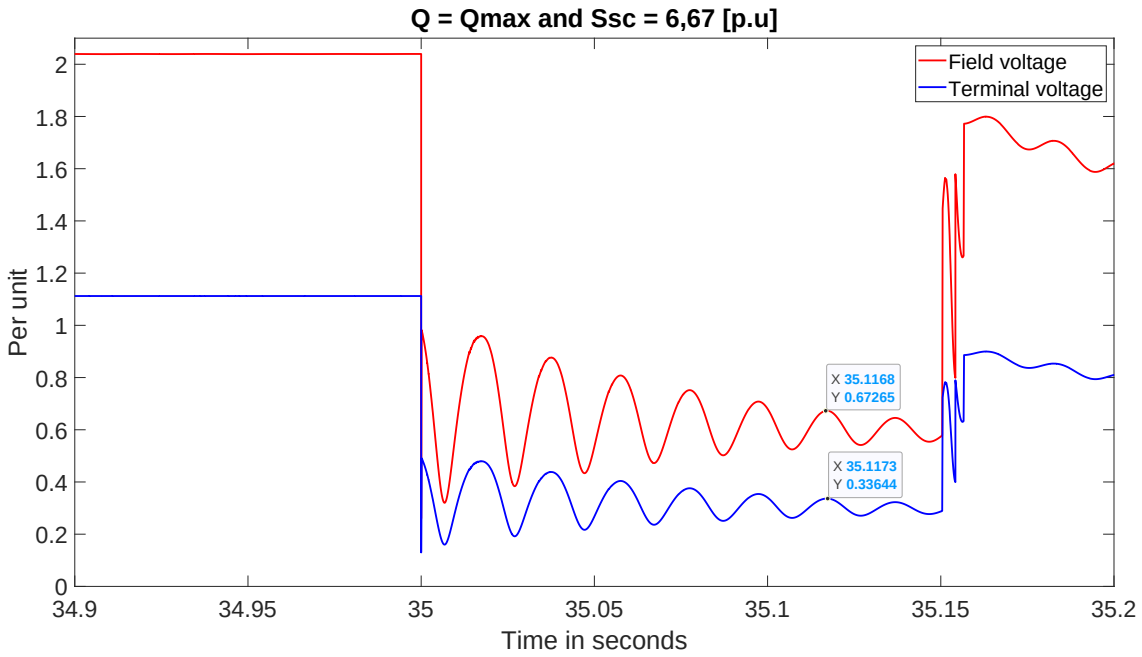

Figure A.13: Plot of the terminal voltage and field voltage with Q = Qmax and X_{th} = 0,15 [p.u].

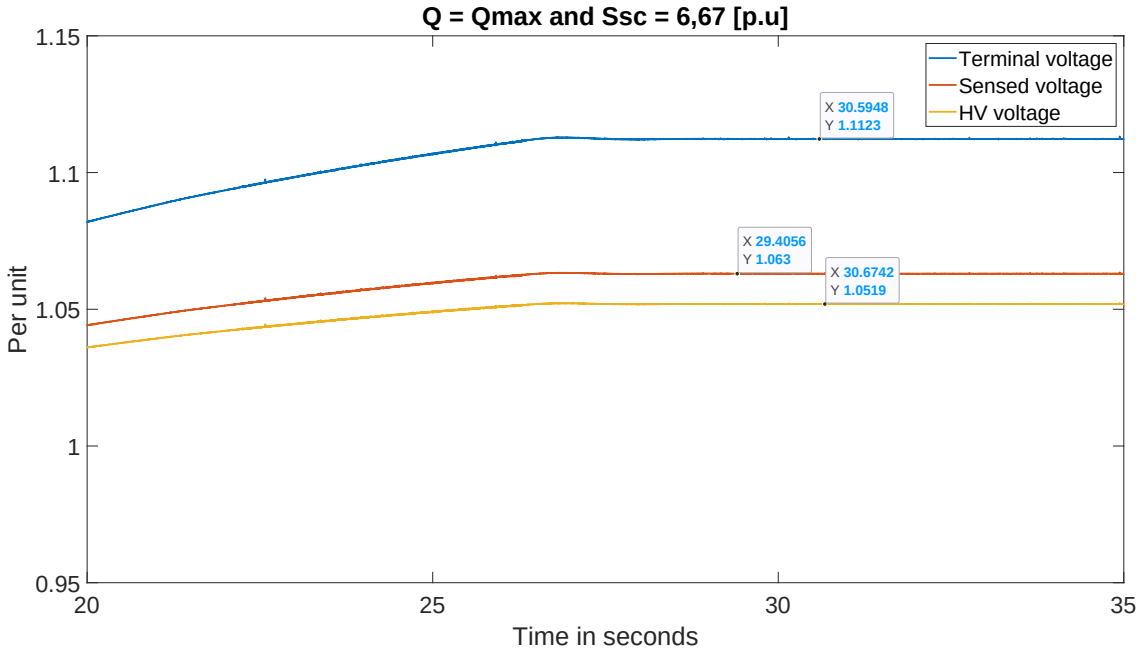

Figure A.14: Figure of the voltage drop between the terminals and the HV side of the transformer, with Q = Qmax and X_{th} = 0,15 [p.u].

A.2 Appendix 2: Active power before and after the fault

A.2.1 Case 1A

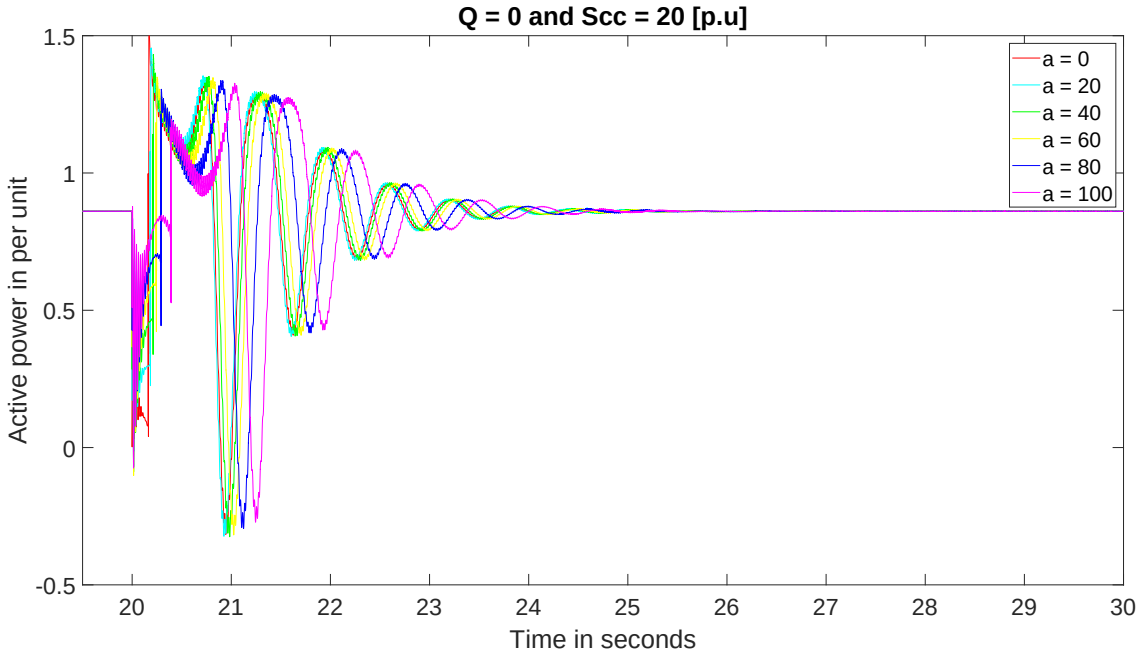

Figure A.15: Figure of the active power flow before and after the fault, with Q = 0 and X_{th} = 0,05 [p.u].

A.2.2 Case 1B

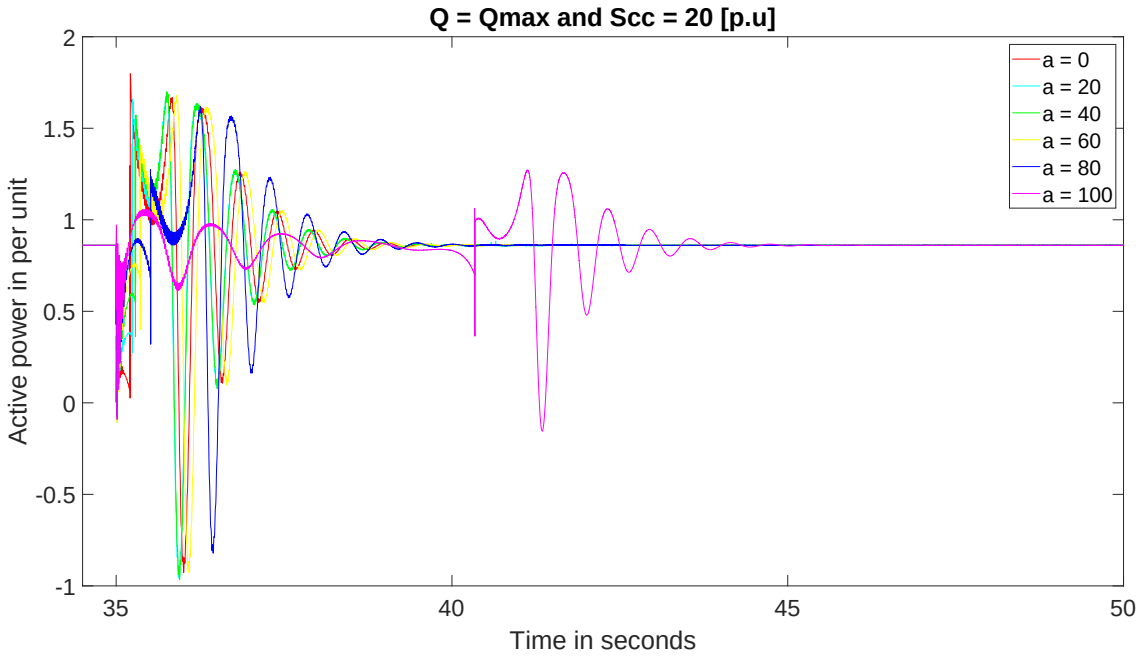

Figure A.16: Figure of the active power flow before and after the fault, with Q = Qmax and X_{th} = 0,05 [p.u].

A.2.3 Case 2A

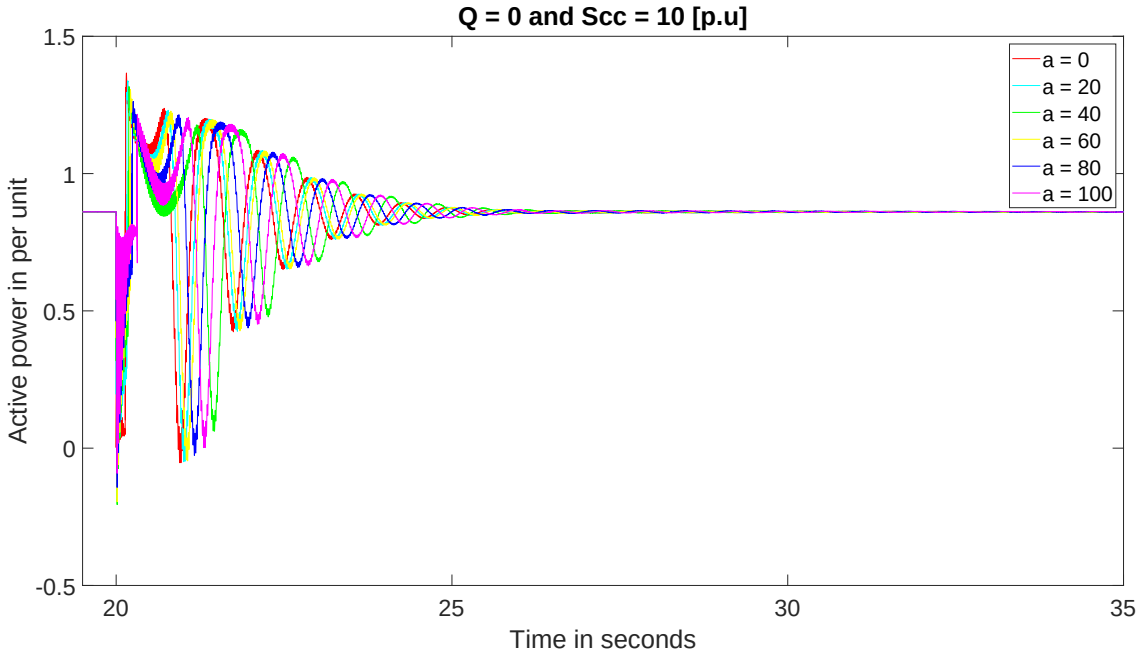

Figure A.17: Figure of the active power flow before and after the fault, with Q = 0 and X_{th} = 0,1 [p.u].

A.2.4 Case 2B

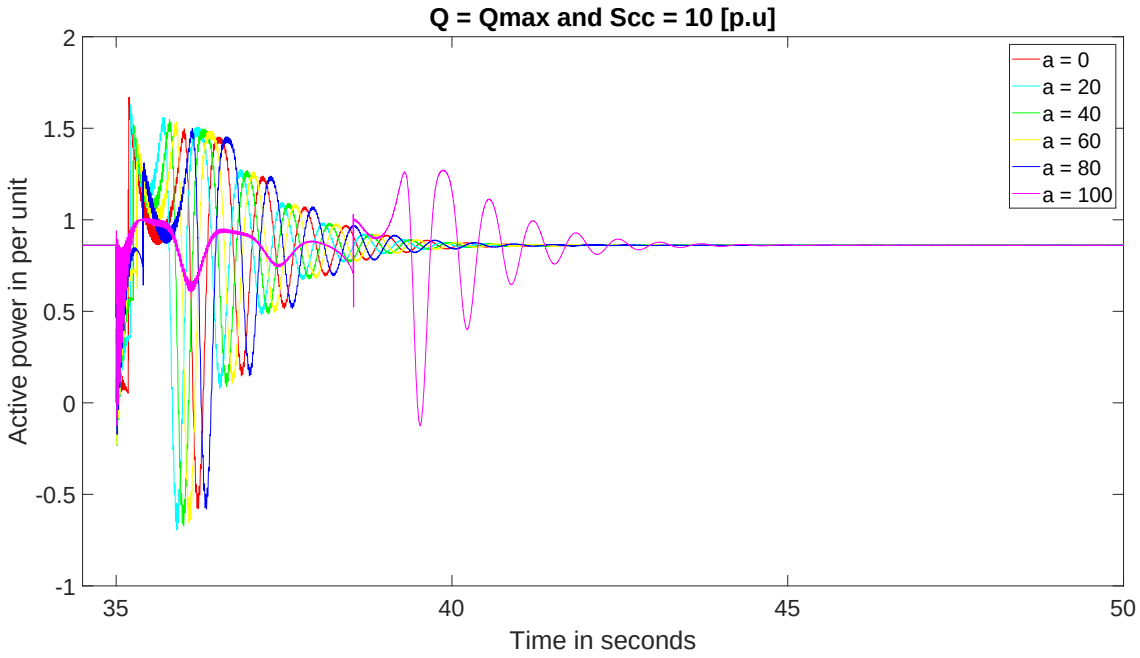

Figure A.18: Figure of the active power flow before and after the fault, with Q = Qmax and X_{th} = 0,1 [p.u].

A.2.5 Case 3A

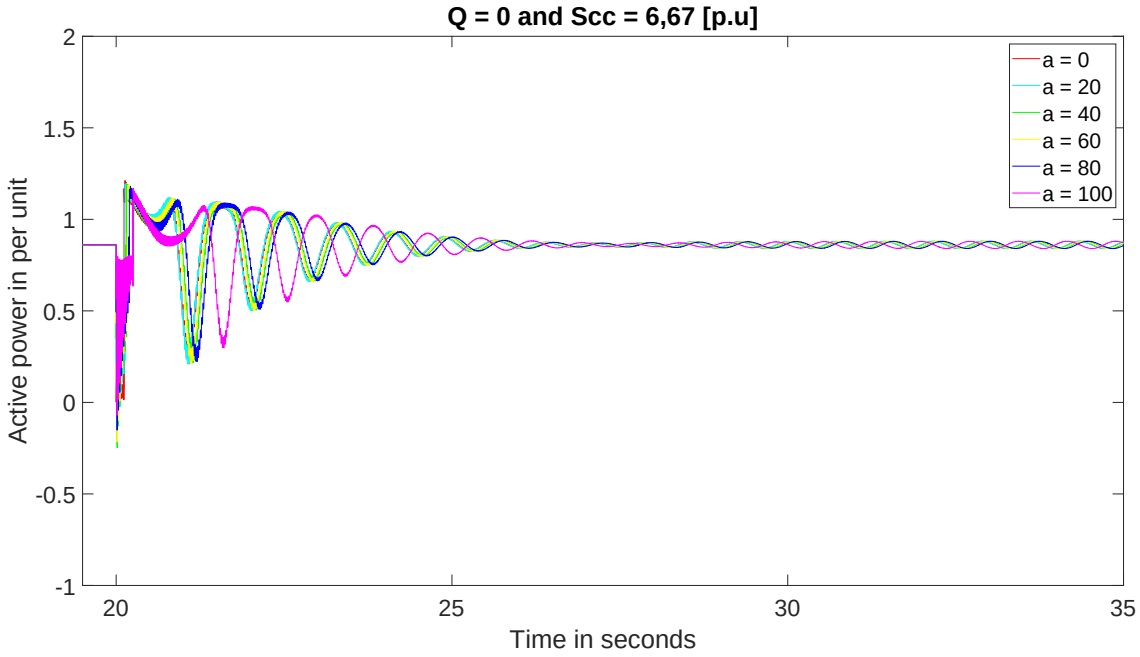

Figure A.19: Figure of the active power flow before and after the fault, with Q = 0 and X_{th} = 0,15 [p.u].

A.2.6 Case 3B

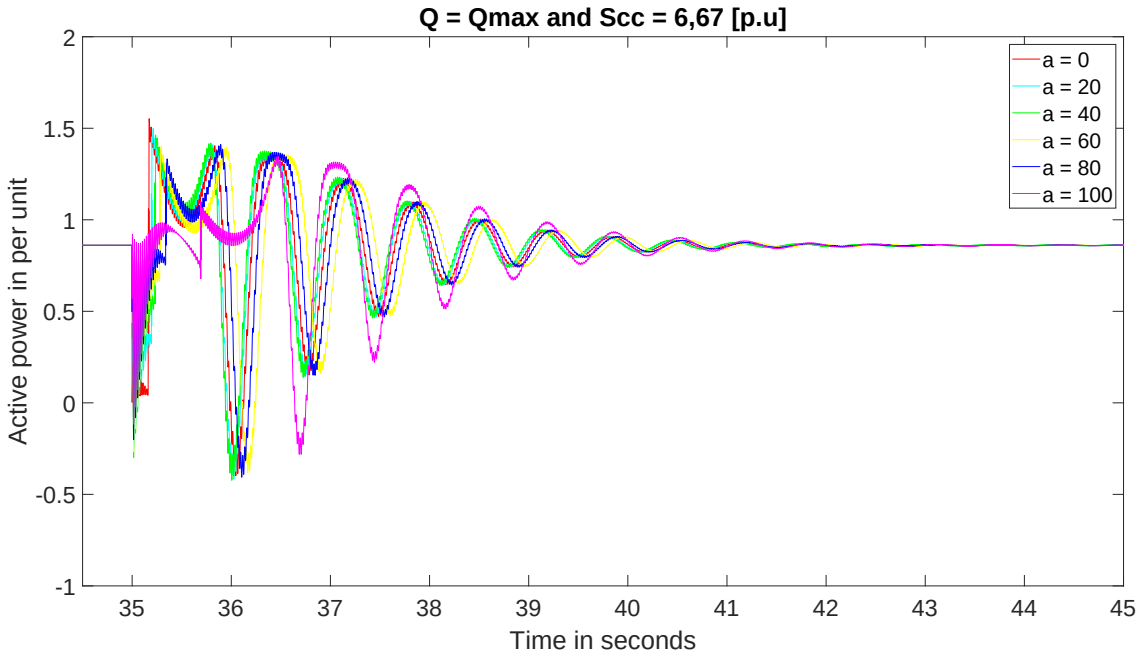

Figure A.20: Figure of the active power flow before and after the fault, with Q = Qmax and X_{th} = 0,15 [p.u].

A.3 Appendix 3: Critical clearing time for Qmax, S_{sc} = 20 [p.u] and S_{sc} = 10 [p.u]

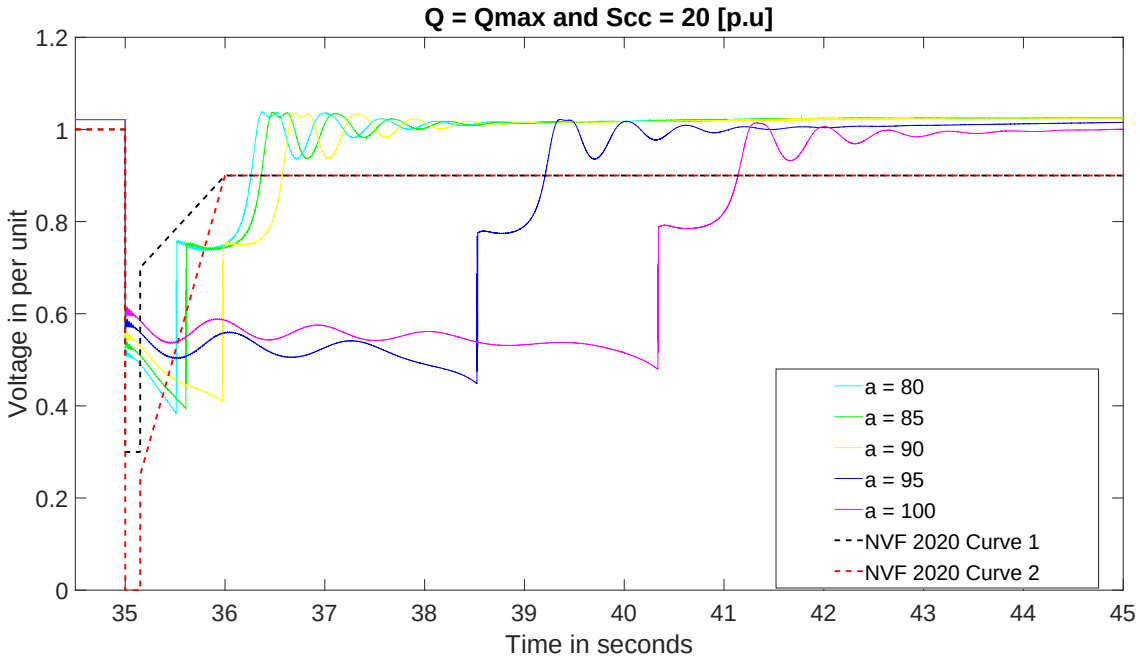

Figure A.21: Plot of the voltage profiles on the HV side of the step-up transformer with a reactive power at Q = Qmax and X_{th} = 0,05 [p.u]. The plots shows the voltage drop when "a" is changed from 80 to 100 in steps of 5 to show the exponential increase in critical clearing time.

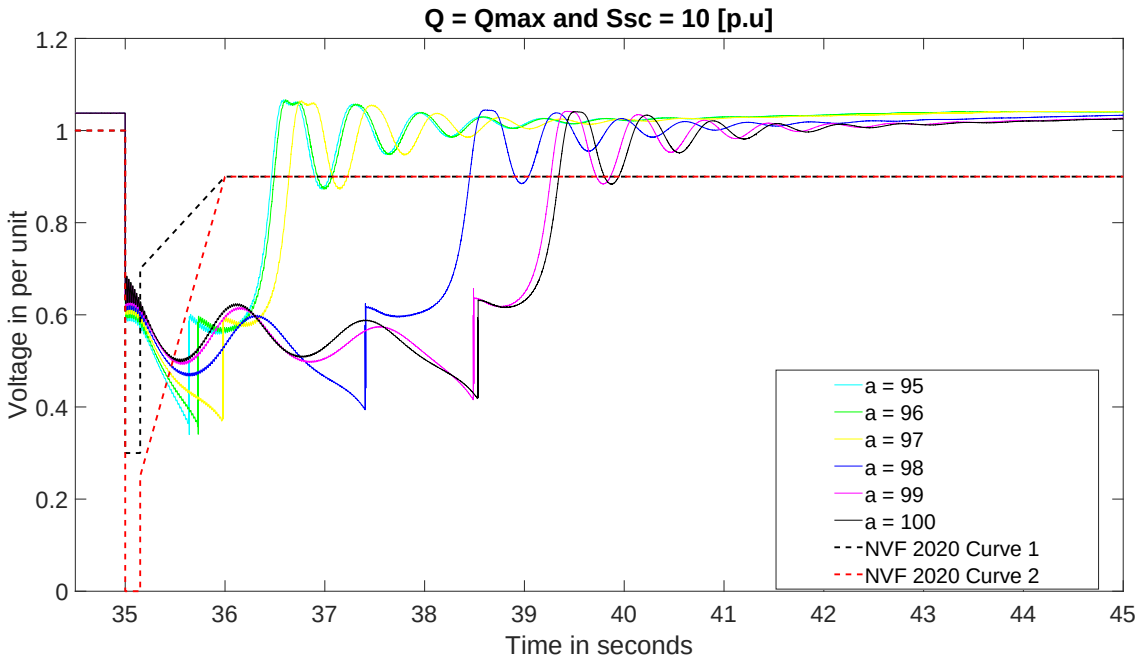

Figure A.22: Plot of the voltage profiles on the HV side of the step-up transformer with a reactive power at Q = Qmax and X_{th} = 0,1 [p.u]. The plots shows the voltage drop when "a" is changed from 95 to 100 in steps of 1 to show the exponential increase in critical clearing time.

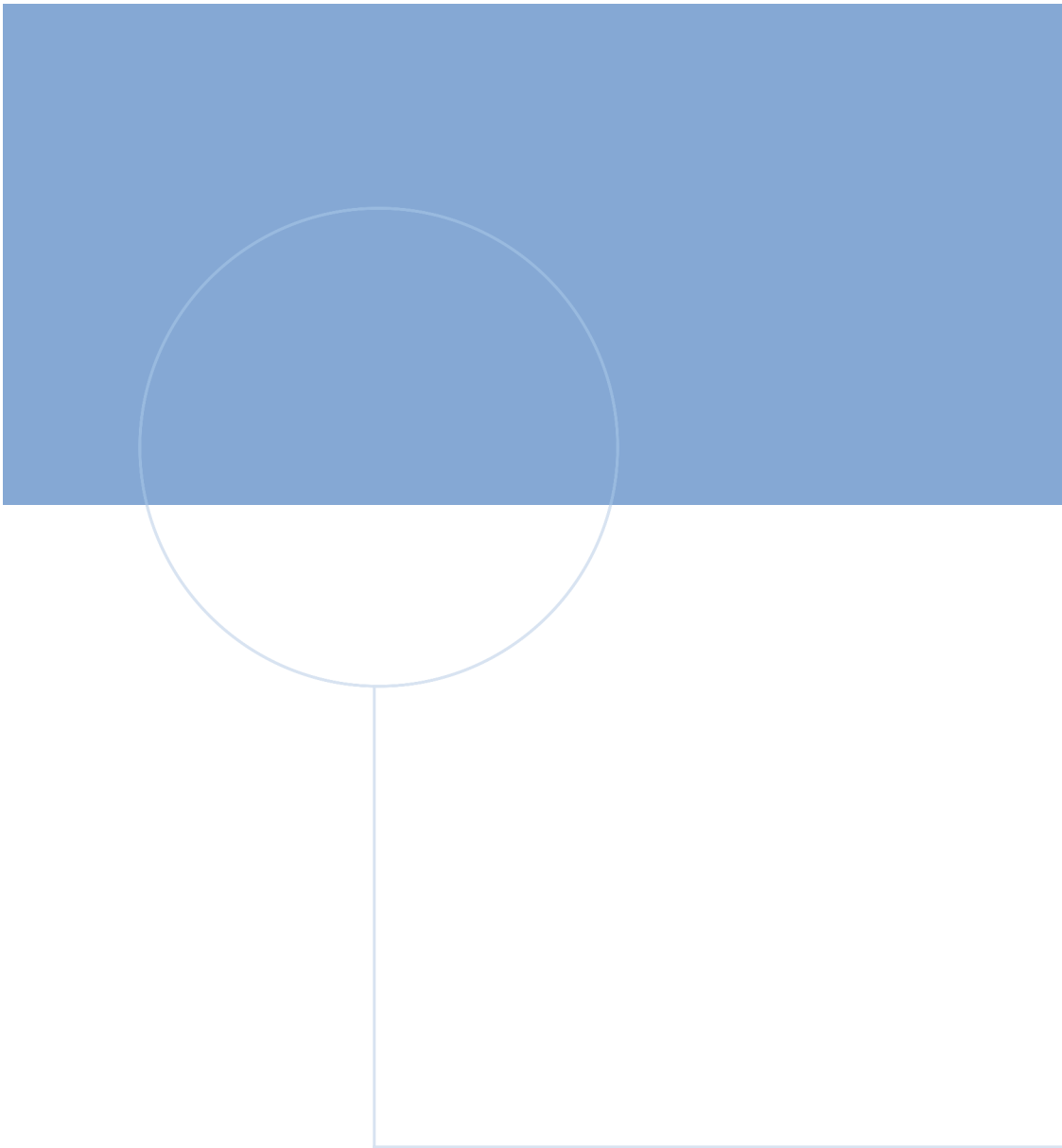

NTNU

Norwegian University of
Science and Technology